AD_____

Award Number: W81XWH-07-1-0466

TITLE: Studies on Axonal Transport in an Animal Model for Gulf War Syndrome

PRINCIPAL INVESTIGATOR: Peter W. Baas, Ph.D.

CONTRACTING ORGANIZATION: Drexel University College of Medicine
Philadelphia, PA 19129

REPORT DATE: July 2008

TYPE OF REPORT: Final

PREPARED FOR: U.S. Army Medical Research and Materiel Command
Fort Detrick, Maryland 21702-5012

DISTRIBUTION STATEMENT: Approved for Public Release;
Distribution Unlimited

The views, opinions and/or findings contained in this report are those of the author(s) and should not be construed as an official Department of the Army position, policy or decision unless so designated by other documentation.

REPORT DOCUMENTATION PAGE

Form Approved
OMB No. 0704-0188

Public reporting burden for this collection of information is estimated to average 1 hour per response, including the time for reviewing instructions, searching existing data sources, gathering and maintaining the data needed, and completing and reviewing this collection of information. Send comments regarding this burden estimate or any other aspect of this collection of information, including suggestions for reducing this burden to Department of Defense, Washington Headquarters Services, Directorate for Information Operations and Reports (0704-0188), 1215 Jefferson Davis Highway, Suite 1204, Arlington, VA 22202-4302. Respondents should be aware that notwithstanding any other provision of law, no person shall be subject to any penalty for failing to comply with a collection of information if it does not display a currently valid OMB control number. **PLEASE DO NOT RETURN YOUR FORM TO THE ABOVE ADDRESS.**

1. REPORT DATE	2. REPORT TYPE	3. DATES COVERED
01-07-2008	Final	1 JUL 2007 - 30 JUN 2008

4. TITLE AND SUBTITLE

Studies on Axonal Transport in an Animal Model for Gulf War Syndrome

5a. CONTRACT NUMBER

5b. GRANT NUMBER
W81XWH-07-1-0466

5c. PROGRAM ELEMENT NUMBER

6. AUTHOR(S)
Peter W. Baas, Ph.D.

E-Mail: pbaas@drexelmed.edu

5d. PROJECT NUMBER

5e. TASK NUMBER

5f. WORK UNIT NUMBER

7. PERFORMING ORGANIZATION NAME(S) AND ADDRESS(ES)

Drexel University College of Medicine
Philadelphia, PA 19129

8. PERFORMING ORGANIZATION REPORT NUMBER

9. SPONSORING / MONITORING AGENCY NAME(S) AND ADDRESS(ES)
U.S. Army Medical Research and Materiel Command
Fort Detrick, Maryland 21702-5012

10. SPONSOR/MONITOR'S ACRONYM(S)

11. SPONSOR/MONITOR'S REPORT NUMBER(S)

12. DISTRIBUTION / AVAILABILITY STATEMENT
Approved for Public Release; Distribution Unlimited

13. SUPPLEMENTARY NOTES

14. ABSTRACT

Gulf War Veterans are more prone to neurodegeneration, presumably due to a combination of toxins to which they were exposed together with stress. The hypothesis of the project was that these toxins might adversely affect the transport of subcellular elements called microtubules within the nerves, and that potential therapies could be developed accordingly. The one year of work did not resolve the issue, but progress was made toward refining the best experimental paradigm in which to test the hypothesis, and progress was made toward refining therapies based on novel tools that target a microtubule-based motor protein called kinesin-5 and microtubule-severing proteins called katanin and spastin.

15. SUBJECT TERMS
Gulf War Syndrome, ALS, microtubule, neuron, neurodegeneration, axonal transport

16. SECURITY CLASSIFICATION OF:			17. LIMITATION OF ABSTRACT	18. NUMBER OF PAGES	19a. NAME OF RESPONSIBLE PERSON
a. REPORT	b. ABSTRACT	c. THIS PAGE			19b. TELEPHONE NUMBER *(include area code)*
U	U	U	UU	44	USAMRMC

Standard Form 298 (Rev. 8-98)
Prescribed by ANSI Std. Z39.18

Table of Contents

Introduction

Veterans of the first Gulf War are twice as likely to develop amyotrophic lateral sclerosis (ALS) as the general population. ALS is a debilitating neurodegenerative disease that typically afflicts both upper and lower motor neurons, and causes widespread degeneration throughout the central nervous system. The disease is thought to affect axonal transport, because neurons with the longest axons appear to be most vulnerable. During the Gulf War, soldiers were exposed to a number of different chemicals including pesticides, drugs to protect against nerve agents, and botulinum toxin vaccine. Any of these chemicals, potentially in combination with one another or with the stress of the military operation, could have triggered the degenerative nerve disease in these soldiers. Unfortunately, the number of veterans of the Gulf War comprise too small of a cluster to study environmental effects potentially contributing to the onset of ALS. Therefore, we proposed to use a recently established animal model to determine whether the various chemicals to which the soldiers were exposed during the Gulf War may diminish the vitality of axonal transport, which could, in turn, contribute to nerve degeneration underlying ALS. Our overall hypothesis was that the pathology mainly affects the mechanisms of slow axonal transport, which is the movement of the cytoskeletal elements themselves, as opposed to fast axonal transport, which is the movement of membranous organelles along the cytoskeletal elements. We posited that the primary deficit is to slow the frequency of the transport of microtubules. Our objectives were to test this hypothesis and test potential experimental approaches for alleviating the deficits that we identify.

Body

There are many reasons why we felt that pursuing these studies could be very beneficial. The primary reason was to develop strategies for helping the veterans of the Gulf War to live a higher quality of life. In addition, we felt that new information on the etiology of the disease would be valuable for understanding how to better protect soldiers (as well as other citizens exposed to potential toxins) in the future.

Our study plan was somewhat risky, which is why we only asked for one year of funding under the Exploration/Hypothesis Development category. Our plan was to culture neurons from experimental (and control) animals, and use live-cell imaging to directly visualize the transport of microtubules and other elements of the cytoplasm. Then, based on the results of these studies, we planned to pursue experiments aimed at developing therapies to restore the transport deficits to normal. In this case, the animal model was adult male rats, treated with toxins and stress. Assuming that our hypothesis is correct, and the major deficit relates to impaired transport of microtubules, our plan was to pursue two strategies for restoring microtubule transport to normal. One strategy was to suppress a molecular motor termed kinesin-5, which we have shown to be a “brake” on the transport of microtubules. We posited that removing the brake should allow for enhanced transport of microtubules. The other strategy was based on the finding that only very short microtubules are transported down the axon. Short microtubules are

generated by a process called microtubule-severing in which long microtubules are severed into shorter pieces by proteins called katanin and spastin. We planned to investigate whether the flaw in transport relates to too much severing or too little severing, and then we planned to evaluate whether we can restore transport levels to normal by experimentally manipulating katanin and/or spastin.

The reviewers of the application expressed skepticism about using the rat model for Gulf War Syndrome. This animal model, developed by Abdel-Rahman and co-workers involves exposing adult male rats to three different toxins to which soldiers were exposed in the Gulf War, together with stress. The reviewers were concerned that the type of stress that can be imposed on the rat in the laboratory is not similar to that which the soldiers endured in the Gulf War and that there is not a similar genetic backdrop against which the poisons and stress are imposed. For example, humans have certain genetic predispositions to diseases such as ALS that are exacerbated by the toxins, and this would not be the same in a rat. Moreover, the reviewers were quite concerned with our ability to verify the model system before conducting the experiments. The reviewers stated that "Overall, the hypothesis, as stated, is narrow and appears to overlook other possible causes of GWI." The reviewers also wisely pointed out that our proposed timetable did not take into account the potential for failed experiments, and that we were only using published work from Abdel-Rahman as a guide for developing the animal model in our own laboratory. Even so, the reviewers felt that looking into microtubule-related causes of degeneration and microtubule-based therapies could have a "huge impact."

We these very real concerns in mind, we decided to respond to the reviewers by altering our plan. Rather than using the animal model, which we discovered would take over half of the funding time to establish and verify in our laboratory, we decided to culture neurons from healthy rats and then expose the cultures of neurons to the toxins directly. This way, we could obtain very direct and specific data on the effects of each toxin on the neurons, rather than obtaining confusing data from an uncertain animal model. We also focused our attention on the two potential therapeutic strategies, to hone our base of knowledge and tools. We devoted 4 months to working on the effects of kinesin-5 inhibition on cultured neurons, and 4 months working on the effects of spastin/katanin manipulation in cultured neurons. Given that flaws in spastin are the chief cause of hereditary spastic paraplegia in humans, we felt that expanding our base of knowledge on this molecule would also assist us in understanding genes that might be risk factors in humans for nerve degeneration. These experimental studies were done on embryonic or juvenile rat neurons, because methods for culturing them are routine. For the last 4 months of the funding period, we have been working to develop cultures of adult rat neurons, so that we can begin testing the detrimental effects of the toxins and the capacity of our kinesin-5 and spastin/katanin manipulations to overcome the deficits in microtubule transport caused by the poisons.

On the favorable side, we can report that the reviewers were of great assistance in putting us on the path to a much more tractable experimental paradigm that we feel should yield insightful results. Using this more reductionist approach, for example, we can compare the toxins against one another, and rank them in terms of their degenerative effects. In

addition, we can discover whether different therapeutic options might be advantage for each of the different toxins. On the negative side, we regret to report that the one-year frame of time was not sufficient for us to actually results using the toxins. We do feel, however, that we are on a very tractable pathway and that the investment in the project will ultimately pay off.

The original task 1 in the Statement of Work was to establish the animal model, and we incorrectly estimated that this would take us only 2 months. After further investigation and consultation with advisors, we abandoned this approach, and decided on the alternative approach described above. The original task 2 was to establish cultures of adult rat DRG neurons in our laboratory, and to begin to use them for microtubule-based assays. We estimated five months of labor for this. We have accomplished the goal (using healthy rats) of mastering this approach, and it has taken us 4 months (see above). The final task was to begin to use the therapeutic approaches on these cultures, and we have made progress on both kinesin-5 (4 months) and katanin/spastin (4 months).

With regard to katanin and spastin, we performed studies on cultured embryonic hippocampal neurons, with a focus on axonal branch formation as a "readout" for the physiological effects of manipulating the two microtubule-severing proteins. Katanin is more highly expressed in the neuron, but spastin is more concentrated at sites of branch formation. Overexpression of spastin dramatically enhanced the formation of branches, whereas overexpression of katanin did not. The excess spastin resulted in large numbers of short microtubules, whereas the excess katanin resulted in short microtubules intermingled with longer microtubules. We hypothesized that these different microtubule-severing patterns may be due to the presence of molecules such as tau on the microtubules that more strongly shield them from being severed by katanin than by spastin. Consistent with this hypothesis, we found that axons depleted of tau show a greater propensity to branch, and that this is true whether or not the axons are also depleted of spastin. We proposed that there are two modes by which microtubule-severing is orchestrated during axonal branch formation, one based on the local concentration of spastin at branch sites and the other based on local detachment from microtubules of molecules such as tau that regulate the severing properties of katanin. These studies, published in 2008 (see reportable outcomes), provide a great deal of information and establish tools we will need for our proposed therapeutic approach on the adult DRG neurons.

Our next project with spastin and katanin focused on the propensity of spastin to participate in neurodegeneration. Autosomal dominant mutations in the SPG4 locus corresponding to spastin are the commonest cause of hereditary spastic paraplegia (HSP), a neurodegenerative disease that afflicts the adult corticospinal tracts. Here we sought to evaluate whether SPG4-based HSP is best understood as a "loss of function" disease. Using various rat tissues, we found that katanin levels are much higher than spastin levels during development. In the adult, katanin levels plunge dramatically but spastin levels decline only slightly. Quantitative data of spastin expression in specific regions of the nervous system failed to reveal any obvious explanation for the selective sensitivity of adult corticospinal tracts to loss of spastin activity. An alternative explanation relates to

the fact that the mammalian spastin gene has two start codons, resulting in a 616 aa protein called M1, and a slightly shorter protein called M85. We found that M1 is almost absent from developing neurons and most adult neurons, but comprises 20-25% of the spastin in the adult spinal cord, the location of the axons that degenerate during HSP. Experimental expression in cultured neurons of a short dysfunctional M1 polypeptide (but not a short dysfunctional M85 peptide) is deleterious to normal axonal growth. In squid axoplasm, the M1 peptide dramatically inhibits fast axonal transport, whereas the M85 peptide does not. These results are consistent with a "gain of function" mechanism underlying HSP wherein spastin mutations produce a cytotoxic protein in the case of M1, but not M85. This work has been published in 2008 (see reportable outcomes), and is important for knowing which spastin isoform to target for our therapeutic strategies.

With regard to kinesin-5, a homotetrameric motor protein that interacts with adjacent microtubules in the mitotic spindle, we found that it is also highly expressed in developing postmitotic neurons. Axons of cultured neurons experimentally depleted of kinesin-5 grew up to five times longer than controls, and displayed more branches. The faster growth rates were accompanied by a doubling of the frequency of transport of short microtubules, suggesting a major role for kinesin-5 in the balance of motor-driven forces on the axonal microtubule array. Live-cell imaging revealed that the effects on axonal length of kinesin-5 depletion were due partly to a lower propensity of the axon and newly forming branches to undergo bouts of retraction. Overexpression of wild-type kinesin-5, but not a rigor mutant of kinesin-5, had the inverse effect on axonal length. These results indicate that kinesin-5 imposes restrictions on the growth of the axon, and does so at least in part by generating forces on the axonal microtubule array. These studies lay the groundwork for the use of more modern anti-kinesin-5 drugs to be used to improve the vitality of degenerating axons. This work was published in 2007 (see reportable outcomes).

Key Research Accomplishments

1. Establishment of adult rat neuronal cultures for use in microtubule related assays.
2. Refinement of knowledge and tools related to katanin/spastin approach for potential therapies for Gulf War Syndrome-related neurodegeneration.
3. Refinement of knowledge and tools related to kinesin-5 approach for potential therapies for Gulf War Syndrome-related neurodegeneration.
4. Development of a tractable plan for obtaining meaningful data in the future on whether or not these approaches are effective at improving the status of axonal degeneration associated with the Gulf War toxins.

Reportable Outcomes

Myers, K.A., and P.W. Baas. 2007. Kinesin-5 regulates the growth of the axon by acting as a break on its microtubule array. J. Cell Biol. 178: 1081-1091.

Solowska, J.M, G. Morfini, A. Falnikar., B.T. Himes, S.T. Brady, D. Huang, and P.W. Baas. 2008. Quantitative and functional analyses of spastin in the nervous system: implications for hereditary spastic paraplegia. Journal of Neuroscience 28: 2147-2157.

Yu, W., L. Qiang, J.M. Solowska, A. Karabay, S. Korulu, and P.W. Baas. 2008. Spastin is more specialized than P60-katanin to participate in the formation of axonal branches. Molecular Biology of the Cell 19: 1485-1498.

Conclusions

The "exploration" nature of this grant funding mechanism enabled us to propose a rather risky plan that met with some skepticism from the reviewers. Taking the advice of the reviewers, we revised the plan and were able to put ourselves on a more certain path toward producing meaningful results on the effects of toxins associated with neurodegeneration in soldiers suffering from Gulf War Syndrome. Even so, one year of work was sufficient only to lay the groundwork toward determining the effects of the therapies. We look forward to pursuing the next phase of the work.

References: None

Appendices: Included in the appendices are PDFs of the three published articles.

Supporting Data: All figures, graphs and tables are shown in the three published papers.

Kinesin-5 regulates the growth of the axon by acting as a brake on its microtubule array

Kenneth A. Myers and Peter W. Baas

Department of Neurobiology and Anatomy, Drexel University College of Medicine, Philadelphia, PA 19104

Kinesin-5 is a homotetrameric motor protein that interacts with adjacent microtubules in the mitotic spindle. Kinesin-5 is also highly expressed in developing postmitotic neurons. Axons of cultured neurons experimentally depleted of kinesin-5 grow up to five times longer than controls and display more branches. The faster growth rates are accompanied by a doubling of the frequency of transport of short microtubules, suggesting a major role for kinesin-5 in the balance of motor-driven forces on the axonal microtubule array. Live-cell imaging reveals that the effects on axonal length of kinesin-5 depletion are caused partly by a lower propensity of the axon and newly forming branches to undergo bouts of retraction. Overexpression of wild-type kinesin-5, but not a rigor mutant of kinesin-5, has the inverse effect on axonal length. These results indicate that kinesin-5 imposes restrictions on the growth of the axon and does so at least in part by generating forces on the axonal microtubule array.

Introduction

The growth and maintenance of the axon is dependent on a continuous array of microtubules that extends from the cell body of the neuron into the growth cone. Individual microtubules assume a variety of lengths within the array, ranging from <1 to >100 μm (Yu and Baas, 1994). Very short microtubules are able to move rapidly and in both directions (Wang and Brown, 2002). In contrast, the longer microtubules in the axon are essentially immobile (Ma et al., 2004; Ahmad et al., 2006). Twice as many short microtubules move in the anterograde direction, presumably to ensure that more tubulin enters the axon than is moved back to the cell body. In addition to supplying tubulin for axonal growth, mobility within the microtubule array promotes the morphological plasticity underlying events such as growth-cone motility and branch formation (Yu and Baas, 1994; Dent et al., 1999). The longer microtubules are important too because they act as compression-bearing struts that prevent the axon from retracting under the myosin-II–based contractile forces imposed on the cortical actin (Myers et al., 2006b). We have proposed a model whereby the same molecular motors that transport the short microtubules impinge upon the long microtubules to regulate the degree to which they can resist the myosin-based contractile forces (Baas et al., 2006).

We have begun to study the panoply of microtubule-based motors that generate forces against long and short microtubules. We have found that if we deplete cytoplasmic dynein or if we depolymerize actin filaments, the frequency of anterograde microtubule transport is reduced by about half (Hasaka et al., 2004; He et al., 2005). These results are consistent with a scenario in which short microtubules move anterogradely via a "sliding filament" mechanism in which the cargo domain of the motor interacts (indirectly) with actin filaments (Pfister, 1999; Myers et al., 2006a). The motor domain is then available to transport the short microtubules. Consistent with our model for long and short microtubules, depletion of cytoplasmic dynein also renders the long microtubules less capable of resisting the myosin-II–based contractile forces that cause the axon to retract (Ahmad et al., 2000; Myers et al., 2006a). The fact that not all of the mobility within the microtubule array depends on cytoplasmic dynein indicates that there are other participating motors, presumably kinesins.

The relevant kinesins are the so-called mitotic kinesins, which generate forces between adjacent microtubules rather than between microtubules and membranous cargo (Dent et al., 1999). We have shown that many of these specialized kinesins continue to be expressed in terminally postmitotic neurons (Sharp et al., 1997; Ferhat et al., 1998; Buster et al., 2003). We are particularly interested in kinesin-5 (also known as Eg5), which forms homotetramers consisting of two sets of antiparallel motor domains (Kashina et al., 1996). In the mitotic spindle, the primary function of kinesin-5 is to maintain spindle bipolarity by generating centrosome-directed forces between antiparallel microtubules in the midzone (Blangy et al., 1995; Sharp et al., 1999a,b; Kapitein et al., 2005). In neurons, pharmacological inhibition of kinesin-5

Correspondence to Peter W. Baas: pbaas@drexelmed.edu

Abbreviations used in this paper: DIC, differential interference contrast; PDL, poly-D-lysine.

The online version of this article contains supplemental material.

© The Rockefeller University Press $30.00
The Journal of Cell Biology, Vol. 178, No. 6, September 10, 2007 1081–1091
http://www.jcb.org/cgi/doi/10.1083/jcb.200702074

Supplemental Material can be found at:
http://www.jcb.org/cgi/content/full/jcb.200702074/DC1

THE JOURNAL OF CELL BIOLOGY

Downloaded from www.jcb.org on September 10, 2007

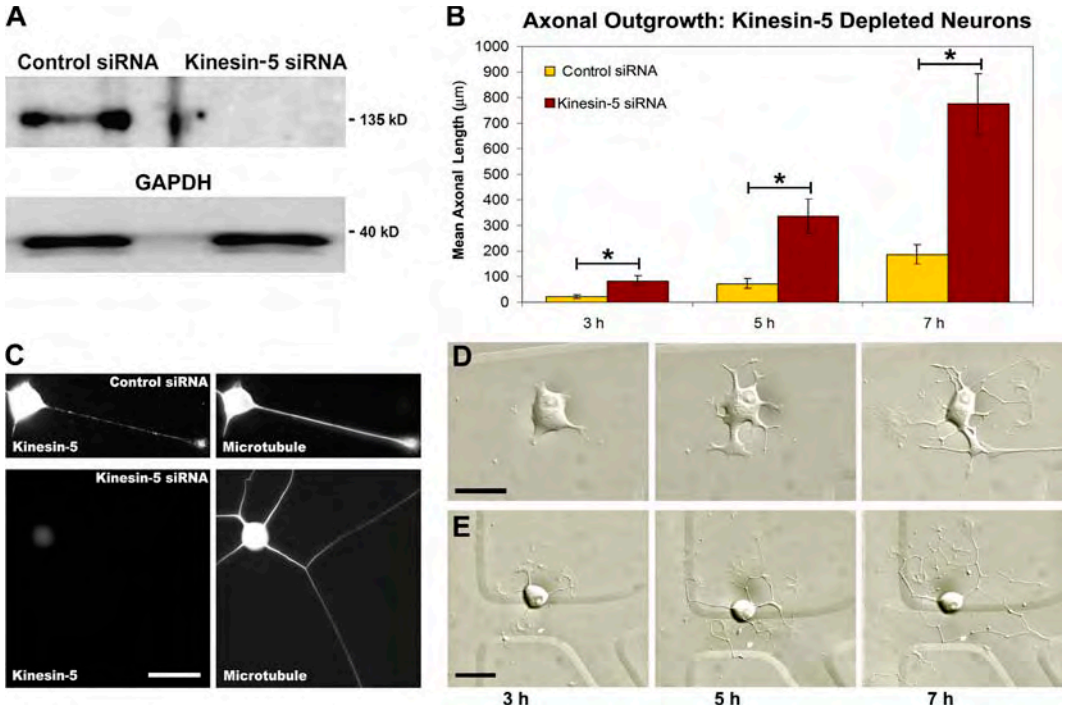

Figure 1. **Kinesin-5 depletion results in increased axonal length.** (A) Western blot showing kinesin-5 protein levels in cultured sympathetic neurons treated with control siRNA and kinesin-5 siRNA. The bottom panel shows the glyceraldehyde-3-phosphate dehydrogenase (GAPDH) loading control for both protein samples. (B) Quantification of mean axonal outgrowth reveals significantly longer axons of kinesin-5–depleted neurons at all time points observed, with a 4.3-fold mean increase in axonal length (mean ± SEM; 3 h, control = 21.3 ± 6.45 μm, experimental = 82.8 ± 19.7 μm; 5 h, control = 71.8 ± 20.0 μm, experimental = 335 ± 66.8 μm; 7 h, control = 187 ± 37.1 μm, experimental = 774 ± 120 μm) (control siRNA, $n = 17$; kinesin-5 siRNA, $n = 21$; *, $P < 0.01$). (C) Fluorescence images of kinesin-5 immunostaining in control siRNA (top) and kinesin-5 siRNA–treated neurons (bottom). The corresponding microtubule staining for these two cells is shown in the panels on the right. (D) DIC images of a control siRNA neuron taken at 3, 5, and 7 h after replating. (E) DIC images of a kinesin-5–depleted neuron at 3, 5, and 7 h after replating revealed the notable increases in axonal length quantified in B. Bars, 20 μm.

results in longer axons (Haque et al., 2004; Yoon et al., 2005), suggesting a key role for this motor in the development of the nervous system. In the present study, we have investigated the underlying mechanisms by which kinesin-5 influences the development of the axon.

Results

Although monastrol (the drug used in the earlier studies on neurons; Haque et al., 2004; Yoon et al., 2005) is quite specific for kinesin-5 (Kapoor et al., 2000; Maliga et al., 2002; Kwok et al., 2006; Maliga and Mitchison, 2006), we wished to pursue an additional approach that would deplete kinesin-5 rather than inhibit it. For this we used siRNA, which has been shown to be highly effective at depleting kinesin-5 from other cell types (Weil et al., 2002). For the current experiments, rat sympathetic neurons were transfected with 10 μM siRNA (control or kinesin-5), plated densely on plastic dishes, and then allowed time for the protein to be depleted. As determined by Western blotting, 3 d after transfection was sufficient time to deplete over 95% of the kinesin-5 protein from the neurons (Fig. 1 A). The neurons were then replated at a lower density onto glass coverslips treated with polylysine and laminin, and allowed to grow axons anew. For some studies, we also performed side-by-side monastrol experiments.

Effects of kinesin-5 depletion on axonal morphology

For evaluation of the effects of siRNA-based depletion of kinesin-5 on axonal morphology, neurons were chosen randomly and then imaged at successive time points beginning 1 h after plating, and continuing every 2 h thereafter until 7 h. Although at the 1 h time point there were very few neurons that had extended axons in either the control or experimental groups; analyses of mean axonal length at 3, 5, and 7 h all revealed significant increases in the experimental neurons. Specifically, quantification of axonal length revealed a 4.3-fold increase in mean axonal lengths at all three time points, a change that was statistically significant (3 h, $P < 0.008$; 5 h, $P < 0.002$; 7 h, $P < 0.0003$; two-tailed t test; Fig. 1 B). These differences (Fig. 1, C and D) were comparable to those obtained in parallel experiments using monastrol (see Fig. 8).

In addition to being longer, the experimental axons were also more branched than the control axons (Fig. 2, A and B). For quantification of this effect, total branch numbers were normalized to total axonal length, so that the values were comparable between control and kinesin-5–depleted neurons (control, $n = 27$; kinesin-5 siRNA, $n = 37$). Statistical analyses of axonal branching data revealed a significant increase in branching frequency of kinesin-5–depleted neurons to levels nearly four times higher than controls (Fig. 2 C). When branching frequency was quantified based on the location of the branches, a statistically

Downloaded from www.jcb.org on September 10, 2007

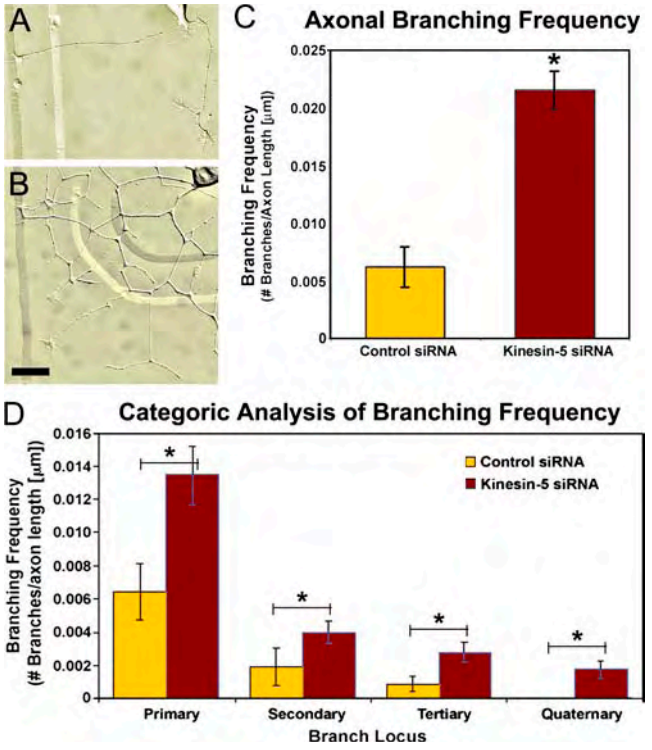

Figure 2. **Axonal branching is enhanced when kinesin-5 is depleted.** (A and B) DIC images of typical control (A) and kinesin-5–depleted (B) neurons. Note the increase in branch number in axons depleted of kinesin-5. (C) Quantitative analysis of axonal branch number (normalized to total axonal length) revealed a statistically significant increase when compared with control siRNA–treated neurons (mean ± SEM; control siRNA = 0.006 ± 0.002, kinesin-5 siRNA = 0.022 ± 0.002; *, $P = 5.76 \times 10^{-8}$). (D) Categorical analysis at various branching loci (control siRNA, $n = 27$; kinesin-5 siRNA, $n = 37$) revealed a statistically significant increase in branching frequency at all branch positions (mean ± SEM; primary branch: control = 0.006 ± 0.002, kinesin-5 siRNA = 0.013 ± 0.002, *, $P < 0.02$; secondary branch: control = 0.002 ± 0.001, kinesin-5 siRNA = 0.004 ± 0.001, *, $P < 0.03$; tertiary branch: control = 0.001 ± 0.0004, kinesin-5 siRNA = 0.003 ± 0.001, *, $P < 0.03$; quaternary branch: control = 0.00 ± 0.00, kinesin-5 siRNA = 0.001 ± 0.0005, *, $P < 0.007$). Bars, 20 μm.

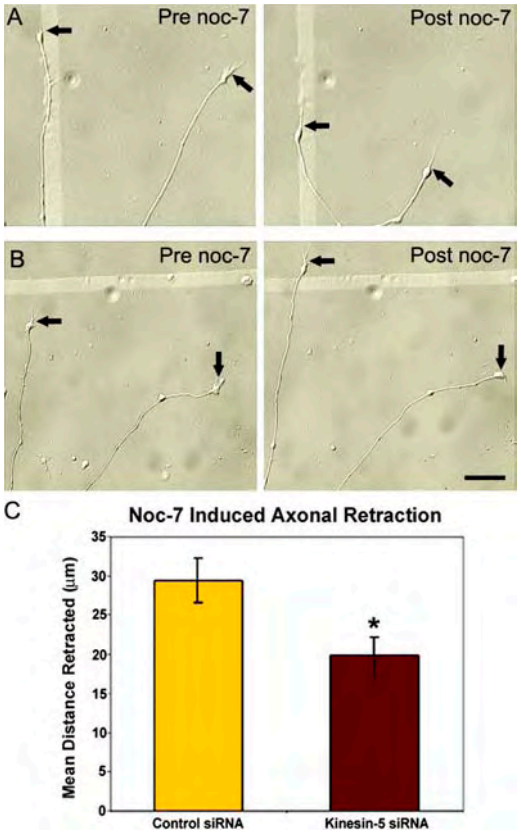

Figure 3. **Depletion of kinesin-5 reduces the distance of axonal retraction.** (A and B) DIC images of control axons (A) and kinesin-5–depleted axons (B) before and 30 min after treatment with 0.3 mM noc-7. (B) Kinesin-5–depleted axons continue to elongate even in the presence of noc-7. Arrows demarcate the distal tips of growth cones before and after noc-7 treatment. (C) Quantitative analysis of noc-7–induced axonal retraction revealed a statistically significant reduction in mean distance retracted in neurons depleted of kinesin-5 (mean ± SEM; control, $n = 54$; kinesin-5 siRNA, $n = 55$; *, $P = 0.011$). Bar, 20 μm.

significant increase in branching frequency was identified in kinesin-5–depleted neurons at all branch loci (Fig. 2 D). In neurons depleted of kinesin-5, primary branch frequency was increased to 217% of controls ($P < 0.02$; $n = 14$), secondary branch frequency was increased to 200% of controls ($P < 0.03$; $n = 14$), and tertiary branch frequency was elevated to 298% of control neurons ($P < 0.03$; $n = 12$). There were no quaternary branches observed in the control siRNA group of neurons during the observation time period ($n = 12$). The change between control and kinesin-5 siRNA was found to be statistically significant ($P < 0.007$).

We next investigated whether the kinesin-5–depleted axons differed from controls in their propensity to retract in response to physiological cues. For this, we used noc-7 (a donor of nitric oxide and potent inducer of axonal retraction; Ernst et al., 2000; He et al., 2002). After allowing neurons depleted of kinesin-5 to undergo 12–16 h of axonal growth, differential interference contrast (DIC) images were taken of individual neurons whose axons were >100 μm, followed by treatment with 0.3 mM noc-7 for 30 min. These same neurons were then relocated and imaged once again, and the before-and-after images were analyzed for mean differences in axonal length. Quantification of mean distance retracted revealed that the axons of neurons transfected with control siRNA underwent significantly greater distances of retraction than the axons of neurons depleted of kinesin-5 (control siRNA, $n = 54$; kinesin-5 siRNA, $n = 55$). In some cases, the axons of the neurons depleted of kinesin-5 actually continued to grow in the presence of noc-7, which virtually never occurred in the case of the controls (Fig. 3, A and B). On average, neurons treated with control siRNA retracted their axons 29.5 ± 2.87 μm after 30-min exposure to noc-7, whereas neurons depleted of kinesin-5 retracted their axons 19.8 ± 2.45 μm (mean ± SEM, $P = 0.011$; Fig. 3 C). Thus depletion of kinesin-5 reduces the distances over which the axons would normally have retracted. Similar results were obtained with monastrol (unpublished data).

Effects of kinesin-5 depletion on axonal transport of short microtubules

For studies on microtubule transport (Fig. 4 A), the culture regimes were the same as for the morphological studies, except that replating was performed at 60 h after transfection, and cells

Downloaded from www.jcb.org on September 10, 2007

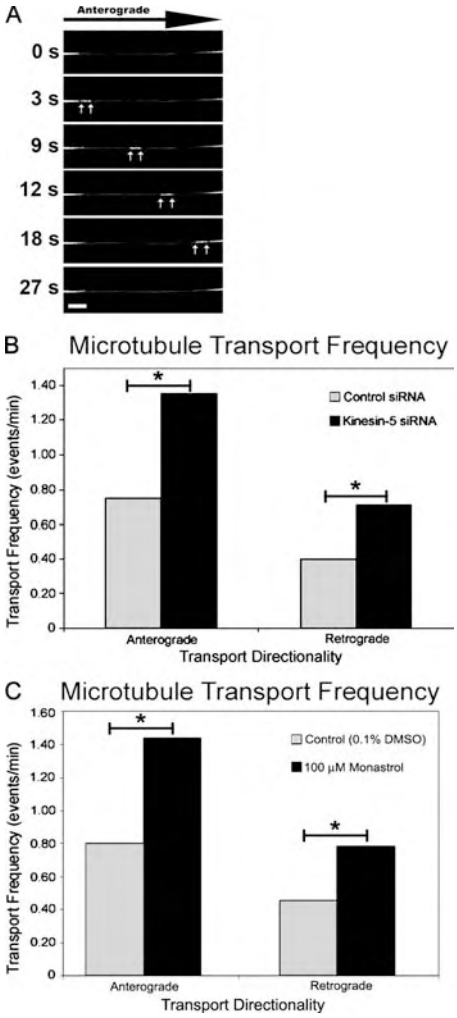

Figure 4. **Depletion of kinesin-5 enhances the transport frequency of short microtubules.** (A) Time-lapse images of a neuron expressing GFP-tubulin reveal a short microtubule moving in the anterograde direction through a photobleached axon. White arrows mark the leading and trailing ends of the microtubule. (B) Quantification of short microtubule transport frequency using siRNA-based depletion of kinesin-5 resulted in the increased frequency of bidirectional short microtubule transport (anterograde: control siRNA, 0.752 events/min; kinesin-5 siRNA, 1.35 events/min; retrograde: control siRNA, 0.400 events/min; kinesin-5 siRNA, 0.705 events/min; *, $P \leq 0.025$). (C) Inhibition of kinesin-5 with monastrol produced a result similar to siRNA-based depletion of kinesin-5, with an increase in bidirectional transport frequency to levels approximately twofold higher than observed in control neurons (anterograde: DMSO, 0.801 events/min; monastrol, 1.438 events/min; retrograde: DMSO, 0.458 events/min; monastrol, 0.788 events/min; *, $P < 0.01$). Bar, 5 μm.

were allowed to grow axons for 12–16 h before imaging. These times were used because they coincide with the depletion of kinesin-5 via siRNA (Fig. 1 A) and because this period of incubation is optimal for EGFP-tubulin expression in these cells. For control siRNA, the total number of movements was 121 over a period of 105 min of image acquisition, with 79 in the anterograde direction and 42 in the retrograde direction. For kinesin-5 siRNA, the total number of movements over 105 min of imaging was 216, representing the sum of 142 movements in the anterograde direction and 74 movements in the retrograde direction. With respect to transport directionality, these data represent a 179% increase over controls in anterograde movement frequency, and a 176% increase over controls in retrograde movement frequency, both statistically significant increases (anterograde, $P \leq 0.01$; retrograde, $P \leq 0.025$; χ^2; Fig. 4 B). Enhanced frequencies of short microtubule transport were also observed when monastrol was used to inhibit kinesin-5 activity, and these changes were comparable to the siRNA experiments (Fig. 4 C). For the monastrol studies, there was a 178% increase in anterograde transport frequency and a 172% increase in retrograde transport frequency (anterograde, $P < 0.001$; retrograde, $P < 0.001$; χ^2). These results suggest that kinesin-5 imposes limitations on the number of short microtubules that are in transit (in both directions) within the axon.

To investigate whether this effect on transport is specific to microtubules, we added fluorescently labeled markers of either vesicles or mitochondria and analyzed their movements under control- and kinesin-5–inhibited conditions. Using a rhodamine–dextran tracer to monitor pinocytosed vesicular transport (Fig. 5 A), we found that there was no statistical variation in axonal vesicle trafficking under conditions of kinesin-5 depletion in either the distance or direction that the moving vesicles were transported (anterograde, $P = 0.232$; retrograde, $P = 0.431$; two-tailed *t* test; Fig. 5 B). We next investigated the effects of kinesin-5 depletion on the axonal transport of mitochondria using the mitotracker label, which is a fluorescent label that is specific for mitochondria (Buckman et al., 2001). For these experiments we measured both the length of the mitochondria, as well as the distance moved during the imaging period. Stationary mitochondria were not analyzed, although there was no noticeable difference between the numbers of stationary mitochondria between control and kinesin-5–depleted neurons (unpublished data). Similar to our studies of vesicle transport, no statistical difference was found when mitochondrion lengths were compared between control and kinesin-5–depleted axons ($P = 0.08$, two-tailed *t* test). Analysis of mitochondrion transport distances revealed a similar, nonsignificant variation between control and kinesin-5–depleted specimens ($P = 0.677$, two-tailed *t* test; Fig. 5, C and D). These data are consistent with the effects of kinesin-5 on axonal transport being specific to the transport of microtubules.

Depletion of kinesin-5 accelerates axonal growth by decreasing stepwise retraction events

Live-cell movies were used to further investigate the effects of depleting kinesin-5 on axonal length. Phase-contrast images were acquired for 5 h at 3-min intervals beginning 2 h after the neurons were replated. Consistent with the still images (Figs. 1 and 2), the movies show that axons depleted of kinesin-5 grow more rapidly and undergo dramatic increases in branching as compared with controls (Fig. 6 A). The movies indicate that these effects are due, at least in part, to diminution in retraction events that normally accompany axonal development. Control neurons undergo relatively consistent bouts of growth and retraction, with the net result being axonal elongation. In contrast, kinesin-5–depleted neurons undergo substantially fewer bouts of retraction, resulting in enhanced stepwise growth. Analysis of the data indicates a significant change in the distribution of

Downloaded from www.jcb.org on September 10, 2007

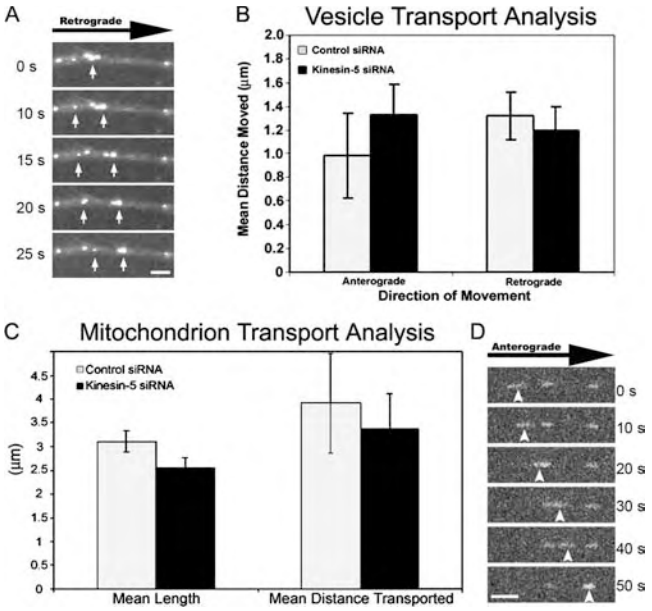

Figure 5. **Depletion of kinesin-5 motor does not affect axonal transport of membranous elements.** (A) Time-lapse images of rhodamine-dextran–labeled vesicles being transported retrogradely within the axon. White arrows demarcate two mobile vesicles observed during the period of imaging. (B) Quantification of vesicular transport direction and frequency revealed no difference between control and kinesin-5–depleted neurons (mean ± SEM; anterograde: control = 0.983 ± 0.357, kinesin-5 = 1.33 ± 0.262; retrograde: control = 1.32 ± 0.201, kinesin-5 = 1.19 ± 0.206) (control axons, $n = 14$; kinesin-5–depleted axons, $n = 14$). (C) Analysis of mitochondrion transport revealed that the depletion of kinesin-5 does not have an effect on mitochondrion length (mean length ± SEM; control = 3.10 ± 0.232 μm, kinesin-5 siRNA = 2.55 ± 0.206 μm) or distance of transport (mean ± SEM; control = 3.91 ± 1.05 μm, kinesin-5 siRNA = 3.37 ± 0.742 μm) (control siRNA, $n = 38$; kinesin-5 siRNA, $n = 39$). (D) Time-lapse images of a mitotracker FM–labeled mitochondrion being transported anterogradely within the axon. Arrowheads mark the moving mitochondrion. Bars, 5 μm.

growth steps and retraction steps between control neurons and neurons depleted of kinesin-5 (control, $n = 13$; kinesin-5 siRNA, $n = 13$; $P \leq 0.001$; χ^2) (Fig. 6, B and D). The effect on retraction was even more dramatic with regard to the stepwise movements of axonal branches, commonly resulting in branches that retracted entirely back into the primary axon (control, $n = 8$; kinesin-5 siRNA, $n = 13$; $P \leq 0.001$; χ^2; Fig. 6 C and Video 1, available at http://www.jcb.org/cgi/content/full/jcb.200702074/DC1). Of the 198 stepwise movements measured in control branches, 112 were growth oriented, whereas 68 were retractile, and the remaining 18 constituted time points when the axon did not grow or retract (neutral steps). In neuronal branches that had been depleted of kinesin-5, a total of 356 stepwise movements were recorded, the sum of 298 growth-oriented, 34 retractile, and 24 neutral steps (Fig. 6 E). Thus, it appears that depletion of kinesin-5 results in enhanced frequencies of axonal branching by causing the axon to retract branches less frequently, thus allowing greater numbers of branches to persist.

The effects of kinesin-5 overexpression are the inverse of kinesin-5 depletion

We wished to further test the specificity of our results by ascertaining whether an increase in kinesin-5 produces the inverse effect of depletion. To investigate this, neurons were transfected to express either GFP alone (control) or to express EGFP–kinesin-5, after which they were replated and allowed to grow axons for 7 h, as described for the siRNA experiments. For these experiments, we used mCherry-tubulin to visualize microtubule transport. Investigations of mean axonal length in GFP control neurons ($n = 20$) were analyzed at 3, 5, and 7 h after replating. Axons were found to be of similar lengths to controls from siRNA-based experiments from respective time points (mean ± SEM; GFP control, 3 h = 64.5 ± 10.2 μm, 5 h = 108 ± 16.1 μm, 7 h = 205 ± 21.3 μm). Consistent with the prediction of adding a large number of additional kinesin-5 molecules, the most highly expressing neurons displayed very short axons (typically <30 μm; Fig. 7 B). Comparison of axonal lengths of the low expressers ($n = 21$; Fig. 7 A) revealed a statistically significant decrease in mean axonal length when compared with GFP controls at all three observed time points (3 h, $P < 0.004$; 5 h, $P < 0.004$; 7 h, $P < 0.0005$; two-tailed t test; Fig. 7 C). When normalized to controls, these reductions represent a decrease of 252, 225, and 209% (at 3, 5, and 7 h, respectively) in the mean axonal lengths of neurons expressing EGFP–kinesin-5.

We next analyzed microtubule transport in the axons of the low expressers (Fig. 7 A). Analysis of GFP control neurons revealed frequencies of short microtubule transport that did not differ significantly from control siRNA–treated transport frequencies. For GFP control axons, the total number of movements was 93, with 60 in the anterograde direction and 33 in the retrograde direction over a period of 77 min of image acquisition. For EGFP–kinesin-5–expressing neurons, the total number of movements was 82, with 40 in the anterograde direction and 42 in the retrograde direction over 98 min of image acquisition. The decrease in transport was statistically significant, but only in the anterograde direction, where EGFP–kinesin-5 expression reduced transport by 190% (anterograde, $P \leq 0.01$; retrograde, $P \leq 1$; χ^2; Fig. 7 D). These results further demonstrate the capacity of kinesin-5 to restrict the number of microtubules in transit, but suggest that kinesin-5 may have a preference for restricting transport in the anterograde direction. There were no notable effects on microtubule bundling or organelle distribution associated with the overexpression of kinesin-5 at these levels (unpublished data).

Kinesin-5 elicits its effects in a force-dependent manner

It is noteworthy that monastrol-based inhibition of kinesin-5 produced indistinguishable results from siRNA-based depletion of kinesin-5 in all of our studies on axonal morphology (Fig. 8) and microtubule transport (Fig. 4). Monastrol functions as an allosteric inhibitor of the motor by preventing the release of ADP bound to kinesin-5 (Lockhart and Cross, 1996). The functional outcome of this allosteric inhibition is the locking of the kinesin-5 motor in a weak and diffusible microtubule-binding state, capable of eliciting a reduced and passive drag against microtubules in motility assays (Crevel et al., 2004). Thus, treatment with monastrol would eliminate the force-generating properties of kinesin-5 but would presumably not eliminate other properties of kinesin-5, such as its capacity to passively interact with

Downloaded from www.jcb.org on September 10, 2007

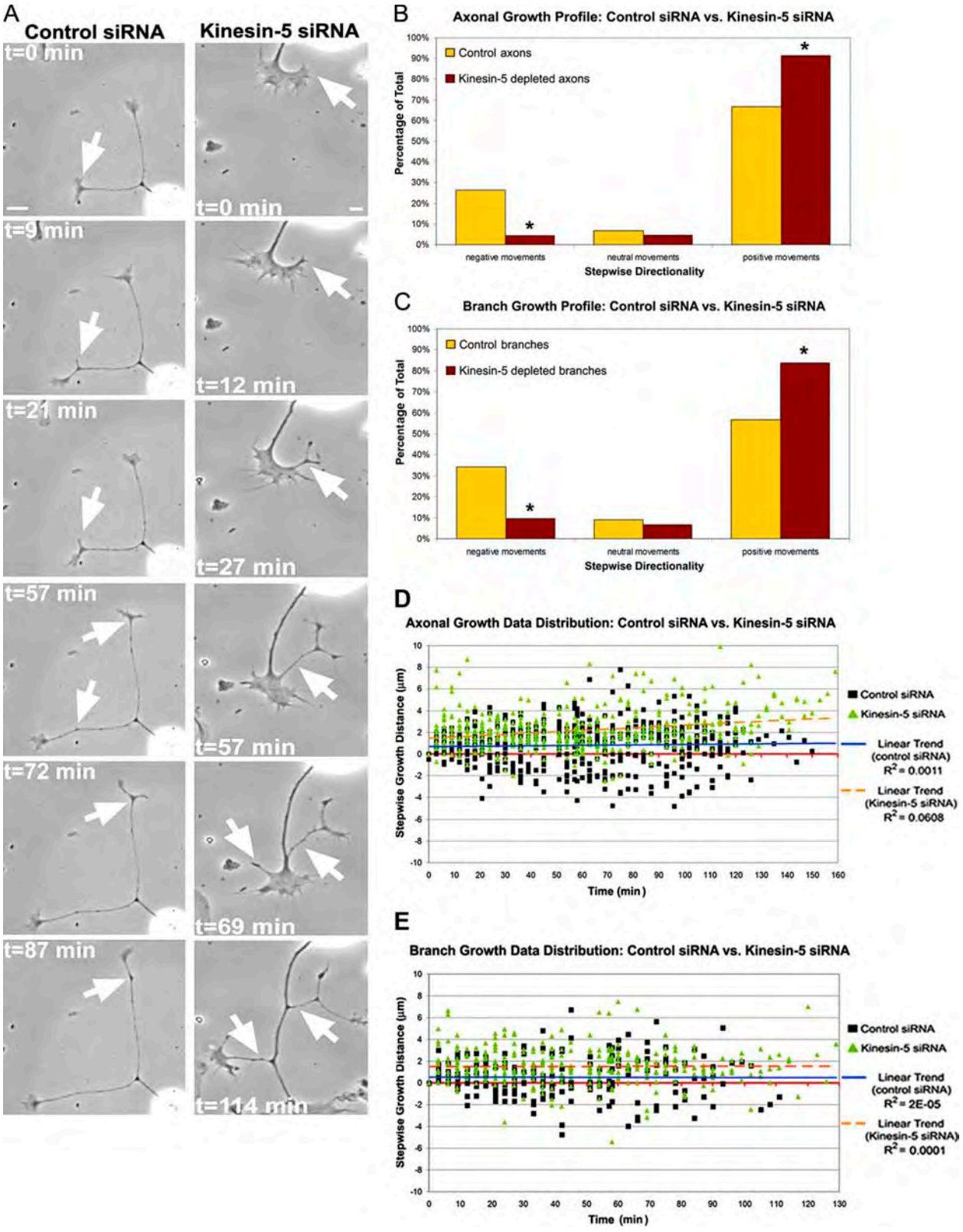

Figure 6. **Kinesin-5 depletion results in fewer bouts of retraction of axons and axonal branches.** (A) Time-lapse, phase-contrast images of a control (left) and a kinesin-5–depleted neuron (right). Notice that whereas control axons form early branches, the branches typically undergo retraction events (left, arrows). Kinesin-5–depleted branches display robust growth and are typically observed to elongate (right, arrows). (B) Quantitative comparison of axonal growth profiles revealed a significant shift toward stepwise bouts of growth in axons depleted of kinesin-5 (*, $P \leq 0.001$; χ^2). (C) Analysis of branching profiles revealed a similar and significant shift toward stepwise bouts of growth when kinesin-5 was depleted (*, $P \leq 0.001$; χ^2). (D and E) Data distribution graphs of the stepwise growth/retraction of control and kinesin-5–depleted axons (D) and branches (E). Bars, 20 μm.

Downloaded from www.jcb.org on September 10, 2007

neighboring microtubules and potentially displace other motors, preventing them from interacting with the microtubules. Therefore, it would appear that kinesin-5 must elicit forces in order for it to exert its regulatory effects on axonal growth. To further test this, we expressed in cultured neurons either a wild-type EGFP–kinesin-5 construct or an EGFP-labeled ATPase rigor mutant of kinesin-5 (T112N point mutant). Originally studied by Blangy et al. (1998), this mutation blocks ATP hydrolysis, locking the kinesin-5 motor in a strong microtubule-binding state that is able to promote microtubule–microtubule interactions, but is unable to generate forces against microtubules. In conducting these experiments, we decided to perform them on neurons that had been treated with either control or kinesin-5 siRNA. This experimental approach allowed us to test whether the observed effects on axonal growth require the force-generating properties of the motor and also provided an opportunity to conduct an additional control regarding the specificity of the results observed with siRNA-based depletion of kinesin-5. EGFP fluorescence intensity was used to ensure that we compared similarly expressing cells in each experimental group. There was some initial concern that the kinesin-5 siRNA that persisted in the cells might impede our capacity to express the EGFP–kinesin-5 at sufficiently high concentrations to elicit an effect, but this did not prove to be a problem. The results of these experiments are shown in Fig. 8.

Expression of the wild-type kinesin-5 in neurons treated with control siRNA confirmed our earlier overexpression data (Fig. 7 C), resulting in axonal lengths that were significantly shorter than neurons expressing endogenous levels of kinesin-5 (control siRNA alone, mean ± SEM = 187 ± 37.1 μm; control siRNA + wild-type kinesin-5, 121 ± 29.9 μm; $P < 0.008$, two-tailed *t* test). This effect was not observed in control siRNA–treated neurons expressing the rigor mutant. Rather, under these conditions, expression of the rigor mutant kinesin-5 produced mean axonal lengths nearly identical to control cells (control siRNA + rigor mutant, mean ± SEM = 171 ± 58.2 μm; control siRNA alone, 187 ± 37.1 μm; $P = 0.471$, two-tailed *t* test).

Rescue of kinesin-5–depleted neurons with the wild-type construct resulted in axonal lengths that were statistically similar to neurons treated with control siRNA alone after 7 h of growth (wild-type rescue, mean ± SEM = 257 ± 46.1 μm; control siRNA alone, 187 ± 37.1 μm; $P > 0.05$, two-tailed *t* test). When the rigor mutant was introduced into kinesin-5– depleted neurons, mean axonal lengths were observed to be statistically indistinguishable from those recorded in neurons treated with monastrol or kinesin-5 siRNA alone (rigor mutant rescue, mean ± SEM = 546 ± 86.5 μm, $n = 17$; monastrol, 722 ± 97.9 μm, $n = 17$; kinesin-5 siRNA alone, 774 ± 120 μm, $n = 21$; $P = 0.135$, two-tailed *t* test). Moreover, when compared with other experimental treatments, axonal lengths in the rigor mutant rescue group persisted at levels twice as long as the wild-type rescue group, and nearly three times longer than neurons treated with control siRNA alone (wild-type rescue, 257 ± 46.1 μm, $P < 0.02$; control siRNA alone, 187 ± 37.1 μm, $P < 0.001$, two-tailed *t* test; Fig. 8). These data indicate that the force-generating properties of kinesin-5 are central to its capacity to restrict axonal lengths.

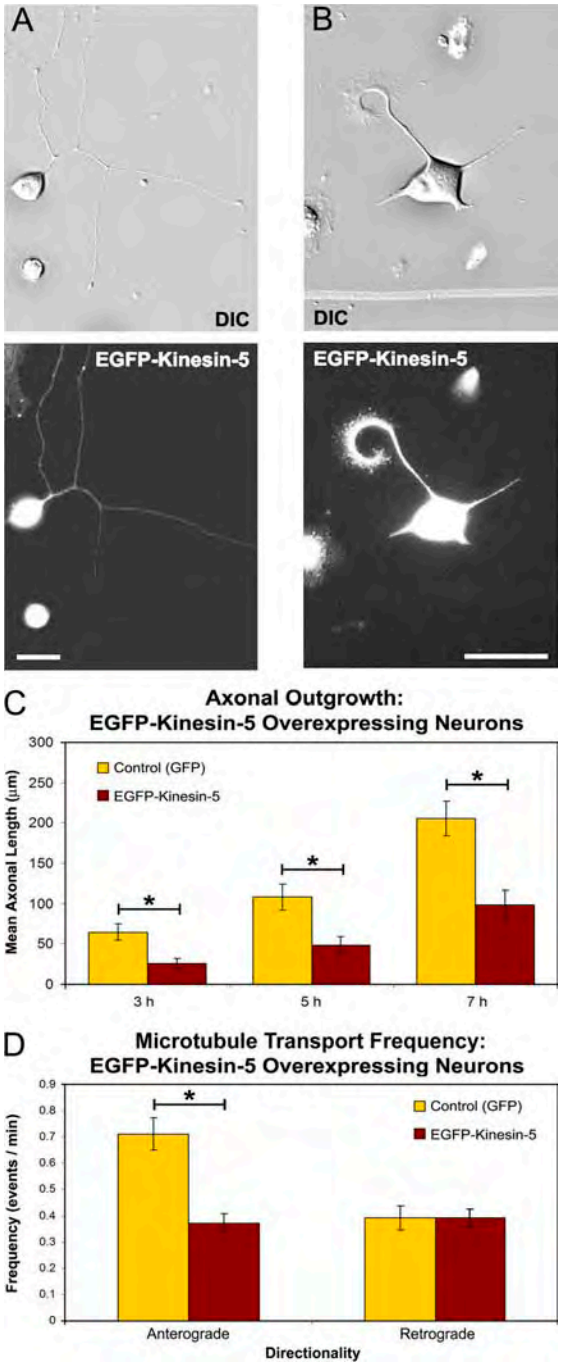

Figure 7. **Axonal growth and microtubule transport frequency are affected by kinesin-5 overexpression.** (A and B) DIC (top) and corresponding anti-GFP immunocytochemistry (bottom) in neurons transfected with a wild-type EGFP–kinesin-5 construct demonstrating that axon length is coordinated with the level of EGFP–kinesin-5 expression. (C) Quantitative analysis of mean axonal length revealed a statistically significant reduction in mean axonal length in neurons expressing EGFP–kinesin-5 when compared with GFP control axons (mean ± SEM; EGFP–kinesin-5: 3 h = 25.6 ± 6.38 μm, 5 h = 48.1 ± 10.7 μm, 7 h = 98.1 ± 18.2 μm; *, $P < 0.0005$). (D) Analysis of short microtubule transport frequency in EGFP–kinesin-5 expressers revealed a significant reduction in anterograde transport, but no change in retrograde transport frequency (mean ± SEM; anterograde: GFP control = 0.779 ± 0.041 events/min; EGFP–kinesin-5 = 0.408 ± 0.016 events/min; retrograde: GFP control = 0.429 ± 0.033 events/min; EGFP–kinesin-5 = 0.449 ± 0.017 events/min; *, $P \leq 0.01$). Bars, 30 μm.

Downloaded from www.jcb.org on September 10, 2007

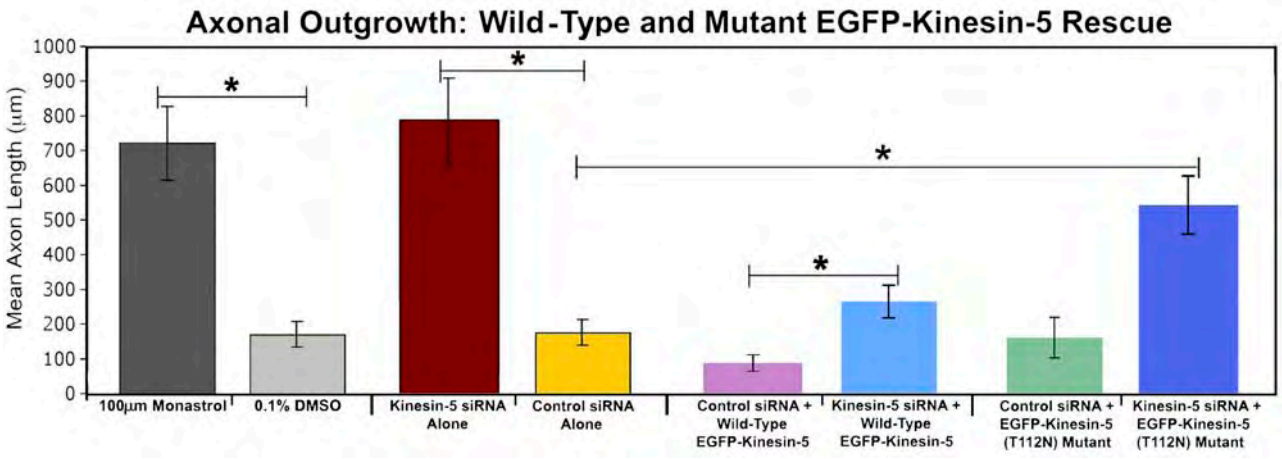

Figure 8. **Kinesin-5 elicits it effects in a force-dependent manner.** Inhibition of kinesin-5 by monastrol treatment or depletion of kinesin-5 by siRNA produces mean axonal lengths that are approximately four times greater than neurons treated with DMSO (control) or control siRNA. When a wild-type kinesin-5 construct is introduced into control siRNA–treated neurons, there is a corresponding diminution in mean axon length. Parallel experiments using a rigor mutant (T112N) kinesin-5 construct in control siRNA–treated neurons revealed that mean axonal lengths were indistinguishable from the control siRNA alone group. A similar effect was observed in kinesin-5–depleted neurons that were rescued by introduction of the wild-type EGFP–kinesin-5, with mean axonal lengths that were statistically similar to control siRNA neurons expressing endogenous levels of the motor protein (mean ± SEM, wild-type rescue = 257 ± 46.1 μm; control siRNA alone, 187 ± 37.1 μm; $P > 0.05$; two-tailed *t* test). Finally, in kinesin-5–depleted neurons that we attempted to rescue with the EGFP–kinesin-5 mutant, the mean length of axons were found to be nearly three times longer than the control siRNA–treated group, and more than twice the length of kinesin-5–depleted neurons rescued with wild-type kinesin-5 (mean ± SEM, rigor mutant rescue = 546 ± 86.5 μm; wild-type rescue, 257 ± 46.1 μm; $P < 0.002$; control siRNA alone, 187 ± 37.1 μm, $P < 0.001$; two-tailed *t* test). *, $P < 0.02$.

Discussion

We previously speculated that kinesin-5 might be the motor that transports microtubules retrogradely in the axon, based on the premise that axonal growth rates may be determined by the ratio of anterograde/retrograde microtubule transport (Haque et al., 2004; Baas et al., 2006). In this view, depleting kinesin-5 would cause axons to grow faster because of a marked increase in this ratio. However, the current results show something quite different, i.e., that the frequency of microtubule transport in both directions is markedly increased when kinesin-5 is depleted. These results indicate that kinesin-5 is not the motor that transports microtubules retrogradely. Instead, it appears that kinesin-5 restricts the transport of short microtubules by other motors. The results of the depletion studies (Fig. 4) suggest that there is no directional preference on this effect, as removing kinesin-5 results in marked increases in both directions. In this sense, it may not be the ratio of anterograde/retrograde transport that is most critical to axonal growth, but rather, the overall vitality of the transport. The overexpression studies (Fig. 7), however, raise the possibility of a directional preference, suggesting that kinesin-5 may be more suited to opposing microtubule transport in the anterograde direction. This possibility is consistent with other studies in which kinesin-5 was shown to antagonize minus end–directed motors such as cytoplasmic dynein and kinesin-14a (Gaglio et al., 1996; Walczak et al., 1998; Mountain et al., 1999; Tao et al., 2006). It may be that kinesin-5 restricts microtubule transport in both directions, but preferentially in the anterograde direction.

Additional observations suggest that the greater length of kinesin-5–depleted axons is not solely explicable (or even principally explicable) on the basis of the changes in microtubule transport. The axons depleted of kinesin-5 are also far less prone to retraction, and this appears to be a major factor in their capacity to achieve greater lengths. This phenomenon is particularly evident with regard to the greater number of branches displayed by axons depleted of kinesin-5, where the numbers of branches appear to be dependent on the propensity of newly formed branches to retract. This is important because the proclivity of the axon to retract is not regulated by short microtubules, but rather by the microtubules that are long enough to act as compression-bearing struts (He et al., 2002; Baas et al., 2006; Myers et al., 2006b). Thus, we would contend that kinesin-5's principal role in regulating axonal length may be to influence the balance of forces on the long microtubules, which is consistent with our overall view that the various motors that transport microtubules are not selective for short microtubules but rather impinge upon microtubules of all lengths (Baas et al., 2006).

How does kinesin-5 elicits these effects? In the mitotic spindle, kinesin-5 is known to act between microtubules of opposite polarity orientation (interpolar microtubules). Although kinesin-5 was originally believed to function mainly to assist in the separation of the half spindles, newer studies indicate that it can alternatively function to resist separation of the half spindles by other motor proteins (Kapitein et al., 2005; Tao et al., 2006; Saunders et al., 2007). In this newer role, kinesin-5 has recently been likened to a brake on the microtubules within the spindle because it acts as a rate-limiting factor on the ability of the microtubules to slide relative to one another. The analogy of kinesin-5 acting as a brake on microtubule sliding is also quite applicable to our observations on the axon. The difference is that the mitotic spindle consists of regions of uniform and nonuniform microtubule polarity orientation, whereas nearly all of the microtubules in the axon are thought to be of the same orientation (Baas, 1998;

Downloaded from www.jcb.org on September 10, 2007

Hasaka et al., 2004). Thus it remains unclear whether the mechanism underlying the kinesin-5 brake is the same in the axon as in the mitotic spindle or one that is quite different.

It is important to note that kinesin-5 can also generate forces between neighboring microtubules of the same orientation within the mitotic spindle (Kapoor et al., 2000). Indeed, some of the earliest studies indicating antagonism between kinesin-5 and minus-end directed motors were conducted on monoasters of uniform polarity orientation (Gaglio et al., 1996). More recent studies suggest a complexity of possibilities for how kinesin-5 is able to generate different kinds of forces between microtubules of the same or different polarity orientations (Kapetein et al., 2005; Saunders et al., 2007). One possibility is that the two ends of the homotetramer are not always in synchrony with regard to force generation, thus generating options for the manner by which forces impact the relevant microtubules. It appears that kinesin-5 is also quite different from other kinesins with regard to how it reacts to changes in load (Valentine et al, 2006), which would likely influence kinesin-5's force-dependent functions. Whatever the case, understanding the complexities of force generation by kinesin-5 may clarify how kinesin-5 is capable of opposing transport of microtubules in both directions within the axon.

In discussing its mechanism of action, it is also important to consider that not all of the properties of kinesin-5 are force dependent. Kinesin-5 has been observed to cross-link neighboring microtubules (Sharp et al., 1999a) and to do so in a passive manner that does not require ATP (Tao et al., 2006). In this sense, kinesin-5 could antagonize microtubule sliding simply by cross-linking adjacent microtubules or by displacing other motors from the microtubule lattice, even when kinesin-5 is not undergoing a power stroke. Our studies using the rigor mutant indicate that the force-dependent properties of kinesin-5 are required for it to elicit its effects on axonal growth. Even so, we are reluctant to completely dismiss the possibility that the force-independent properties of kinesin-5 might contribute to its functions in the axon. For example, the growth cones of kinesin-5–depleted axons are clearly broader than those of control axons (Fig. 6), suggesting that the microtubules within these growth cones may be less cross-linked in the absence of kinesin-5. Thus it may be that the dual properties of kinesin-5 are manifested differently in the growth cone and in the axonal shaft. In this regard, it will be prudent in the future to conduct studies with the rigor mutant specifically on growth cone behaviors.

Another open question is whether kinesin-5 opposes all other motors equally, or if kinesin-5 specifically or preferentially antagonizes minus end–directed motors in the neuron. We have not yet studied kinesin-14a in neurons, but we have conducted a great deal of work on cytoplasmic dynein. As noted in the Introduction, these studies have enabled us to propose a model whereby cytoplasmic dynein generates forces between the longer microtubules in the axon and the cortical actin meshwork. These dynein-driven forces antagonize the contractile forces imposed on the cortical actin array by myosin-II (Ahmad et al., 2000; Myers et al., 2006b). Our finding that kinesin-5 promotes axonal retraction is consistent with a scenario by which forces generated by kinesin-5 antagonize the forces generated by cytoplasmic dynein. Our tentative thinking is that the microtubules nearest the cortex interact with the cortical actin via cytoplasmic dynein, and that these same microtubules sometimes interact with adjacent microtubules via kinesin-5. When the kinesin-5 is engaged there is an increase in the load on the cytoplasmic dynein, thereby attenuating its ability to antagonize the contractility of the cortical actin.

Clearly, an important goal for the future will be to further test the various possibilities of exactly how kinesin-5 elicits such a profound role in restricting the growth of the axon. In addition to elucidating its mechanism of action, an even more important question may be to ascertain why it is that developing neurons express such a potent brake on the growth potential of their axons. Also, of course, the question remains as to how kinesin-5's functions are regulated within the axon. In particular, local regulation of kinesin-5 would enable the axon to increase or decrease the relevant forces to comply with the needs of the axon. For example, branch formation would benefit both from a local increase in short microtubule transport and from a diminished propensity of the branch to retract once long microtubules have been established in the branch. This kind of regulation could be accomplished by signaling pathways, given that the association of kinesin-5 with microtubules is regulated by phosphorylation (Blangy et al., 1995; Sawin and Mitchison, 1995). Finally, it will be important to ascertain whether our findings on kinesin-5 apply to adult axons as well as developing axons because the ability to enhance axonal growth so dramatically by inhibiting kinesin-5 could be a powerful tool for augmenting axonal regeneration after injury (Baas, 2002).

Materials and methods

Cell culture and transfection

Cultures of dissociated neurons from rat superior cervical ganglia were prepared as previously described (He et al., 2005). For experiments using siRNA, dissociated neurons were transfected with 10 μM (final concentration) of either control siRNA or kinesin-5 siRNA (*Silencer* KIF11 [Eg5] siRNA; Ambion). Once transfected, the neurons were cultured in L-15 medium on 35-mm plastic dishes that had been coated with 0.1 mg/ml poly-D-lysine (PDL) for 3 h and repeatedly rinsed in double-distilled H_2O. The following morning 5 μg/ml laminin and 5 μM arabinose C were added to the culture medium. For transport studies, the neurons were replated (He et al., 2005) at a density of ~7,500 cells/dish at 60 h after transfection onto grided glass coverslips that had been coated with 0.1 mg/ml PDL and 25 μg/ml laminin. Replating was performed 72 h after transfection. The EGFP-tubulin construct (CLONTECH Laboratories, Inc.) and the mCherry-tubulin construct (provided by R. Tsien, University of California, San Diego, La Jolla, CA) were transfected at 15 μg. Wild-type and mutant kinesin-5 constructs were provided by M. Kress (Institut André Lwoff, Centre National de la Recherche Scientifique, Villejuif, France) and A. Blangy (Centre de Recherches en Biochimie Macromoléculaire, Centre National de la Recherche Scientifique Unité Propre de Recherche, Montpellier, France), and then engineered in our laboratory as fusions with EGFP. The mutant construct, termed T112N, is described in detail by Blangy et al. (1998). For kinesin-5 overexpression studies, 12 μg of either GFP (control) or EGFP–kinesin-5 was cotransfected with mCherry-tubulin.

In one study, we wished to determine if expression of wild-type and/or the mutant kinesin-5 could "rescue" the phenotype obtained with siRNA-based depletion of kinesin-5. For these experiments, neurons were first transfected with siRNA. 48 h after transfection with siRNA, either the wild-type EGFP–kinesin-5 or the rigor mutant EGFP–kinesin-5 (T112N) was introduced using Lipofectamine 2000 (Invitrogen) as previously described (Yu et al., 2005), except that Lipofectamine treatments were performed for 4.5 h duration and were followed by rinsing and medium replacement with L-15 plating medium. Neurons were then replated 24–30 h after Lipofectamine

Downloaded from www.jcb.org on September 10, 2007

treatment and morphological analysis was performed as described below for siRNA experiments. Expression was observed in ~15–20% of neurons, and data analysis used neurons with expression levels greater than the mean expression value (determined by arbitrary fluorescence units) for that experimental group.

Immunological techniques and Western blotting
See the online supplemental Materials and methods.

Morphological studies
For all morphological investigations, neurons were cultured and replated after the 72-h replating regimen. For axonal length and branching experiments, neurons were identified at 1 h after replating (before they had established axons). The neurons were then imaged sequentially at 3, 5, and 7 h after replating. Axonal lengths were measured using the "measure/curve" application of Axiovision LE 4.5 (Carl Zeiss MicroImaging, Inc.), and mean values were quantified. Analysis of branching frequency was performed by counting the total number of branches per neuron and dividing these values by total axonal length for individual neurons. For both total branching and categorical branching analysis, we used normalization of branch number to total axonal length to ensure accurate evaluation of branching frequency.

Nitric oxide–induced axonal retraction
60 h after transfection with control or kinesin-5 siRNA, neurons were replated onto gridded PDL (0.1 mg/ml) and laminin-treated (25 μg/ml) glass-bottom culture dishes. By 72 h the neurons had generated extensive axons. The nitric oxide donor, noc-7 (Calbiochem), was prepared and applied as previously described (He et al., 2002), except that it was used at a working concentration of 0.3 mM. DIC images of axons were recorded before and 30 min after addition of noc-7. Axonal lengths (from growth cone to cell body or to the first bifurcation point) were measured using the "measure/curve" application in Axiovision LE 4.5. Raw data were processed and graphs were produced using Excel (Microsoft Corp.).

Transport assays
The microtubule transport assay was performed essentially as described previously (Hasaka et al., 2004), except that for experiments using pharmacological inhibition of kinesin-5 with monastrol, the neurons were plated directly onto glass coverslips in drug-containing medium and were imaged 24–36 h later. For siRNA-based studies, neurons transfected with either control siRNA or kinesin-5 siRNA were replated at 60 h as described in the previous paragraph. A total of 211 time-lapse images were taken at 700–900-ms exposure using 3-s intervals for each axon. Transport analysis included all microtubules observed to move continuously through the photobleached region during the imaging period. Transport frequencies were calculated by dividing the total number of movements by the total imaging time for individual movies.

Vesicle and mitochondrion transport assays
See the online supplemental Materials and methods.

Live-cell imaging and analysis of stepwise axonal growth/retraction
Neurons transfection with control or kinesin-5 siRNA (see Cell culture and transfection) were replated in L-15 medium (supplemented with FBS) onto PDL- and laminin (25 μg/ml)-coated glass coverslips. The L-15 medium was coated with 2 ml of mineral oil (Sigma-Aldrich) as a means to prevent medium evaporation and to maintain nutrient concentrations over time. Phase-contrast time-lapse images were acquired using either a 40 or 20× objective lens with 700-ms exposure time and 1 × 1 binning. Image acquisition was performed at 3-min intervals for 5 h using a heated stage apparatus to maintain the temperature at 37°C. Stepwise axon and branch growth were analyzed using the "Apps/Track Points" application of Metamorph software (Molecular Devices) by establishing a point of origin and then using automated tracking of axonal outgrowth. Data were exported from Metamorph to Excel and were analyzed for the relative change in distance to origin. A camera (Orca ER; Hamamatsu) was used. For additional details on statistical analysis and image processing, see online supplemental materials.

Online supplemental material
Video 1 shows that kinesin-5 depletion results in fewer bouts of retraction of axons and axonal branches. Online supplemental material is available at http://www.jcb.org/cgi/content/full/jcb.200702074/DC1.

We thank Gianluca Gallo and Jonathan Scholey for helpful discussions. We thank Anne Blangy and Michel Kress for providing kinesin-5 constructs and antibodies and Roger Y. Tsien for providing the mCherry-tubulin construct.

This work was supported by grants to P.W. Baas from the National Institutes of Health (NIH; R01NS28785), the Alzheimer's Association (IIRG-06-26604), the Department of the Army (GW060062), and the Craig H. Neilsen Foundation (2784). K.A. Myers was supported by a predoctoral National Research Service Award (SF3INS053022) from the NIH.

Submitted: 12 February 2007
Accepted: 9 August 2007

References

Ahmad, F.J., J. Hughey, T. Wittmann, A. Hyman, M. Greaser, and P.W. Baas. 2000. Motor proteins regulate force interactions between microtubules and microfilaments in the axon. *Nat. Cell Biol.* 2:276–280.

Ahmad, F.J., Y. He, K.A. Myers, T.P. Hasaka, F. Francis, M.M. Black, and P.W. Baas. 2006. Effects of dynactin disruption and dynein depletion on axonal microtubules. *Traffic*. 7:524–537.

Baas, P.W. 1998. The role of motor proteins in establishing the microtubule arrays of axons and dendrites. *J. Chem. Neuroanat.* 14:175–180.

Baas, P.W. 2002. Microtubule transport in the axon. *Int. Rev. Cytol.* 212:41–62.

Baas, P.W., C. Vidya Nadar, and K.A. Myers. 2006. Axonal transport of microtubules: the long and short of it. *Traffic*. 7:490–498.

Blangy, A., H.A. Lane, P. d'Herin, M. Harper, M. Kress, and E.A. Nigg. 1995. Phosphorylation by p34cdc2 regulates spindle association of human Eg5, a kinesin-related motor essential for bipolar spindle formation in vivo. *Cell*. 83:1159–1169.

Blangy, A., P. Chaussepied, and E.A. Nigg. 1998. Rigor-type mutation in the kinesin-related protein HsEg5 changes its subcellular localization and induces microtubule bundling. *Cell Motil. Cytoskeleton*. 40:174–182.

Buckman, J.F., H. Hernandez, G.J. Kress, T.V. Votyakova, S. Pal, and I.J. Reynolds. 2001. MitoTracker labeling in primary neuronal and astrocytic cultures: influence of mitochondrial membrane potential and oxidants. *J. Neurosci. Methods*. 104:165–176.

Buster, D.W., D.H. Baird, W. Yu, J.M. Solowska, M. Chauviere, A. Mazurek, M. Kress, and P.W. Baas. 2003. Expression of the mitotic kinesin Kif15 in postmitotic neurons: implications for neuronal migration and development. *J. Neurocytol.* 32:79–96.

Crevel, I.M., M.C. Alonso, and R.A. Cross. 2004. Monastrol stabilises an attached low-friction mode of Eg5. *Curr. Biol.* 14:R411–R412.

Dent, E.W., J.L. Callaway, G. Szebenyi, P.W. Baas, and K. Kalil. 1999. Reorganization and movement of microtubules in axonal growth cones and developing interstitial branches. *J. Neurosci.* 19:8894–8908.

Ernst, A.F., G. Gallo, P.C. Letourneau, and S.C. McLoon. 2000. Stabilization of growing retinal axons by the combined signaling of nitric oxide and brain-derived neurotrophic factor. *J. Neurosci.* 20:1458–1469.

Ferhat, L., R. Kuriyama, G.E. Lyons, B. Micales, and P.W. Baas. 1998. Expression of the mitotic motor protein CHO1/MKLP1 in postmitotic neurons. *Eur. J. Neurosci.* 10:1383–1393.

Gaglio, T., A. Saredi, J.B. Bingham, M.J. Hasbani, S.R. Gill, T.A. Schroer, and D.A. Compton. 1996. Opposing motor activities are required for the organization of the mammalian mitotic spindle pole. *J. Cell Biol.* 135:399–414.

Haque, S.A., T.P. Hasaka, A.D. Brooks, P.V. Lobanov, and P.W. Baas. 2004. Monastrol, a prototype anti-cancer drug that inhibits a mitotic kinesin, induces rapid bursts of axonal outgrowth from cultured postmitotic neurons. *Cell Motil. Cytoskeleton*. 58:10–16.

Hasaka, T.P., K.A. Myers, and P.W. Baas. 2004. Role of actin filaments in the axonal transport of microtubules. *J. Neurosci.* 24:11291–11301.

He, Y., W. Yu, and P.W. Baas. 2002. Microtubule reconfiguration during axonal retraction induced by nitric oxide. *J. Neurosci.* 22:5982–5991.

He, Y., F. Francis, K.A. Myers, W. Yu, M.M. Black, and P.W. Baas. 2005. Role of cytoplasmic dynein in the axonal transport of microtubules and neurofilaments. *J. Cell Biol.* 168:697–703.

Kapitein, L.C., E.J. Peterman, B.H. Kwok, J.H. Kim, T.M. Kapoor, and C.F. Schmidt. 2005. The bipolar mitotic kinesin Eg5 moves on both microtubules that it crosslinks. *Nature*. 435:114–118.

Kapoor, T.M., T.U. Mayer, M.L. Coughlin, and T.J. Mitchison. 2000. Probing spindle assembly mechanisms with monastrol, a small molecule inhibitor of the mitotic kinesin, Eg5. *J. Cell Biol.* 150:975–988.

Kashina, A.S., R.J. Baskin, D.G. Cole, K.P. Wedaman, W.M. Saxton, and J.M. Scholey. 1996. A bipolar kinesin. *Nature*. 379:270–272.

Kwok, B.H., L.C. Kapitein, J.H. Kim, E.J. Peterman, C.F. Schmidt, and T.M. Kapoor. 2006. Allosteric inhibition of kinesin-5 modulates its processive directional motility. *Nat Chem Biol*. 2:480–485.

Downloaded from www.jcb.org on September 10, 2007

Lockhart, A., and R.A. Cross. 1996. Kinetics and motility of the Eg5 microtubule motor. *Biochemistry*. 35:2365–2373.

Ma, Y., D. Shakiryanova, I. Vardya, and S.V. Popov. 2004. Quantitative analysis of microtubule transport in growing nerve processes. *Curr. Biol.* 14:725–730.

Maliga, Z., and T.J. Mitchison. 2006. Small-molecule and mutational analysis of allosteric Eg5 inhibition by monastrol. *BMC Chem. Biol.* 6:2.

Maliga, Z., T.M. Kapoor, and T.J. Mitchison. 2002. Evidence that monastrol is an allosteric inhibitor of the mitotic kinesin Eg5. *Chem. Biol.* 9:989–996.

Mountain, V., C. Simerly, L. Howard, A. Ando, G. Schatten, and D.A. Compton. 1999. The kinesin-related protein, HSET, opposes the activity of Eg5 and cross-links microtubules in the mammalian mitotic spindle. *J. Cell Biol.* 147:351–366.

Myers, K.A., Y. He, T.P. Hasaka, and P.W. Baas. 2006a. Microtubule transport in the axon: re-thinking a potential role for the actin cytoskeleton. *Neuroscientist*. 12:107–118.

Myers, K.A., I. Tint, C.V. Nadar, Y. He, M.M. Black, and P.W. Baas. 2006b. Antagonistic forces generated by cytoplasmic dynein and myosin-II during growth cone turning and axonal retraction. *Traffic*. 7:1333–1351.

Pfister, K.K. 1999. Cytoplasmic dynein and microtubule transport in the axon: the action connection. *Mol. Neurobiol.* 20:81–91.

Saunders, A.M., J. Powers, S. Strome, and W.M. Saxton. 2007. Kinesin-5 acts as a brake in anaphase spindle elongation. *Curr. Biol.* 17:R453–R454.

Sawin, K.E., and T.J. Mitchison. 1995. Mutations in the kinesin-like protein Eg5 disrupting localization to the mitotic spindle. *Proc. Natl. Acad. Sci. USA*. 92:4289–4293.

Sharp, D.J., R. Kuriyama, R. Essner, and P.W. Baas. 1997. Expression of a minus-end-directed motor protein induces Sf9 cells to form axon-like processes with uniform microtubule polarity orientation. *J. Cell Sci.* 110:2373–2380.

Sharp, D.J., K.L. McDonald, H.M. Brown, H.J. Matthies, C. Walczak, R.D. Vale, T.J. Mitchison, and J.M. Scholey. 1999a. The bipolar kinesin, KLP61F, cross-links microtubules within interpolar microtubule bundles of *Drosophila* embryonic mitotic spindles. *J. Cell Biol.* 144:125–138.

Sharp, D.J., K.R. Yu, J.C. Sisson, W. Sullivan, and J.M. Scholey. 1999b. Antagonistic microtubule-sliding motors position mitotic centrosomes in *Drosophila* early embryos. *Nat. Cell Biol.* 1:51–54.

Tao, L., A. Mogilner, G. Civelekoglu-Scholey, R. Wollman, J. Evans, H. Stahlberg, and J.M. Scholey. 2006. A homotetrameric kinesin-5, KLP61F, bundles microtubules and antagonizes Ncd in motility assays. *Curr. Biol.* 16:2293–2302.

Walczak, C.E., I. Vernos, T.J. Mitchison, E. Karsenti, and R. Heald. 1998. A model for the proposed roles of different microtubule-based motor proteins in establishing spindle bipolarity. *Curr. Biol.* 8:903–913.

Wang, L., and A. Brown. 2002. Rapid movement of microtubules in axons. *Curr. Biol.* 12:1496–1501.

Weil, D., L. Garcon, M. Harper, D. Dumenil, F. Dautry, and M. Kress. 2002. Targeting the kinesin Eg5 to monitor siRNA transfection in mammalian cells. *Biotechniques*. 33:1244–1248.

Yoon, S.Y., J.E. Choi, J.W. Huh, O. Hwang, H.S. Lee, H.N. Hong, and D. Kim. 2005. Monastrol, a selective inhibitor of the mitotic kinesin Eg5, induces a distinctive growth profile of dendrites and axons in primary cortical neuron cultures. *Cell Motil. Cytoskeleton*. 60:181–190.

Yu, W., and P.W. Baas. 1994. Changes in microtubule number and length during axon differentiation. *J. Neurosci.* 14:2818–2829.

Yu, W., J.M. Solowska, L. Qiang, A. Karabay, D. Baird, and P.W. Baas. 2005. Regulation of microtubule severing by katanin subunits during neuronal development. *J. Neurosci.* 25:5573–5583.

Downloaded from www.jcb.org on September 10, 2007

Neurobiology of Disease

Quantitative and Functional Analyses of Spastin in the Nervous System: Implications for Hereditary Spastic Paraplegia

Joanna M. Solowska,[1] Gerardo Morfini,[2] Aditi Falnikar,[1] B. Timothy Himes,[1,3] Scott T. Brady,[2] Dongyang Huang,[2] and Peter W. Baas[1]

[1]Department of Neurobiology and Anatomy, Drexel University College of Medicine, Philadelphia, Pennsylvania 19129, [2]Department of Anatomy and Cell Biology, University of Illinois at Chicago, Chicago, Illinois 60612, and [3]Department of Veterans Affairs Medical Center, Philadelphia, Pennsylvania 19104

Spastin and P60-katanin are two distinct microtubule-severing proteins. Autosomal dominant mutations in the SPG4 locus corresponding to spastin are the most common cause of hereditary spastic paraplegia (HSP), a neurodegenerative disease that afflicts the adult corticospinal tracts. Here we sought to evaluate whether SPG4-based HSP is best understood as a "loss-of-function" disease. Using various rat tissues, we found that P60-katanin levels are much higher than spastin levels during development. In the adult, P60-katanin levels plunge dramatically but spastin levels decline only slightly. Quantitative data of spastin expression in specific regions of the nervous system failed to reveal any obvious explanation for the selective sensitivity of adult corticospinal tracts to loss of spastin activity. An alternative explanation relates to the fact that the mammalian spastin gene has two start codons, resulting in a 616 amino acid protein called M1 and a slightly shorter protein called M85. We found that M1 is almost absent from developing neurons and most adult neurons but comprises 20–25% of the spastin in the adult spinal cord, the location of the axons that degenerate during HSP. Experimental expression in cultured neurons of a short dysfunctional M1 polypeptide (but not a short dysfunctional M85 peptide) is deleterious to normal axonal growth. In squid axoplasm, the M1 peptide dramatically inhibits fast axonal transport, whereas the M85 peptide does not. These results are consistent with a "gain-of-function" mechanism underlying HSP wherein spastin mutations produce a cytotoxic protein in the case of M1 but not M85.

Key words: **microtubule; neuron; axon; spastin; katanin; hereditary spastic paraplegia**

Introduction

Hereditary spastic paraplegia (HSP) is a late-onset debilitating disease of the CNS that specifically afflicts the corticospinal tracts in the adult spinal cord. Mutations in SPG4, the gene that encodes for a protein called spastin, are the most common cause of HSP (Hazan et al., 1999; Salinas et al., 2007). Spastin is one of two well studied AAA ATPases expressed in vertebrate cells that sever microtubules (Errico et al., 2002). The other is called P60-katanin (McNally and Vale, 1993; Karabay et al., 2004; Yu et al., 2005). The severing of microtubules by these enzymes is functionally important for the axon. Within the axon, long microtubules are not highly mobile (Ma et al., 2004; Ahmad et al., 2006) and must be severed into shorter pieces before undergoing rapid transport (Wang and Brown, 2002; Baas and Qiang, 2005; Baas et al., 2005). Spatial control of microtubule severing is important for mobilizing large numbers of microtubules at growth-related locales such as the centrosome (Ahmad et al., 1999), sites of branch formation (Yu et al., 1994), and growth cones (Dent et al., 1999). In the adult, severing of microtubules need not be as robust as during development but is still required to ensure that a portion of the microtubule array remains mobile (Yu et al., 2007).

Most disease-related mutations of spastin render the protein dysfunctional and hence reduce the degree to which microtubules can be severed. In theory, this could lead to flaws in cytoskeletal organization and microtubule-based transport. At present, haploinsufficiency is the favored mechanism for the degeneration of axons in HSP, but there are several questions that cannot be easily answered by this mechanism (Zhao et al., 2001; Schickel et al., 2007). For example, there are no detectable flaws in neuronal development associated with the spastin mutations, despite the greater need for microtubule severing during development (Fink and Rainier, 2004). One possibility is that longer axons are more at risk than shorter axons, but this does not explain why peripheral neurons with long axons are unaffected. Another possibility is that the selective vulnerability of certain axons is related to the absolute

Received July 11, 2007; revised Dec. 19, 2007; accepted Jan. 8, 2008.

This work was supported by grants from the National Institutes of Health (NIH), the Spastic Paraplegia Foundation, the Alzheimer's Association, the Department of Defense, and the Craig H. Nielsen Foundation (P.W.B.), from the Amyloid Lateral Sclerosis Association and Huntington's Disease Society of America (G.M.), and from the NIH and Muscular Dystrophy Association (S.T.B.). We thank Elena Rugarli for providing us with human spastin constructs that were used for preliminary studies. We thank Wenqian Yu, Liang Qiang, Jed Shumsky, Douglas Baird, Bin Wang, Yuka Atagi, Katie Liu, Sarah Pollema, and Gustavo Pigino for advice, support, and technical assistance.

Correspondence should be addressed to either of the following: Peter W. Baas, Department of Neurobiology and Anatomy, Drexel University College of Medicine, 2900 Queen Lane, Philadelphia, PA 19129, E-mail: pbaas@drexelmed.edu; or Gerardo Morfini, Department of Anatomy and Cell Biology, University Of Illinois at Chicago, MC512, 808 South Wood Street, Room 578, Chicago, IL 60612, E-mail: gmorfini@uic.edu.

DOI:10.1523/JNEUROSCI.3159-07.2008

Copyright © 2008 Society for Neuroscience 0270-6474/08/282147-11$15.00/0

levels of P60-katanin and spastin, given that these two proteins have overlapping properties.

Here, we quantitatively analyzed the absolute levels of each of the two microtubule-severing proteins in various regions of the rat nervous system during development and in the adult. These studies provided an unprecedented opportunity to assess the merits of a "loss-of-function" scenario for HSP. During the course of these studies, we discovered that the adult spinal cord contains significant levels of an isoform of spastin (termed M1), which is not readily detectable in any other nervous tissue at any other stage of life. On this basis, we conducted studies to determine whether pathogenic spastin peptides containing the sequence unique to M1 may have deleterious effects on the health of the axon. The results of these studies challenge the idea that HSP is best understood as a loss-of-function disease.

Materials and Methods

Preparation of spastin constructs and antibody. Mouse cDNA encoding full-length spastin was purchased from Invitrogen (Carlsbad, CA). Spastin constructs were generated by cloning mouse cDNA encoding spastin M1 (amino acids 2–614) and M85 (amino acids 86–614) into mammalian expression vector pCMV-Tag (Stratagene, La Jolla, CA) downstream from and in frame with the myc-tag. The vector provides a perfect Kozak consensus sequence and the first methionine encoding triplet: GCC GCCatgG for both M1 and M85 constructs. The M1 construct does not have 5′ untranslated region. ΔMIT was generated as a construct starting at amino acid 192 so as to delete a domain called MIT, which is the "microtubule interacting and endosomal trafficking" domain (Claudiani et al., 2005; Roll-Mecak and Vale, 2005). To generate truncated M1 and M85 constructs for functional studies in squid axoplasm, plasmids were digested with *Nco*I restriction enzyme before *in vitro* transcription/translation. The constructs for functional studies in neuronal cells were prepared by cloning cDNA encoding the first 280 amino acids of M1 or the first 195 amino acids of M85 spastin into pEGFP-C vector (Clontech, Palo Alto, CA). These expressed proteins were termed M85-STOP and M1-STOP. To prepare a polyclonal antibody against spastin, a fragment of spastin cDNA encoding amino acids 337–465 was cloned into the bacterial expression vector pRSET (Invitrogen). A peptide termed SP/AAA was purified, and a rabbit antiserum Sp/AAA was prepared by Cocalico Biologicals (Reamstown, PA). IgG fraction was purified by protein A-Sepharose chromatography. The specificity of the antibody was tested using mock-transfected cells, cells transfected with M1 or M85 spastin as positive controls, and cells transfected with P60-katanin as a negative control.

Quantitative Western blotting. For quantitative Western blotting, we calibrated the Sp/AAA antibody as described previously (Yu et al., 2005). We also used the polyclonal P60-katanin antibody that we previously generated, described, and calibrated (Karabay et al., 2004; Yu et al., 2005). To obtain standard curves, SDS-PAGE was performed using 10–60 fmol of purified M85 spastin or 20–200 fmol of purified, full-length P60-katanin. After electrophoresis, proteins were transferred to nitrocellulose and immunoblotted with the anti-P60-katanin or the anti-spastin antibody (diluted 1:20,000). Optical density (OD) was measured for each protein band corresponding to different concentrations of spastin or P60-katanin, and standard curves were drawn. Rat neuronal tissues and non-neuronal tissues were isolated at different stages of development [embryonic day 18 (E18), postnatal day 0 (P0), P6, P12, and adult] and homogenized in Laemli's sample buffer using 1 ml of buffer/100 mg of tissue (Yu et al., 2005). Protein extracts obtained from 1000 μg of tissue from different developmental stages were used. One half of the extract was used for Western blotting with anti-spastin antibody, and the other half was used simultaneously for Western blotting with anti-P60-katanin antibody. After reaction with chemiluminescent peroxidase substrate (Super Signal; Pierce, New York, NY), each blot was covered with x-ray film. For OD readings, we used different exposure times from 5 s to 4 min. P60-katanin or spastin concentrations were read from standard curves drawn for each blot on which all sample proteins and standard proteins were visualized under identical conditions. Films were imaged using an Epson Perfection 1240U scanner. The optical densities were measured for bands corresponding to spastin and P60-katanin using a Macintosh computer (Apple Computers, Cupertino, CA) running NIH Image. Lysates of the RFL-6 cells (a rat lung fibroblast cell line) transfected with M1 and M85 recombinant myc-tagged spastin isoforms were used to indicate the molecular weight (MW) of spastins expressed *in vivo*. Myc-tag is 11 amino acids long, and there are three more amino acids added to spastin as a result of cloning. Altogether, this adds ~1.7 kDa to the recombinant spastins MW, and therefore the control recombinant M1 and M85 spastins migrate slightly above endogenous spastins.

Analysis of hypothetical loss of microtubule-severing activity attributable to spastin mutation. After having obtained values for the absolute levels of P60-katanin and spastin, we considered various possibilities for the loss of total microtubule-severing activity attributable to spastin mutations. It is unknown whether or not P60-katanin and spastin have equal severing activities within the axon, so these calculations enabled us to further evaluate the merits of a loss-of-function scenario for HSP. The absolute levels of P60-katanin and spastin expression in femtomoles were used to calculate the overall loss of microtubule-severing activity resulting from 50% reduction of spastin activity caused by mutations. For these analyses, we reasoned that, if the microtubule-severing activity of P60-katanin *in vivo* equals that of M85-spastin, then 1 fmol of each protein represents one arbitrary microtubule-severing activity unit (AMSU) and therefore the total microtubule-severing activity equals expression of P60-katanin in femtomoles plus expression of spastin in femtomoles. However, if P60-katanin is twice as active as spastin, then 1 fmol of P60-katanin would represent 2 AMSUs, and the total microtubule-severing activity equals two times expression of P60-katanin in femtomoles plus expression of spastin in femtomoles. In a situation in which M85-spastin is twice as active as P60-katanin, 1 fmol of spastin would represent 2 AMSUs, and the total microtubule-severing activity equals expression of P60-katanin in femtomoles plus two times expression of spastin in femtomoles. Calculations were performed for spinal cord and hippocampus in the adult and at various developmental stages using the hypothetical ratios of P60-katanin/spastin activity 2:1, 1:1, 1:2, 1:4, and 1:10. The total microtubule-severing activity in spastin mutants equals the microtubule-severing activity calculated for P60-katanin plus one-half of the microtubule-severing activity calculated for spastin using different hypothetical ratios of P60-katanin/spastin activity. The overall loss of microtubule-severing activity was calculated by subtracting the percentage of activity left in mutant from 100% activity represented by wild-type tissue at a given developmental stage.

Preparation, transfection, and immunolabeling of cell cultures. Cultures of RFL-6 rat fibroblasts were prepared and transfected with spastin constructs using lipofectamine 2000 (catalog #11668-027; Invitrogen) as described previously (Buster et al., 2003). Primary rat cortical neurons were cultured and transfected (with the Amaxa nucleofector; Amaxa Biosystems, Gaithersburg, MD) using the identical approach to that which we used previously for cultured rat hippocampal neurons (Yu et al., 2005). For immunofluorescence studies, cells were fixed with 0.2% glutaraldehyde and 4% paraformaldehyde and then postextracted with 0.1% Triton X-100. In the case of the RFL-6 fibroblasts, the cultures were then double labeled by exposure first to anti-spastin Sp/AAA polyclonal antibody (1:10,000), overnight at 4°C, and then to Alexa Fluor 488-conjugated goat anti-rabbit (catalog #A11008; Invitrogen) and Cy3-conjugated β-tubulin mouse monoclonal antibody for 1 h (at 1:500). Images were obtained on an Axiovert 200 microscope (Zeiss, Oberkochen, Germany) equipped with a high-resolution CCD (Orca ER; Hamamatsu, Hamamatsu City, Japan). Mean gray values (the sum of gray values of all the pixels in a selected cell divided by the number of pixels) were obtained using AxioVision software and presented as arbitrary fluorescence units (AFU). Cells with approximately equal levels of expressed protein were selected, and quantification was performed on the entire cell. In the case of the cortical neurons, the cells were transfected with the truncated green fluorescent protein (GFP)–spastin constructs or GFP control and then double-labeled for GFP and actin, as described previously (Yu et al., 2005). Double-label overlay images were obtained with a Zeiss Pascal LSM 5 confocal microscope (with the pin-

hole wide open). For each experimental condition, neurons were scored according to the stage of development, and the length of the axon for neurons that had entered stage 3 of development was measured using Pascal LSM 5 software (Yu et al., 2005; Qiang et al., 2006). Statistics were done using Mann–Whitney *U* test or χ^2 test.

In vitro *translation.* For studies on vesicle motility in squid axoplasm, spastin polypeptides were produced by *in vitro* transcription/translation (TnT T7 coupled Reticulocyte Lysate system; Promega, Madison, WI), as described previously (Szebenyi et al., 2003; Morfini et al., 2006). Typically, 1–2 μg of plasmids were transcribed in a 50 μl reaction mix, following the procedures of the manufacturer. *In vitro* translation products were briefly centrifuged to eliminate translation machinery, and supernatants were frozen in liquid N_2 until use. Spastin polypeptides were typically perfused at 1–10 nM levels. To ensure that the same levels of spastin peptides were perfused for each experimental condition, parallel reactions were performed using ^{35}S-labeled methionine (GE Healthcare, Little Chalfont, UK), and relative levels were quantified using phosphoimaging scanning methods (Morfini et al., 2006).

Vesicle motility assays in isolated squid axoplasm. Axoplasm was extruded from giant axons of the squid *Loligo pealeii* (Marine Biological Laboratory, Woburn, MA) as described previously (Szebenyi et al., 2003; Morfini et al., 2006, 2007b). Axons were 400–600 μm in diameter and provided ≈5 μl of axoplasm. Recombinant *in vitro* translated spastin peptides were diluted into X/2 buffer (in mM: 175 potassium aspartate, 65 taurine, 35 betaine, 25 glycine, 10 HEPES, 6.5 $MgCl_2$, 5 EGTA, 1.5 $CaCl_2$, and 0.5 glucose, pH 7.2) supplemented with 2–5 mM ATP. Twenty microliters of this mixture was added to perfusion chambers (Brady et al., 1993). Preparations were analyzed on a Zeiss Axiomat with a 100×, 1.3 numerical aperture objective and differential interference contrast optics. Hamamatsu Argus 20 and model 2400 CCDs were used for image processing and analysis. Organelle velocities were measured with a Photonics Microscopy C2117 video manipulator (Hamamatsu). All experiments were repeated at least three times. Unless otherwise stated, the data were analyzed by ANOVA, followed by *post hoc* Student–Newman–Keuls test to make all possible comparisons.

Results

The functions of spastin were completely unknown until sequence homology with P60-katanin suggested that spastin might also be a microtubule-severing protein (Errico et al., 2002). The microtubule-severing properties of spastin have now been confirmed experimentally by overexpression of spastin in cells, as well as by application of recombinant spastin protein to purified microtubules and extracted cells (Errico et al., 2002; Evans et al., 2005; Roll-Mecak and Vale, 2005). However, it is unclear whether alterations in this activity are the principle cause of degeneration of a specific population of axons in the adult spinal cord during HSP. In addition, little is still known about the molecular forms of spastin expressed in different tissues or the relative contribution of spastin and P60-katanin to microtubule function in different neuronal populations.

The vertebrate spastin gene has two start codons that produce a long form and a shorter protein lacking the first 84 amino acids of the full-length protein (Claudiani et al., 2005). We refer to the full-length 68 kDa spastin protein as M1 and the shorter 60 kDa protein as M85 (Fig. 1*A*). We generated DNA constructs for mouse M1 and M85, both driven by strong promoters for use in our experimental studies. In addition, we made a construct starting at amino acid 192 so as to delete a domain called MIT, which is the "microtubule interacting and endosomal trafficking" domain (Claudiani et al., 2005; Roll-Mecak and Vale, 2005). We refer to this last construct as ΔMIT. We also generated constructs that produce truncated, HSP-related versions of M85 and M1 (see below).

To date, there have been no functional studies comparing the microtubule-severing properties of M1 and M85, nor have there been any quantitative studies on the levels of M1 and M85 in different regions of the nervous system at different stages of life. We previously performed quantitative analyses on the absolute levels of P60-katanin in adult and developing rat tissues (Yu et al., 2005). One of the stumbling blocks to performing analogous studies on spastin has been the lack of high-quality antibodies that can be used on rodent tissues. We have now developed a polyclonal antibody against amino acids 337–465 of mouse spastin (Fig. 1*A*). This antibody, which we call Sp/AAA, proved to be highly specific for spastin in our Western blot analyses. The antibody detected M1, M85, and ΔMIT spastin in lysates from RFL-6 cells transfected with corresponding spastin constructs (used as positive controls) but did not detect any band corre-

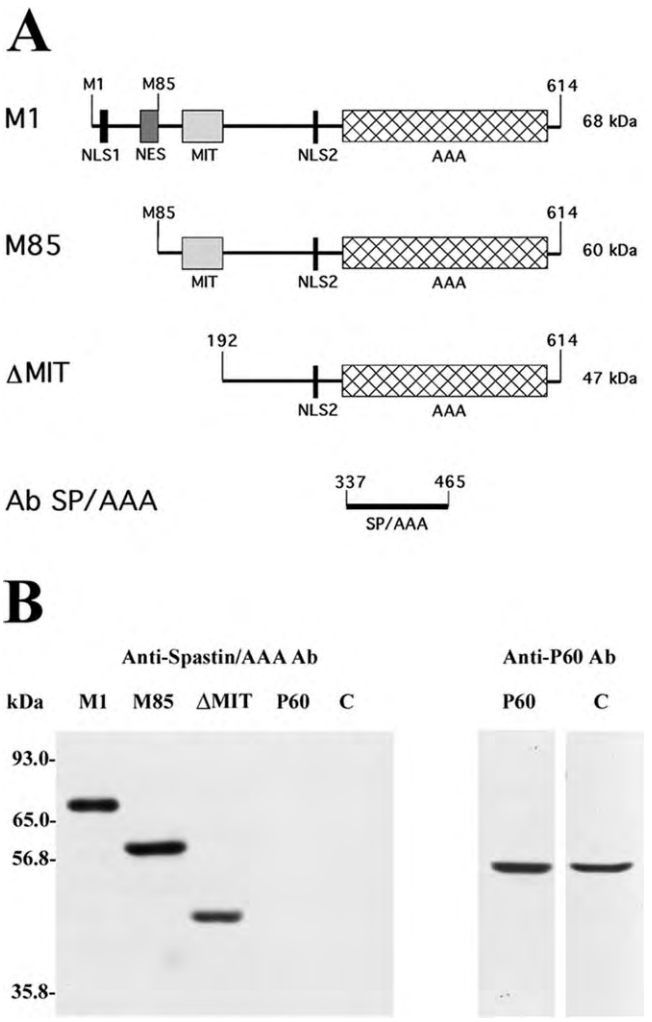

Figure 1. Mouse spastin constructs and antibody. ***A***, Schematic diagram of full-length mouse spastin M1 derived from translation starting at methionine 1, M85 spastin derived from translation starting at methionine 85, and ΔMIT, which corresponds to our construct that lacks the MIT domain. NLS1 and NLS2, Nuclear localization signals; NES, nuclear export signal; MIT, microtubule-interacting and trafficking domain; AAA, AAA domain; Ab Sp/AAA, anti-spastin antibody was prepared against amino acids 337–465. ***B***, Detection of spastin with anti-spastin antibody Sp/AAA. M1 (68 kDa), M85 (60 kDa), or ΔMIT (47 kDa) proteins were specifically detected in lysates from RFL-6 cells transfected with M1, M85, or ΔMIT spastin constructs. Sp/AAA antibody does not cross-react with P60-katanin in a lysate from P60-katanin (P60) transfected cells. Endogenous spastin was not detected in control RFL-6 cells using Sp/AAA antibody when concentration of total protein was comparable with that from transfected cells. When higher amounts of lysates were used, a 60 kDa band corresponding to endogenous M85 spastin was detected (data not shown). P60-katanin was readily detected in both P60-katanin transfected (P60) and control RFL-6 cells with anti-P60-katanin antibody. C, Control lane.

sponding to P60-katanin in lysates obtained from RFL-6 cells transfected with our P60-katanin construct (P60), used as a negative control (Fig. 1*B*). Interestingly, endogenous spastin expression in mock-transfected RFL-6 cells (Fig. 1*B*, lane C), a non-neuronal cell line, is very low; detection of spastin in these cells required larger amounts of cell lysate than those sufficient to detect P60-katanin with the anti-P60-katanin antibody.

Evaluation of microtubule-severing by M1, M85, and ΔMIT

Additional Western blotting, shown later, demonstrates that M85 is the predominant isoform of spastin in all tissues at all stages of development analyzed. This observation raised the question as to whether M1 and M85 differ in their functional properties. To compare their microtubule-severing properties, we transfected myc fusions of M1 and M85 into rat RFL-6 fibroblasts. We also transfected these cells with the ΔMIT construct to compare the degree to which the protein severs microtubules with or without the MIT domain. At 24 h after transfection, the cells were prepared for immunofluorescence microscopy by double labeling with the Sp/AAA antibody and an anti-tubulin antibody. There was no detectable endogenous spastin in interphase RFL-6 cells, so the staining with the Sp/AAA antibody revealed the overexpressed protein only (Fig. 2*A*). Cells were selected for analyses with approximately equivalent levels of expression of the spastin constructs, as assessed by fluorescence intensity of the Sp/AAA antibody staining. Microtubule levels were assessed by quantifying fluorescence intensity with an anti-tubulin antibody. This experiment revealed that all three of the recombinant spastins sever microtubules but to different degrees (Fig. 2*B–D*). The most effective was M85. Microtubule loss in cells overexpressing M85 was the greatest (only ~10% of microtubule staining remained compared with the control cells, indicated by arrowheads; Fig. 2, row B). The remaining microtubules were very short and sparse, rendering the affected cells almost invisible after tubulin staining (Fig. 2, column M85). As previously reported (White et al., 2007), the absence of the MIT domain did not abolish the severing ability of spastin. However, microtubule severing was not as great with ΔMIT as with M85 (~25% of microtubule staining remained, and the remaining microtubules were longer; Fig. 2, column ΔMIT). In cells overexpressing M1, ~60% of the microtubule staining remained and the microtubules were considerably longer than those in cells expressing M85 or ΔMIT (Fig. 2, column M1). On the basis of these results, we conclude that M85 severs microtubules more effectively than M1 and that the MIT domain enhances the severing ability of spastin.

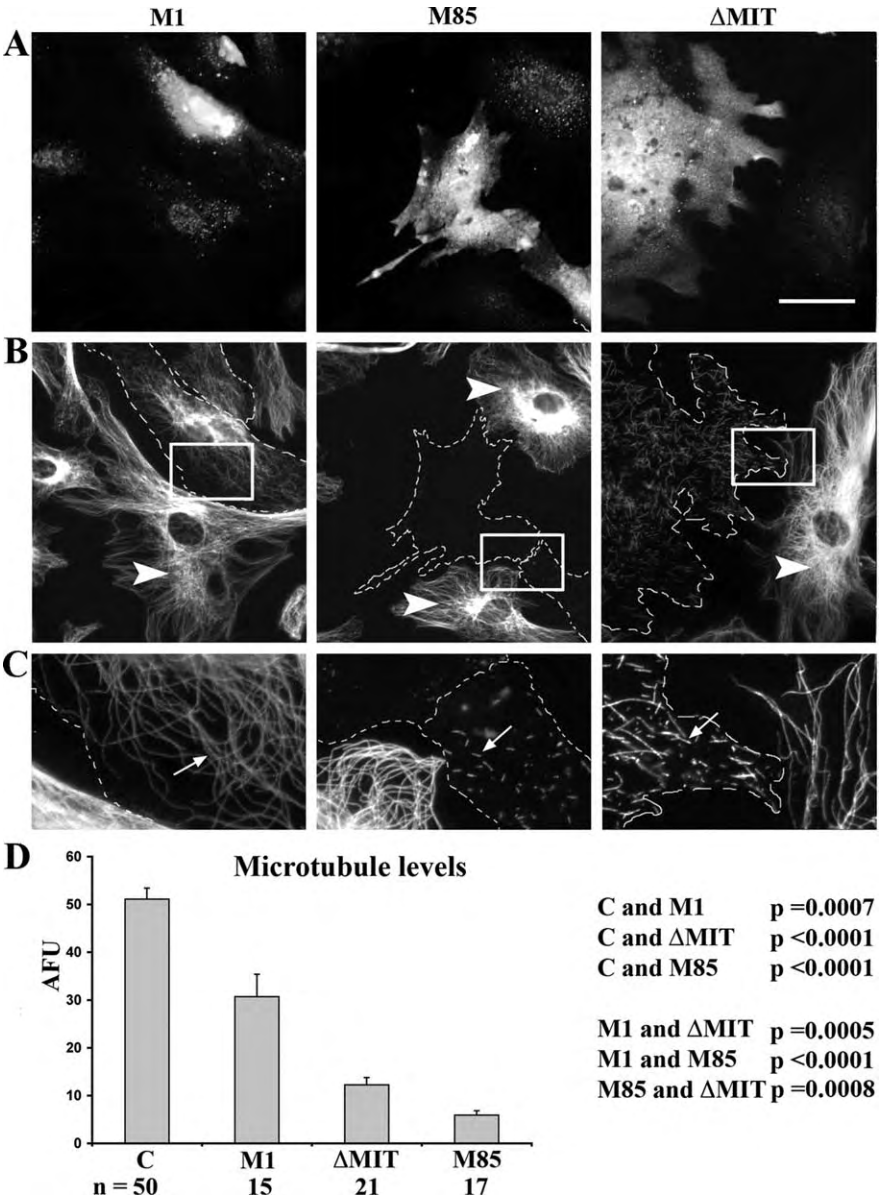

Figure 2. Microtubule severing by recombinant spastins in rat fibroblasts. RFL-6 cells were transfected with myc-tagged spastin constructs M1, M85, or ΔMIT. ***A***, Spastin-transfected cells were detected by immunostaining with Sp/AAA anti-spastin antibody. ***B***, Microtubules were visualized by immunostaining with anti-tubulin antibody. Spastin-overexpressing cells are outlined. Nontransfected cells are indicated by arrowheads. These cells are not readily visible in ***A*** because of very low expression of endogenous spastin. ***C***, Enlargements of boxed areas from ***B***. Arrows point at microtubules stained with anti-tubulin antibody. Microtubules in M1-overexpressing cells are much longer than microtubules in M85-overexpressing or ΔMIT-overexpressing cells. ***D***, Quantification of microtubule levels in control and transfected cells are shown for each recombinant spastin. The *p* values were calculated using Mann–Whitney *U* test. AFUs represent the sum of gray values of all the pixels in a selected cell divided by the number of pixels. Scale bar: ***A***, ***B***, 30 μm; ***C***, 9.5 μm.

Quantification of spastin and P60-katanin in rat tissues

Patients with SPG4-based HSP have one mutated spastin allele that produces a dysfunctional protein, as well as one nonmutated allele. Assuming no compensatory changes exist, this would diminish the pool of functional spastin by 50%. One possibility is that the total levels of both microtubule-severing proteins, P60-katanin and spastin, determine whether a particular neuron will suffer or not from a reduction in functional spastin levels. Western blot analyses indicate that P60-katanin has a broad distribu-

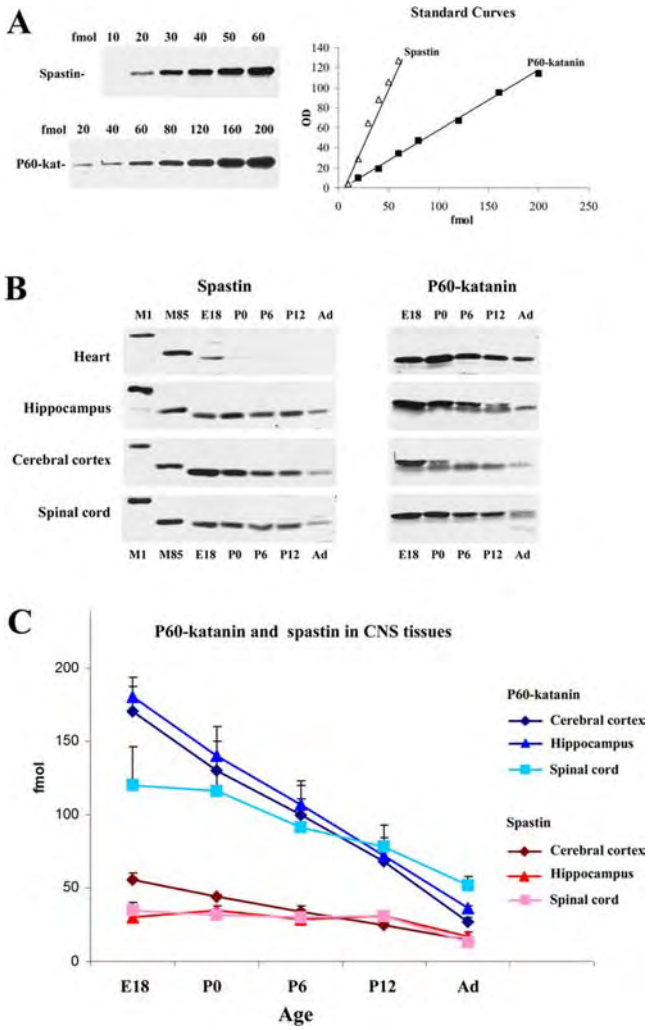

Figure 3. Quantification of P60-katanin and spastin in developing CNS tissues. ***A***, Calibration of anti-spastin and anti-P60-katanin antibodies. Standard curves were obtained using 10–60 fmol of spastin or 20–200 fmol of P60-katanin. ***B***, Western blots of spastin and P60-katanin in developing rat tissues. Tissues (heart, hippocampus, cerebral cortex, and spinal cord) were collected and combined from 12 E18 rats, eight P0 rats, six P6 rats, six P12 rats, and four adult (Ad) rats. Protein extracts from 1000 μg of combined tissues in sample buffer were divided into halves. One half of the lysate was used for Western blotting with anti-spastin antibody, and the other half was blotted simultaneously with anti-P60-katanin antibody. The M1 and M85 recombinant myc-tagged spastin isoforms synthesized in RFL-6 cells transfected with corresponding constructs were used to indicate the MW of spastins expressed in developing tissues. Myc-tag adds ~1.7 kDa to the recombinant spastins MW (see Materials and Methods), and therefore the control recombinant M1 and M85 spastins migrate slightly above endogenous spastins. After short exposure (5–15 s), only M85 was detected. In heart (representing non-neuronal tissue), the levels of spastin expression were considerably lower than in CNS tissues. ***C***, The optical densities were measured for bands representing M85 spastin or P60-katanin in neuronal tissues, and protein concentrations were read from standard curves. At each time point, expression of P60-katanin is higher than that of spastin, but, during development, P60-katanin levels decline much more rapidly than spastin levels. As a result, the total difference in P60-katanin/spastin expression decreases from ~130 fmol/500 μg in embryonic CNS tissues to ~25 fmol/500 μg in adult tissues.

tion across neuronal and non-neuronal tissues (Yu et al., 2005), whereas spastin expression is much more predominant in nervous tissue compared with non-nervous tissue (Fig. 3*B*). The lack of strong expression in non-nervous tissues is consistent with these tissues not being affected by spastin mutations. Additionally, our Western blots analyses show that M85 is the predominant spastin isoform detected in all tissues at all times analyzed (Fig. 3*B*). Quantitative analysis of these blots shows that the absolute levels of P60-katanin always exceed the absolute levels of spastin, with P60-katanin levels being fivefold to sixfold higher than spastin levels in some areas of the nervous system during development. The levels of both severing proteins decline in the adult, but the levels of P60-katanin decline more dramatically than the levels of spastin, so that the disparity between their levels is not nearly as great in the adult as during development (Fig. 3*C*).

At first glance, these results would appear to be consistent with a loss-of-function scenario for HSP, in which high levels of P60-katanin compensate for the loss of spastin at younger ages and in most tissues of the adult nervous system. In such a scenario, the combined levels of P60-katanin and spastin would not be sufficient in the adult corticospinal tracts to compensate for the loss-of-functional spastin associated with disease-related mutations. However, the level of microtubule severing produced by each of these proteins depends not only on the absolute levels of P60-katanin and spastin but also on the relative severing activity of the two enzymes. Both proteins are ATPases that require ATP hydrolysis to sever microtubules. The V_{max} (nanomoles of ATP hydrolyzed per minute per milligram of ATPase) values obtained for both proteins is in the same range: 0.60 for P60-katanin (McNally and Vale, 1993) and 0.66 for spastin (Evans et al., 2005). *In vitro*, the ability to sever purified microtubules seems to be higher for P60-katanin. For example, ~30 nM P60-katanin completely disassembled rhodamine-labeled microtubules within 5 min (McNally and Vale, 1993), whereas 100 nM spastin was used for 17 min to observe the same effect (Evans et al., 2005). However, it is important to note that the spastin used in these experiments was the M1 isoform, which our experiments indicate is less active than the M85 isoform (Fig. 2). Thus, it is likely that the *in vitro* severing activity of M85 spastin (which is the predominant isoform) is more similar to that of P60-katanin. Evaluation of the *in vivo* microtubule-severing activity of P60-katanin and spastin is further complicated by the fact that microtubules in living cells are covered with microtubule-associated proteins, some of which can potentially shield the microtubules from the severing proteins (Qiang et al., 2006).

Given these limitations in determining the actual severing activities of P60-katanin and spastin in living cells, we conducted theoretical analyses considering various possibilities for the relative severing activities of these two proteins (see Materials and Methods). Specifically, our goal was to estimate how different hypothetical ratios of P60-katanin and M85-spastin activity would affect total microtubule-severing activity in various tissues, under conditions wherein a spastin mutation decreased the total spastin activity by 50%. These calculations are based on the levels of P60-katanin and M85-spastin in various regions of the nervous system at various times in development (Fig. 3). The estimated percentage loss of total microtubule-severing activity resulting from a 50% loss of M85-spastin is shown in Figure 4. Calculations were performed for spinal cord and hippocampus in the adult and at various developmental stages, using various hypothetical ratios of P60-katanin/spastin activity (2:1, 1:1, 1:2, 1:4, and 1:10). These calculations revealed that, regardless of the P60-katanin/spastin activity ratio, the loss of total microtubule-severing activity resulting from a spastin mutation would actually be similar or even lower in the adult spinal cord than in developing spinal cord or hippocampus (with the exception of E18 hippocampus).

These results do not appear to support a loss-of-function scenario for HSP, unless the axons in the adult spinal cord are uniquely sensitive to diminutions in microtubule-severing activ-

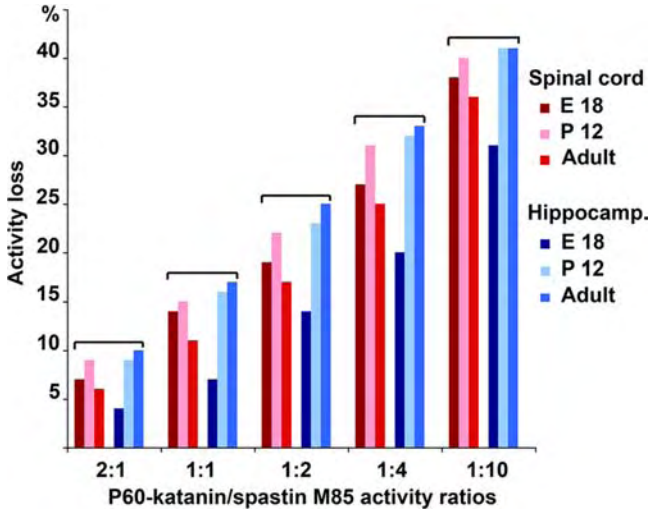

Figure 4. Estimated loss of total microtubule-severing activity attributable to spastin M85 mutation. These analyses are based on the levels of P60-katanin and M85 spastin in various regions of the nervous system at various times of development presented in Figure 3. Calculations were performed for both spinal cord and hippocampus in the adult and at different developmental stages using the hypothetical ratios of P60-katanin/spastin activity 2:1, 1:1, 1:2, 1:4, and 1:10. The loss of total severing activity resulting from spastin mutation would not be greater in an adult spinal cord than in a developing spinal cord or hippocampus (with the exception of E18 hippocampus). Even if we assume that spastin is 10 times as active as P60-katanin, the loss of total severing activity in adult spinal cord would be <40%. Assuming a more realistic scenario wherein spastin might be two times as active as P60-katanin, a total loss of microtubule-severing activity would be only 17% in adult spinal cord. If spastin and P60-katanin activities were equal (1:1), then the loss of activity resulting from spastin mutation would be only ~11% in adult spinal cord.

ity that do not affect axons in the developing spinal cord or other regions of the nervous system (perhaps because of the greater length of axons in the adult spinal cord). However, even if we assume that spastin is 10 times as active as P60-katanin, the loss of total severing activity in adult spinal cord would be <40%. Assuming that P60-katanin and spastin activities are equal, then the loss of activity resulting from spastin mutation would be only ~11% in adult spinal cord. In a more realistic scenario, assuming that spastin might be two times as active as P60-katanin, a total loss of microtubule-severing activity would be only 17% in adult spinal cord. To our knowledge, there is no precedent for neuropathologies resulting from diminutions in enzyme activities in this range, given that virtually all known enzymatic activities exceed what is needed for normal function. In this regard, it is also worth noting that the concentration of P60-katanin alone in neuronal tissues is in the same range as the concentration able to cause complete disassembly of microtubules *in vitro* within minutes. Thus, it seems unlikely that neurons lacking half their normal spastin would suffer from too little microtubule-severing activity.

Quantitative observations on M1 and M85 distribution suggest another potential scenario for HSP pathogenesis. Overexposing the blots (Fig. 5*A*) revealed extremely faint M1 bands in hippocampus and cerebral cortex but only during development. However, there was no M1 band, even on overexposed blots, in the adult hippocampus, the adult cerebral cortex, or the developing spinal cord. The only circumstance in which we detected a substantial M1 band in the nervous system was in the adult spinal cord. We tested three adult animals, 3–8 months old, and found that the level of M1 expression remains approximately the same and comprises ~20–25% of total spastin (and would be equivalent to ~10% of P60-katanin) in the adult spinal cord (Fig. 5*B–D*). At the same time, we were unable to detect even traces of M1 or M85 in sciatic nerves isolated from the same animals (Fig. 5*B*). In contrast, P60-katanin levels were comparable in adult sciatic nerves and spinal cords (Fig. 5*C*). The absence of spastin from the adult sciatic nerve suggests that spastin may be primarily a CNS protein in the adult, which is consistent with the fact that HSP does not involve degeneration of axons of the peripheral nervous system. The presence of M1 strongly correlates with the time and place where the axonal degeneration occurs in HSP, suggesting a possible "gain-of-function" mechanism associated with this spastin isoform.

Effects of dysfunctional spastin peptides on neuronal morphology

The biochemical studies presented thus far led us to hypothesize a potential scenario whereby dysfunctional M1, but not M85, elicits deleterious effects on the axon. Approximately 75% of the disease-related mutations of human SPG4 locus are truncating or splice-site mutations (Fonknechten et al., 2000; Meijer et al., 2002; Sauter et al., 2002). Therefore, as a first measure toward testing this hypothesis, we prepared constructs that would mimic the dysfunctional mutants expressed during HSP by completely eliminating the AAA region of spastin required for microtubule severing (see Materials and Methods). For studies on cultures of embryonic rat cortical neurons, M85-STOP and M1-STOP were prepared as GFP fusion constructs. We chose to use these cultures because cortical neurons give rise to the corticospinal tracts that are afflicted with degeneration in HSP patients. In culture, these neurons undergo stereotyped developmental stages, entirely similar to cultured hippocampal neurons (Yu et al., 2005; Qiang et al., 2006). During stage 1, they extend broad flat lamellae that coalesce during stage 2 into several immature "minor processes." One of these minor processes grows longer than the others and becomes the axon during stage 3. Constructs expressing GFP–M85-STOP, GFP–M1-STOP, or GFP alone were transfected into the neurons just before plating, and the neurons were then fixed and analyzed 2 d later. Cultures were double labeled for GFP and also for actin. The purpose of the actin stain was to ensure that our images captured the full morphology of the neuron, in the event that the GFPs were not distributed into all regions such as the finest filopodia. We attempted to select neurons with similar levels of GFP fluorescence for our analyses, although the neurons expressing GFP–M1-STOP uniformly showed lower levels of expression than the neurons expressing GPP alone or GFP–M85-STOP.

As shown in Figure 6*A*, the proportions of cells in stages 2 and 3 were indistinguishable between the control group and the M85-STOP group ($p = 0.76$). In contrast, a notably greater proportion of the cells have not entered stage 3 in the M1-STOP group ($p = 0.0033$ for control vs M1-STOP cells in stage 3; $p = 0.0074$ for M85-STOP vs M1-STOP cells). Figure 6*B–D* shows the morphology of neurons that had entered stage 3. Control neurons typically had three to six minor processes, and the axon generally showed a few branches along its length and was tipped by a flat growth cone (Fig. 6*B*). Neurons expressing M85-STOP appeared to be equally robust, with no apparent difference in process number or length. The only detectable difference was that axons of neurons expressing M85-STOP appeared to be richer in actin-based lateral extensions emanating from the axon (Fig. 6*D*). In contrast, the neurons expressing M1-STOP had markedly less impressive morphologies, with fewer processes and shorter axons (Fig. 6*C*). Quantification of axonal length indicated no difference

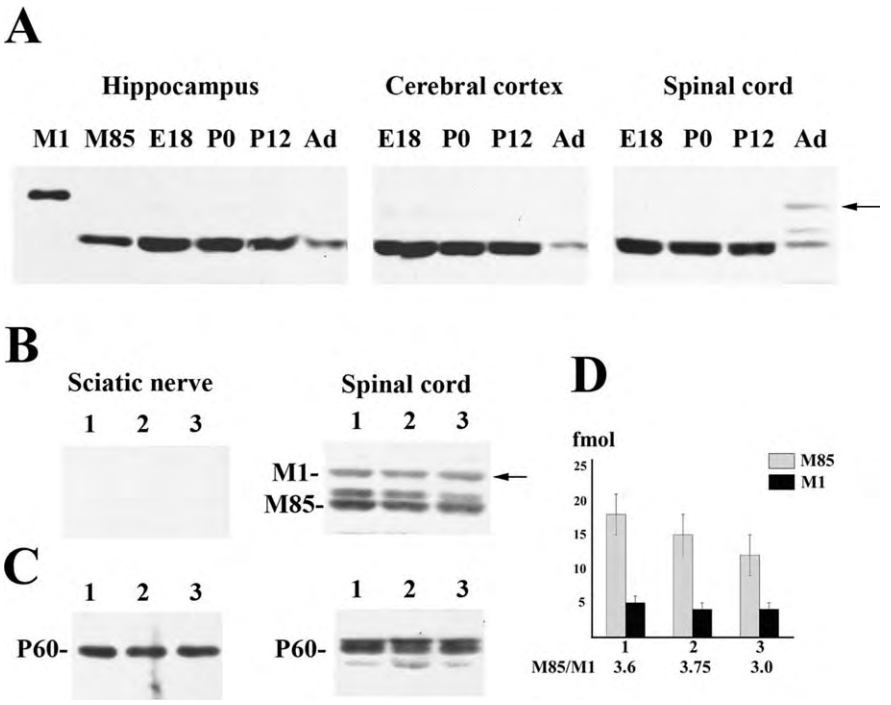

Figure 5. Expression of spastin isoforms in neuronal tissues. ***A***, Western blots of spastin in developing and adult rat CNS tissues. Spastin isoforms were detected in protein extracts from 500 μg of tissues using anti-spastin Sp/AAA antibody and secondary antibody conjugated with HRP. After reaction with chemiluminescent peroxidase substrate and long exposure time (2 min), prominent spastin M85 bands were detected in CNS tissues at all developmental stages, but only adult spinal cord expressed strong levels of spastin M1 (arrow). Very weak spastin M1 bands were detected in embryonic but not adult hippocampus and cerebral cortex. M1, M85, Spastin isoforms from M1- or M85-transfected RFL-6 cells indicate the size of spastin present in developing tissues; Ad, adult. ***B***, Sciatic nerve or spinal cord protein extracts from three rats, 3–8 months old, were blotted with anti-spastin Sp/AAA antibody. Even after long exposure (4 min), no spastin was detected in three adult sciatic nerve lysates, whereas both M85 and M1 spastin were clearly present in lysates from adult spinal cords. ***C***, Aliquots blotted with anti-P60-katanin antibody show that P60-katanin is expressed in both adult sciatic nerves and spinal cords. ***D***, Quantification of M85 and M1 spastin in spinal cords of 3-month-old (1), 7-month-old (2), and 8-month-old (3) rats.

between axons in the control group and the M85-STOP group ($p = 0.1$), but the axons were significantly shorter in the M1-STOP group ($p = 0.0024$ compared with controls; $p < 0.0001$ compared with M85-STOP) (Fig. 6*E*). These results reveal that expression of M1-STOP is deleterious to neuronal development and axonal growth, whereas the same is not true for expression of M85-STOP.

Effects of dysfunctional spastin peptides on fast axonal transport

Previous studies on mutant proteins related to other neurodegenerative diseases indicate that such mutants can produce gain-of-function effects by adversely affecting pathways relevant to fast axonal transport (FAT) (Morfini et al., 2002, 2004, 2005, 2006, 2007b; Pigino et al., 2003). Significantly, several lines of evidence link alterations in FAT to HSP-based pathogenesis. For example, loss-of-function mutations in the kinesin-1 motor KIF5A have been identified in patients with an autosomal-dominant form of HSP (Reid et al., 2002). To directly determine whether there is an effect of the dysfunctional spastin molecules on FAT, wild-type and truncated spastin constructs were translated *in vitro* (Fig. 7*A*), and the effects of the resulting peptides on FAT were evaluated using vesicle motility assays in isolated squid axoplasm. In this type of study, video-enhanced microscopic techniques allow for the quantitative analysis of both anterograde (kinesin-dependent) and retrograde (cytoplasmic dynein-dependent) FAT. Typical anterograde rates are 1.5–2.0 μm/s, whereas retrograde rates are 1–1.3 μm/s in perfused axoplasms. These rates are maintained with little (<10%) or no reduction for >1 h after perfusion with control buffer.

Although control reactions with no cDNA did not result in detectable protein synthesis, two functional start codons in the full-length spastin gene (Spastin FL) resulted in the translation of M1 (spastin amino acids 1–614) and M85 (spastin amino acids 85–614), as described previously (Fig. 7*A*) (Claudiani et al., 2005). As shown in Figure 7*B*, perfusion of full-length M1 and M85 (Spastin FL) in squid axoplasm showed no effect on FAT. Similar results were observed after perfusion of ΔMIT (Fig. 7*C*). Quantification of *in vitro* translated spastin constructs indicated that these proteins were perfused at ~1–10 nM concentration, whereas endogenous squid tubulin is present at 50 μM concentration (Morfini et al., 2007a). No abnormalities were seen on the morphology of axoplasmic microtubules (Morfini et al., 2007a), consistent with the large difference (5000-fold to 50,000-fold) in spastin–tubulin stoichiometries (data not shown). The very low concentrations we used were chosen so as to avoid any consequential alterations in microtubule severing in the controls and because concentrations of mutant peptides in this range have produced defects in FAT at comparable levels in the previous studies mentioned above.

Perfusion of the mixture of M1-STOP and M85-STOP in squid axoplasm at these levels resulted in a striking inhibition of both anterograde and retrograde FAT rates (Fig. 7*D*). These data suggest that pathogenic spastin inhibits FAT in a manner that is independent of the microtubule-severing activity of spastin. Additionally, these experiments suggest that protein truncation confers on spastin a toxic gain of function that results in inhibition of FAT. Separate pools of M1-STOP and M85-STOP were then generated by *in vitro* translation and individually perfused in isolated squid axoplasm (Fig. 8). Results from these experiments showed that truncated M1 inhibited FAT (Fig. 8*A*), whereas truncated M85 showed no effect (Fig. 8*B*). These results indicate that the inhibitory effect of pathogenic spastin on FAT depends on the N-terminal 8 kDa region exclusively present in M1 spastin.

Discussion

The present studies are the first to quantify the absolute levels of both P60-katanin and spastin in the nervous system. During development, the levels of P60-katanin are many times higher than the levels of spastin, but the levels of the two proteins are not as different in the adult attributable to a notable plunge in the levels of P60-katanin. It makes sense that the total levels of the two severing proteins are higher during development because the need for microtubule transport and reorganization is presumably much greater when the axon is growing. The fact that spastin mutations in humans result in no developmental abnormalities suggests that the high levels of P60-katanin are able to fully compensate for the diminished levels of spastin. Indeed, a transgenic

mouse lacking functional spastin shows no detectable flaws in development (Tarrade et al., 2006). However, these neurons show some abnormalities when cultured, and some zebrafish neurons display abnormalities in axonal growth when spastin levels are diminished using morpholinos (Wood et al., 2006). These observations suggest that P60-katanin is capable of compensating for spastin under most circumstances but that the two severing proteins are not completely identical with regard to their functions and how they are regulated. We are currently conducting studies to further explore this possibility. For now, our goal was to evaluate potential mechanisms underlying axonal degeneration resulting from spastin mutations.

Detailed analyses of spastin mutations identified to date do not reveal an obvious candidate pathogenic mechanism for HSP (Fink, 2006; Schickel et al., 2007). Most of >150 human disease-related spastin mutations are nonsense, frame-shift, or splice-site mutations that presumably encode truncated spastin molecules lacking the AAA domain. Approximately 25% of spastin mutations are missense mutations falling within the AAA cassette. Because these various mutations would produce a dysfunctional protein unable to sever microtubules, the prevalent view has been that SPG4-based HSP is most probably a loss-of-function disease, with degeneration of axons resulting from affected neurons not reaching a hypothetical threshold of microtubule severing (Svenson et al., 2001; Errico et al., 2002). The main purpose of our quantitative Western blot analyses was to test the viability of this scenario. Consistent with the late-onset characteristic of HSP, we found that developing neurons contain far more P60-katanin than adult neurons, and hence developing neurons would be far better equipped to compensate for reductions in functional spastin levels associated with SPG4 mutations. In light of our tissue distribution studies, the lack of degeneration of long peripheral axons observed in HSP also makes sense, because adult peripheral neurons appear to express no spastin whatsoever and hence would be dependent on P60-katanin for microtubule severing.

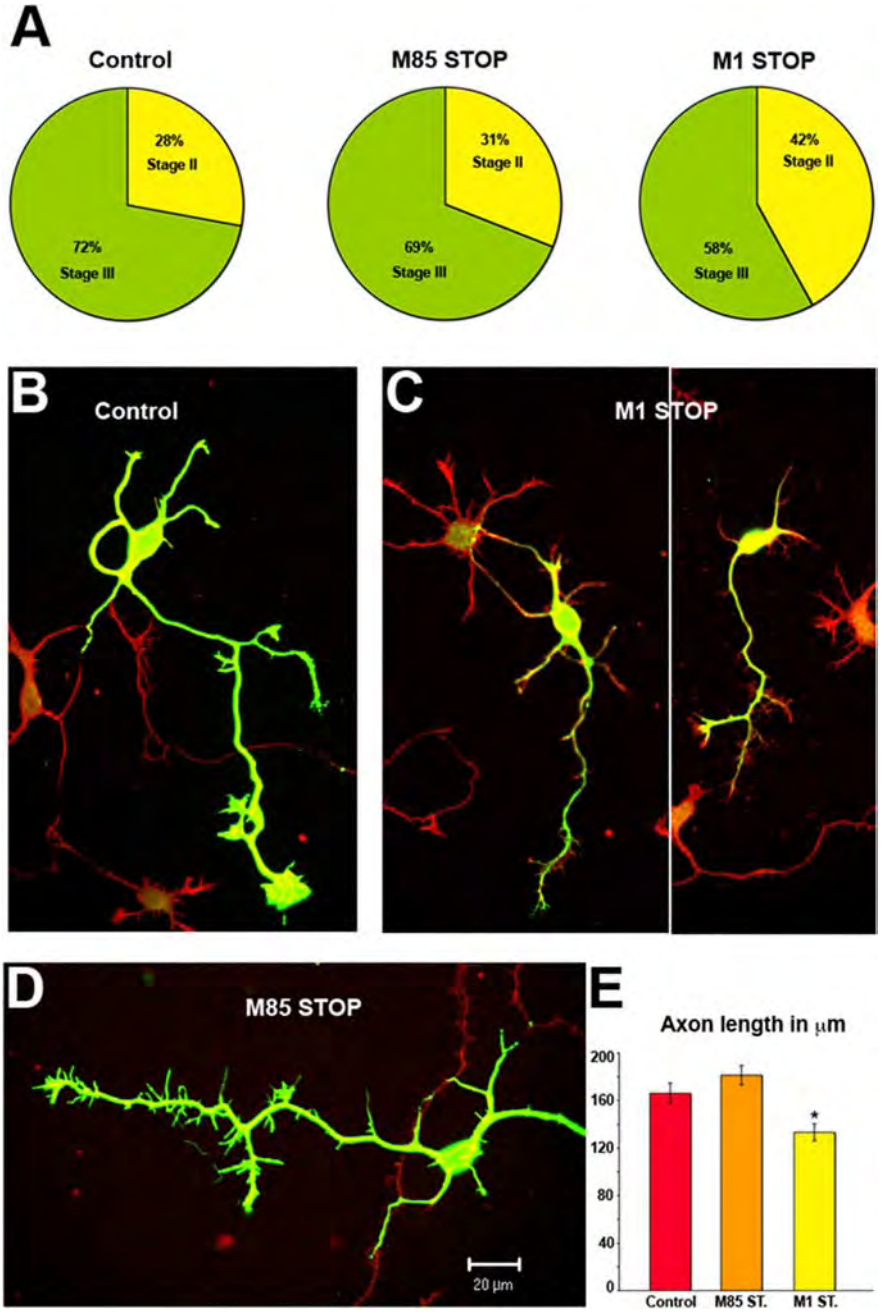

Figure 6. Effects of dysfunctional spastins on neuronal morphology. ***A***, A total of 302, 350, and 272 cortical neurons transfected, respectively, with control GFP construct, GFP–M85-STOP, and GFP–M1-STOP were examined and classified as stage 2 or stage 3 neurons. The quantitative analysis revealed no significant differences between the control and M85-STOP groups. In contrast, the M1-STOP group was delayed in development compared with the other two groups. ***B–D***, Transfected cortical neurons were double labeled for GFP (green) and actin (red). The control group (***B***) and the M85-STOP group (***D***) show a morphology more robust than the M1-STOP group (***C***). The M85-STOP group was somewhat different from the control group in that it displayed more actin-rich lateral extensions along the length of the axon. ***E***, The M1-STOP group ($n = 52$) had significantly shorter axons than the control group ($n = 57$) or the M85-STOP group ($n = 60$) ($p = 0.0024$ and $p < 0.0001$, respectively). There was no difference in axonal length between the control group and the M85-STOP group ($p = 0.1052$). All error bars represent SEM.

At present, it is unknown whether equal amounts of P60-katanin and spastin have the same or different microtubule-severing activities in the axon. With regard to P60-katanin, its severing activity can be dampened by the presence of microtubule-associated proteins on the microtubules (Buster et al., 2002; Qiang et al., 2006) but enhanced by the presence of a cofactor termed P80-katanin (Hartman et al., 1998; Yu et al., 2005). Whether or not spastin is similarly regulated remains to be tested. Whatever the relative microtubule-severing activity of the two proteins may be *in vivo*, our calculations indicate no obvious scenario that can explain why a 50% loss of spastin activity would reduce the overall microtubule-severing activity in the adult spinal cord to a greater extent than in other regions of the adult or developing nervous system. Thus, the only apparent way to reconcile our data with a loss-of-function scenario for HSP is to posit that the health of particularly long CNS axons is more sen-

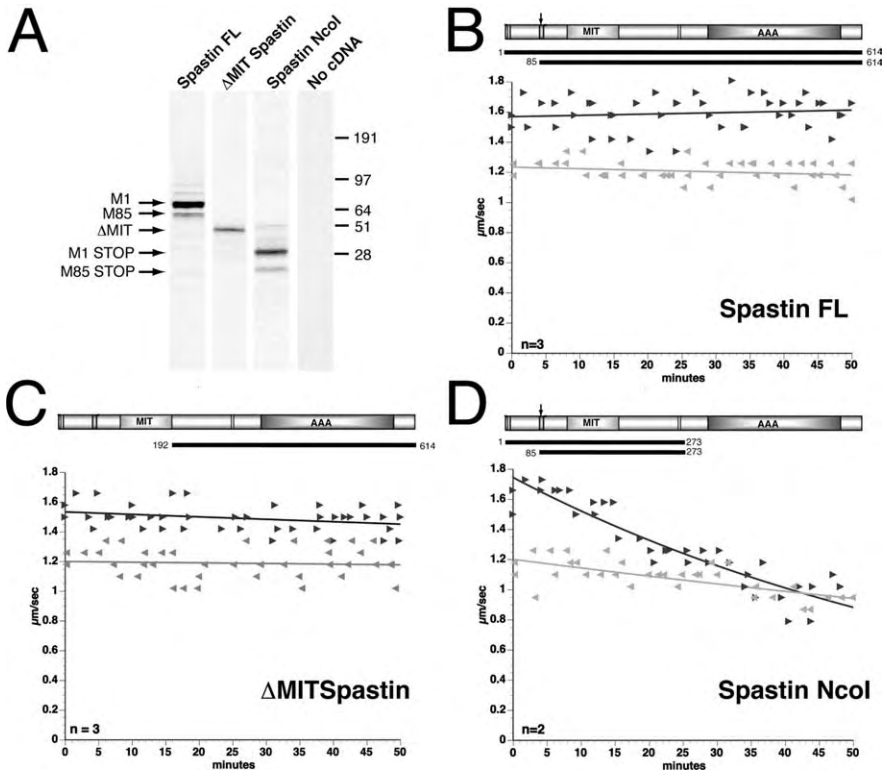

Figure 7. Effects of wild-type and truncated spastin peptides on fast axonal transport. ***A***, Autoradiogram showing *in vitro* translated, [^{35}S]methionine-labeled spastin constructs used for squid axoplasm perfusion experiments. The presence of two functional start codons in the mammalian full-length spastin cDNA construct (Spastin FL) results in the production of both 68 kDa (M1 spastin, amino acids 1–616), and 60 kDa (M85 spastin, amino acids 85–616) spastin products when translated *in vitro*. Digestion of full-length spastin plasmid with *Nco*I (Spastin *Nco*I) before *in vitro* translation results in the synthesis of 29 kDa (M1-STOP, amino acids 1–273) and 21 kDa (M85-STOP, amino acids 85–273) truncated spastin polypeptides. The spastin construct lacking the MIT domain (spastin ΔMIT, amino acids 192–614) was also effectively translated. Control reactions (no cDNA) did not result in detectable protein synthesis. ***B–D***, Vesicle motility assays in isolated squid axoplasm. Individual velocity measurements (arrowheads) are plotted as a function of time. Anterograde (dark arrows and line) and retrograde FAT (reverse gray arrows and line) rates are shown. *In vitro* translated control reactions as shown in ***A*** were perfused in axoplasm, and FAT rates were monitored by video microscopy. A schematic depicting spastin constructs perfused for each experiment is also shown above each plot. Both MIT and AAA spastin domains are indicated. An arrow at amino acid position 85 indicates the second start codon that gives raise to M85. ***B***, ***C***, Perfusion of either full-length spastin or ΔMIT spastin peptides did not affect FAT rates. ***D***, However, perfusion of truncated spastin *Nco*I polypeptides significantly inhibited FAT rates in both directions. *n* indicates the number of independent experiments.

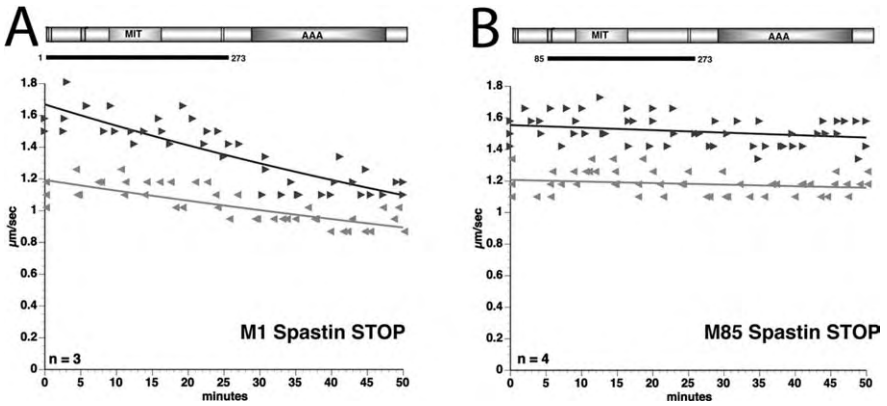

Figure 8. Truncated M1 inhibits fast axonal transport in squid axoplasm. *In vitro* translation reactions were performed using spastin plasmids engineered to produce M1-STOP spastin or M85-STOP spastin, respectively (see Material and Methods), and recombinant peptides were then perfused into squid axoplasm. A schematic depicting spastin peptides perfused in each experiment is shown above each plot. ***A***, Perfusion of M1-STOP spastin inhibits anterograde and retrograde FAT, much as seen with spastin *Nco*I. ***B***, Perfusion of M85-STOP spastin showed no effect on FAT. *n* indicates the number of independent experiments.

sitive to relatively moderate diminutions in microtubule-severing activity than other long axons of the body. This seems unlikely, however, because enzymes are generally expressed in excess of the levels needed (see Results). Finally, it is interesting to note that the age of onset of HSP is considerably earlier in patients who bear a function-blocking mutation on one spastin gene and a non-functional-blocking mutation on the other spastin gene (Svenson et al., 2004). Together, these observations are difficult to reconcile with a loss-of-function scenario.

An alternative scenario is suggested by our observations on the distribution, expression pattern, and properties of the M1 isoform of spastin. M1 is a much less effective severing protein than M85. M1 is even less effective than ΔMIT, indicating that the N-terminal region of M1 more strongly inhibits the severing properties of spastin than the MIT domain enhances its severing properties. M1 is virtually absent from all axons at all stages of life, except for those within the adult spinal cord, in which it accounts for 20–25% of the total spastin. This is provocative because the spinal cord is the precise location of the corticospinal tracts that degenerate during HSP. These observations led us to hypothesize that disease-related mutations in spastin could generate a cytotoxic protein but only in the case of M1. In this scenario, for the spastin protein to be cytotoxic, it would have to contain the N-terminal region specific to M1 and also be functionally compromised by a mutation or by the lack of an AAA domain. To test this hypothesis, we compared the effects of truncated versions of M1 and M85 spastin lacking the AAA domain on cultures of embryonic cortical neurons. These studies demonstrated just how detrimental M1 mutants would be if they were robustly expressed during development. Neurons induced to express the truncated M1 are slower to develop, have shorter axons, and have generally less robust morphologies. Interestingly, the truncated M85 spastin (which would correspond to the mutant spastin expressed during development in HSP patients) did not cause any developmental problems in neuronal cell cultures.

To further investigate the mechanism of HSP, we tested the effects of truncated spastin M1 and M85 on FAT. Our premise that pathogenic spastin mutants could be deleterious to FAT is based on several lines of evidence linking FAT defects to HSP pathogenesis (Fink, 2003). Genetic evidence shows that loss-of-function mutations in a kinesin-1 gene (kinesin-1A,

KIF5A) can also give rise to HSP, namely in the form of HSP termed SPG10 (Reid et al., 2002). Kinesin-1 is the principal molecular motor driving anterograde FAT (Morfini et al., 2005), and, hence, it is provocative that suppression of its functions would elicit essentially the same phenotype as mutations of spastin. Supporting this notion, analysis of SPG4–HSP patients show a length-dependent "dying back" pattern of axonal degeneration, which is consistent with deficits in FAT (Deluca et al., 2004; Morfini et al., 2007b). In our studies on squid axoplasm, perfusion of full-length spastin (M1 plus M85) showed no effect on FAT, and the same was true for the truncated M85 without the ability to sever microtubules. However, the truncated M1 polypeptide strongly inhibited FAT, indicating that it is the 8 kDa N-terminal region of M1 that elicits these deleterious effects. Notably, this domain failed to show any effect on FAT when present in the context of the full-length M1 spastin protein. One possibility is that pathogenic spastin mutations induce a conformational change that results in abnormal exposure of the 8 kDa N terminal unique to M1. Consistent with this view, intragenic polymorphisms of spastin have been found within the 8 kDa N terminus that dramatically modify the HSP phenotype (Svenson et al., 2004). In addition, spastin is known to interact with another HSP-related protein called atlastin via the 8 kDa N-terminal region of M1 (Evans et al., 2006; Sanderson et al., 2006). Interestingly, recessive mutations in atlastin also lead to HSP (Zhao et al., 2001), suggesting that the binding of atlastin or other polypeptides to the N terminal of M1 could help prevent M1-induced pathology.

It has been suggested that, at least in the case of certain spastin mutations, the dysfunctional protein could associate with microtubules and impair their ability to interact with the motor proteins that fuel FAT (McDermott et al., 2003). We are skeptical of this idea because the endogenous levels of spastin expressed in neurons are probably much too low to adversely affect FAT simply by coating the microtubules. Indeed, in our experiments, truncated M1 inhibited FAT when perfused at <100-fold the levels of the motor proteins themselves (i.e., kinesin-1, 500 nM) (Morfini et al., 2006). Although the precise mechanism by which pathogenic M1 inhibits FAT is not directly addressed by our experiments, it may be instructive that other neuropathogenic polypeptides similarly inhibit FAT by activating kinases and phosphatases involved in the regulation of molecular motor proteins (Morfini et al., 2002, 2004, 2005, 2006, 2007b; Pigino et al., 2003; Szebenyi et al., 2003). Collectively, these experimental results provide an initial set of clues that will be helpful in identifying the molecular pathway(s) by which spastin mutations may lead to axonal degeneration through a novel gain-of-function mechanism.

References

Ahmad FJ, Yu W, McNally FJ, Baas PW (1999) An essential role for katanin in severing microtubules in the neuron. J Cell Biol 145:305–315.

Ahmad FJ, He Y, Myers KA, Hasaka TP, Francis F, Black MM, Baas PW (2006) Effects of dynactin disruption and dynein depletion on axonal microtubules. Traffic 7:524–537.

Baas PW, Qiang L (2005) Neuronal microtubules: when the MAP is the roadblock. Trends Cell Biol 15:183–187.

Baas PW, Karabay A, Qiang L (2005) Microtubules cut and run. Trends Cell Biol 15:518–524.

Brady ST, Richards BW, Leopold PL (1993) Assay of vesicle motility in squid axoplasm. Methods Cell Biol 39:191–202.

Buster D, McNally K, McNally FJ (2002) Katanin inhibition prevents the redistribution of gamma-tubulin at mitosis. J Cell Sci 115:1083–1092.

Buster DW, Baird DH, Yu W, Solowska JM, Chauviere M, Mazurek A, Kress M, Baas PW (2003) Expression of the mitotic kinesin Kif15 in postmitotic neurons: implications for neuronal migration and development. J Neurocytol 32:79–96.

Claudiani P, Riano E, Errico A, Andolfi G, Rugarli EI (2005) Spastin subcellular localization is regulated through usage of different translation start sites and active export from the nucleus. Exp Cell Res 309:358–369.

Deluca GC, Ebers GC, Esiri MM (2004) The extent of axonal loss in the long tracts in hereditary spastic paraplegia. Neuropathol Appl Neurobiol 30:576–584.

Dent EW, Callaway JL, Szebenyi G, Baas PW, Kalil K (1999) Reorganization and movement of microtubules in axonal growth cones and developing interstitial branches. J Neurosci 19:8894–8908.

Errico A, Ballabio A, Rugarli EI (2002) Spastin, the protein mutated in autosomal dominant hereditary spastic paraplegia, is involved in microtubule dynamics. Hum Mol Genet 11:153–163.

Evans K, Keller C, Pavur K, Glasgow K, Conn B, Lauring B (2006) Interaction of two hereditary spastic paraplegia gene products, spastin and atlastin, suggests a common pathway for axonal maintenance. Proc Natl Acad Sci USA 103:10666–10671.

Evans KJ, Gomes ER, Reisenweber SM, Gundersen GG, Lauring BP (2005) Linking axonal degeneration to microtubule remodeling by Spastin-mediated microtubule severing. J Cell Biol 168:599–606.

Fink JK (2003) Advances in the hereditary spastic paraplegias. Exp Neurol 184 [Suppl 1]:S106–S110.

Fink JK (2006) Hereditary spastic paraplegia. Curr Neurol Neurosci Rep 6:65–76.

Fink JK, Rainier S (2004) Hereditary spastic paraplegia: spastin phenotype and function. Arch Neurol 61:830–833.

Fonknechten N, Mavel D, Byrne P, Davoine CS, Cruaud C, Bonsch D, Samson D, Coutinho P, Hutchinson M, McMonagle P, Burgander JM, Tartaglione A, Heinzlef O, Feki I, Deufel T, Parfrey N, Brice A, Fontaine B, Prud'homme JF, Weissenbach J, Durr A, Hazan J (2000) Spectrum of SPG4 mutations in autosomal dominant spastic paraplegia. Hum Mol Genet 9:637–644.

Hartman JJ, Mahr J, McNally K, Okawa K, Iwamatsu A, Thomas S, Cheesman S, Heuser J, Vale RD, McNally FJ (1998) Katanin, a microtubule-severing protein, is a novel AAA ATPase that targets to the centrosome using a WD40-containing subunit. Cell 93:277–287.

Hazan J, Fonknechten N, Mavel D, Paternotte C, Samson D, Artiguenave F, Davoine C, Cruaud C, Dürr A, Wincker P, Brottier P, Cattolico L, Barbe V, Burgunder J, Prud'homme J, Brice A, Fontaine B, Heilig B, Weissenbach J (1999) Spastin, a new AAA protein, is altered in the most frequent form of autosomal dominant spastic paraplegia. Nat Genet 23:296–303.

Karabay A, Yu W, Solowska JM, Baird DH, Baas PW (2004) Axonal growth is sensitive to the levels of katanin, a protein that severs microtubules. J Neurosci 24:5778–5788.

Ma Y, Shakiryanova D, Vardya I, Popov SV (2004) Quantitative analysis of microtubule transport in growing nerve processes. Curr Biol 14:725–730.

McDermott CJ, Grierson AJ, Wood JD, Bingley M, Wharton SB, Bushby KM, Shaw PJ (2003) Hereditary spastic paraparesis: disrupted intracellular transport associated with spastin mutation. Ann Neurol 54:748–759.

McNally FJ, Vale RD (1993) Identification of katanin, an ATPase that severs and disassembles stable microtubules. Cell 75:419–429.

Meijer I, Hand C, Cossette P, Figlewicz D, Rouleau G (2002) Spectrum of SPG4 mutations in a large collection of North American families with hereditary spastic paraplegia. Arch Neurol 59:281–286.

Morfini G, Szebenyi G, Elluru R, Ratner N, Brady ST (2002) Glycogen synthase kinase 3 phosphorylates kinesin light chains and negatively regulates kinesin-based motility. EMBO J 23:281–293.

Morfini G, Szebenyi G, Brown H, Pant HC, Pigino G, DeBoer S, Beffert U, Brady ST (2004) A novel CDK5-dependent pathway for regulating GSK3 activity and kinesin-driven motility in neurons. EMBO J 23:2235–2245.

Morfini G, Pigino G, Brady ST (2005) Polyglutamine expansion diseases: failing to deliver. Trends Molec Med 11:64–70.

Morfini G, Pigino G, Szebenyi G, You Y, Pollema S, Brady ST (2006) JNK mediates pathogenic effects of polyglutamine-expanded androgen receptor on fast axonal transport. Nat Neurosci 9:907–916.

Morfini G, Pigino G, Mizuno N, Kikkawa M, Brady ST (2007a) Tau binding to microtubules does not directly affect microtubule-based vesicle motility. J Neurosci Res 85:2620–2630.

Morfini G, Pigino G, Opalach K, Serulle Y, Moreira JE, Sugimori M, Llinas RR, Brady ST (2007b) 1-Methyl-4-phenylpyridinium affects fast axonal

transport by activation of caspase and protein kinase C. Proc Natl Acad Sci USA 104:2442–2447.

Pigino G, Morfini G, Mattson MP, Brady ST, Busciglio J (2003) Alzheimer's presenilin 1 mutations impair kinesin-based axonal transport. J Neurosci 23:4499–4508.

Qiang L, Yu W, Andreadis A, Luo M, Baas PW (2006) Tau protects microtubules in the axon from severing by katanin. J Neurosci 26:3120–3129.

Reid E, Kloos M, Ashley-Koch A, Hughes L, Bevan S, Svenson IK, Graham FL, Gaskell PC, Dearlove A, Pericak-Vance MA, Rubinsztein DC, Marchuk DA (2002) A kinesin heavy chain (KIF5A) mutation in hereditary spastic paraplegia (SPG10). Am J Hum Genet 71:1189–1194.

Roll-Mecak A, Vale RD (2005) The *Drosophila* homologue of the hereditary spastic paraplegia protein, spastin, severs and disassembles microtubules. Curr Biol 15:650–655.

Salinas S, Carazo-Salas RE, Proukakis C, Schiavo G, Warner TT (2007) Spastin and microtubules: functions in health and disease. J Neurosci Res 85:2778–2782.

Sanderson CM, Connell JW, Edwards TL, Bright NA, Duley S, Thompson A, Luzio JP, Reid E (2006) Spastin and atlastin, two proteins mutated in autosomal-dominant hereditary spastic paraplegia, are binding partners. Hum Mol Genet 15:307–318.

Sauter S, Miterski B, Klimpe S, Bönsch D, Schöls L, Visbeck A, Papke T, Hopf H, Engel W, Deufel T, Epplen J, Neesen J (2002) Mutation analysis of the spastin gene (SPG4) in patients in Germany with autosomal dominant hereditary spastic paraplegia. Hum Mutat 20:127–132.

Schickel J, Pamminger T, Ehrsam A, Münch S, Huang X, Klopstock T, Kurlemann G, Hemmerich P, Dubiel W, Deufel T, Beetz C (2007) Isoform-specific increase of spastin stability by N-terminal missense variants including intragenic modifiers of SPG4 hereditary spastic paraplegia. Eur J Neurol 14:1322–1328.

Svenson IK, Ashley-Koch AE, Gaskell PC, Riney TJ, Cumming WJ, Kingston HM, Hogan EL, Boustany RM, Vance JM, Nance MA, Pericak-Vance MA, Marchuk DA (2001) Identification and expression analysis of spastin gene mutations in hereditary spastic paraplegia. Am J Hum Genet 68:1077–1085.

Svenson IK, Kloos MT, Gaskell PC, Nance MA, Garbern JY, Hisanaga S, Pericak-Vance MA, Ashley-Koch AE, Marchuk DA (2004) Intragenic modifiers of hereditary spastic paraplegia due to spastin gene mutations. Neurogenetics 5:157–164.

Szebenyi G, Morfini GA, Babcock A, Gould M, Selkoe K, Stenoien DL, Young M, Faber PW, MacDonald ME, McPhaul MJ, Brady ST (2003) Neuropathogenic forms of huntingtin and androgen receptor inhibit fast axonal transport. Neuron 40:41–52.

Tarrade A, Fassier C, Courageot S, Charvin D, Vitte J, Peris L, Thorel A, Mouisel E, Fonknechten N, Roblot N, Seilhean D, Diérich A, Hauw J, Melk J (2006) A mutation of spastin is responsible for swellings and impairment of transport in a region of axon characterized by changes in microtubule composition. Hum Mol Genet 15:3544–3558.

Wang L, Brown A (2002) Rapid movement of microtubules in axons. Curr Biol 12:1496–1501.

White S, Evans K, Lary J, Cole J, Lauring B (2007) Recognition of C-terminal amino acids in tubulin by pore loops in Spastin is important for microtubule severing. J Cell Biol 176:995–1005.

Wood J, Landers J, Bingley M, McDermott C, Thomas-McArthur V, Gleadall L, Shaw P, Cunliffe V (2006) The microtubule-severing protein Spastin is essential for axon outgrowth in the zebrafish embryo. Hum Mol Genet 15:2763–2771.

Yu W, Ahmad FJ, Baas PW (1994) Microtubule fragmentation and partitioning in the axon during collateral branch formation. J Neurosci 14:5872–5884.

Yu W, Solowska JM, Qiang L, Karabay A, Baird D, Baas PW (2005) Regulation of microtubule severing by katanin subunits during neuronal development. J Neurosci 25:5573–5583.

Yu W, Qiang L, Baas PW (2007) Microtubule-severing in the axon: implications for development, disease, and regeneration after injury. J Environ Biomed 1:1–7.

Zhao X, Alvarado D, Rainier S, Lemons R, Hedera P, Weber CH, Tukel T, Apak M, Heiman-Patterson T, Ming L, Bui M, Fink JK (2001) Mutations in a newly identified GTPase gene cause autosomal dominant hereditary spastic paraplegia. Nat Genet 29:326–331.

Molecular Biology of the Cell
Vol. 19, 1485–1498, April 2008

The Microtubule-severing Proteins Spastin and Katanin Participate Differently in the Formation of Axonal Branches

Wenqian Yu,*† Liang Qiang,*† Joanna M. Solowska,* Arzu Karabay,*‡ Sirin Korulu,*‡ and Peter W. Baas*

*Department of Neurobiology and Anatomy, Drexel University College of Medicine, Philadelphia, PA 19129; and ‡Department of Molecular Biology and Genetics, Istanbul Technical University, 34469 Istanbul, Turkey

Submitted September 7, 2007; Revised November 21, 2007; Accepted January 18, 2008
Monitoring Editor: Erika Holzbaur

Neurons express two different microtubule-severing proteins, namely P60-katanin and spastin. Here, we performed studies on cultured neurons to ascertain whether these two proteins participate differently in axonal branch formation. P60-katanin is more highly expressed in the neuron, but spastin is more concentrated at sites of branch formation. Overexpression of spastin dramatically enhances the formation of branches, whereas overexpression of P60-katanin does not. The excess spastin results in large numbers of short microtubules, whereas the excess P60-katanin results in short microtubules intermingled with longer microtubules. We hypothesized that these different microtubule-severing patterns may be due to the presence of molecules such as tau on the microtubules that more strongly shield them from being severed by P60-katanin than by spastin. Consistent with this hypothesis, we found that axons depleted of tau show a greater propensity to branch, and that this is true whether or not the axons are also depleted of spastin. We propose that there are two modes by which microtubule severing is orchestrated during axonal branch formation, one based on the local concentration of spastin at branch sites and the other based on local detachment from microtubules of molecules such as tau that regulate the severing properties of P60-katanin.

INTRODUCTION

The formation of axonal branches is critical for the development of the nervous system. In order for axonal branches to form, the cytoskeleton within the parent axon must undergo dramatic remodeling. In particular, the parent axon is dominated by very long microtubules that must be locally chopped into short highly mobile pieces that are able to move into the newly forming branch. Over a decade ago, we reported indirect evidence of the local severing of microtubules at sites of impending branch formation using serial reconstructions of election micrographs (Yu *et al.,* 1994). We were then able to directly visualize the severing of microtubules at branch sites using live-cell imaging (Dent *et al.,* 1999). Since then, we have dedicated a great deal of attention to studying P60-katanin, which is the predominant microtubule-severing protein in developing neurons (Ahmad *et al.,* 1999; Karabay *et al.,* 2004; Yu *et al.,* 2005). Inhibition of P60-katanin results in a dramatic shift toward longer microtubules in the axon and severely compromises the axon's growth. This is presumably due to the fact that long microtubules are immobile, whereas short microtubules, produced by the severing of long microtubules, are the ones that undergo the transport events crucial for axonal growth (Baas *et al.,* 2006). On the basis of all of these findings, we had anticipated that overexpressing P60-katanin in cultured neurons would enhance the propensity of their axons to form branches. However, this has not proven to be the case in studies performed thus far (Karabay *et al.,* 2004; Yu *et al.,* 2005).

Since we began our work on P60-katanin, it has become apparent that neurons express another microtubule-severing protein called spastin (Errico *et al.,* 2002; Evans *et al.,* 2005; Roll-Mecak and Vale, 2005, 2006). Spastin is very similar to P60-katanin in the AAA-region responsible for severing microtubules, but different in other regions of the molecule. P60-katanin is broadly expressed across cell types, whereas spastin expression is more restricted to the nervous system (Baas *et al.,* 2005; Ma *et al.,* 2006; Roll-Mecak and Vale, 2006; Salinas *et al.,* 2007). One possibility is that neurons express an entirely redundant microtubule-severing protein because the severing of microtubules is so crucial for axonal growth, branch formation, and the ongoing transport of microtubules throughout the life of the neuron. Another possibility is that the two severing proteins have overlapping but nonidentical functions, properties, and roles to carry out in the neuron. Such a "division of labor" for microtubule-severing proteins has already been demonstrated in the mitotic spindle (Zhang *et al.,* 2007).

To date, there have been no studies that directly compare the functional properties of P60-katanin and spastin in neurons. In the present study, we have rectified this by analyzing the effects on the microtubule array and on the morphology of cultured neurons produced by manipulation of each of the two severing proteins. We have also compared the capacity of tau to regulate the severing of microtubules by each of the two severing proteins. In conducting these studies, our main goal was to test the hypothesis that spastin and P60-katanin participate differently in the formation of axonal branches.

This article was published online ahead of print in *MBC in Press* (http://www.molbiolcell.org/cgi/doi/10.1091/mbc.E07–09–0878) on January 30, 2008.

† These authors contributed equally to this work.

Address correspondence to: Peter W. Baas (pbaas@drexelmed.edu).

© 2008 by The American Society for Cell Biology

MATERIALS AND METHODS

DNA Constructs and Polyclonal Antibodies

Mouse cDNA encoding full-length spastin was purchased from Invitrogen (Carlsbad, CA). Mouse cDNA encoding spastin M85 translated from the second start codon (methionine M85) was cloned into mammalian expression vector pEGFP (Clontech, Palo Alto, CA) downstream from the EGFP tag. Rat cDNA encoding full-length P60-katanin was used to prepare a comparable enhanced green fluorescent protein (EGFP) construct, as previously described (Karabay *et al.,* 2004). To prepare two different polyclonal antibodies against spastin, termed Sp/AAA and Sp/Sp5, two different fragments of spastin cDNA encoding amino acids 333-465 or 90-283, respectively, were cloned into the bacterial expression vector pRSET (Invitrogen, Carlsbad, CA). The two peptides were purified, after which rabbit antisera were prepared by Cocalico Biologicals (Reamstown, PA). IgG fractions were purified by protein A-Sepharose chromatography. Antibody specificity was tested by Western blotting and immunostaining of spastin-transfected and nontransfected fibroblasts. Both antibodies were effective for both Western blotting and immunostaining, but Sp/AAA had properties preferable for Western blotting, whereas Sp/Sp5 had properties preferable for immunostaining.

Preparation and Transfection of Cell Cultures

Cultures of rat hippocampal neurons and RFL-6 rat fibroblasts were prepared as previously described (Yu and Baas, 1994; Buster *et al.,* 2002; Yu *et al.,* 2005; Qiang *et al.,* 2006). For transfection of the EGFP-P60-katanin and EGFP-spastin constructs, we either used a modified electroporation device called a Nucleofector (Amaxa Biosystems, Köln, Germany) before plating, or Lipofectamine 2000 (Invitrogen; 11668-027) at some point after plating the cells. For the former, the single-cell suspension of hippocampal neurons or RFL-6 cells was resuspended in Nucleofector solution (Amaxa Biosystems), and the cells were then transfected with EGFP alone (control) or with the EGFP-P60-katanin or EGFP-spastin construct using the nucleofection device according to manufacturer's instructions and recommended settings (Karabay *et al.,* 2004). After nucleofection, the neurons were plated onto poly-L-lysine–treated glass coverslips as previously described (Yu and Baas, 1994), whereas the RFL-6 cells were plated on untreated glass coverslips (Buster *et al.,* 2002). Lipofectamine 2000 was used for transfecting cells in the culture dish. For this procedure, 0.5–1 μg of DNA and 1.25–2.5 μg of Lipofectamine 2000 were used per 35-mm dish. The ratio of DNA to Lipofectamine 2000 was 1:2.5. The cells were incubated in the DNA/lipofectamine medium for 5 h. After transfection, neurons were transferred to 37°C hippocampal neuron plating medium (Neurobasal medium supplemented with 2% B27, 0.3% glucose, 1 mM glutamine, and 5% FBS). Transfection efficiency was generally 5–10% for neuronal cultures and 15–30% for RFL-6 cell cultures, with EGFP fluorescence appearing within the first several hours after transfection. For experiments involving small interfering RNA (siRNA), neurons were transfected with a pool of four sequences specific to rodent spastin (purchased as a "smartpool" from Dharmacon Research, Boulder, CO; Accession number: XM-343018) or with a nonspecific control sequence (Dharmacon Research; Cat. no. D-001206-03-20), using the Nucleofector as previously described (Qiang *et al.,* 2006). A smartpool of tau siRNA (Dharmacon Research, Cat. no. M-089500-00) was used in some experiments, following our previously described protocol (Qiang *et al.,* 2006). An siRNA sequence that does not correspond to any gene in the rat genome, also purchased from Dharmacon, was used in all siRNA experiments as a control. In some experiments, the RFL-6 fibroblasts were induced to express the human four-repeat form of tau (termed tau 4R; provided by K. S. Kosik, University of California, Santa Barbara, CA) together with EGFP-spastin, EGFP-P60-katanin, or EGFP control for 1 d (using Lipofectamine 2000).

Immunofluorescence Analyses

For immunofluorescence studies on microtubule levels and distribution, cultures were briefly washed with 37°C phosphate buffered-saline (PBS) and then simultaneously fixed and extracted with 4% paraformaldehyde, 0.2% glutaraldehyde, and 0.1% Triton X-100 for 15 min. Cultures were washed with PBS three times for 5 min, quenched with 2 mg/ml sodium borohydride three times for 10 min, and then blocked with 10% normal goat serum and 10 mg/ml BSA in PBS for 1 h. After blocking, cultures were exposed to an anti-EGFP rabbit polyclonal antibody (1:4000; ab6556-25; Abcam, Cambridge, MA) overnight at 4°C. Enhancement of EGFP fluorescence by immunofluorescence assisted in discerning the cells expressing the EGFP, EGFP-P60-katanin, and EGFP-spastin from those that were not expressing, given that the fluorescence of the EGFP itself tended to diminish during the fixation and extraction. Cultures were then rinsed three times for 5 min in PBS, followed by exposure to an anti-β-tubulin antibody directly conjugated to Cy3 (1:400; C4585; Sigma, St. Louis, MO) together with Alexa Fluor-488–conjugated secondary goat anti-rabbit antibody (1:200; A11008; Molecular Probes, Eugene, OR). Cells were then rinsed extensively in PBS and mounted in a medium that reduces photobleaching.

Images were obtained on an Axiovert 200 microscope (Carl Zeiss, Thornwood, NY) equipped with a high resolution CCD (Orca ER, Hamamatsu, Hamamatsu City, Japan). All images were obtained using identical camera, microscope, and imaging criteria such as gain, brightness and contrast, and exposure time. Efforts were made to ensure that the images were not saturated and that minimal bleaching of the fluorescence occurred before image acquisition. Digital gray values of image pixels representing arbitrary fluorescence units (AFU) were obtained using AxioVision software. Fluorescence intensity was quantified for cells that had not been induced to express any of the constructs, cells that had been induced to express EGFP alone, and cells that had been induced to express the P60-katanin or spastin constructs. In some cases, fluorescence images were subjected to the "invert" function in Adobe Photoshop(San Jose, CA) that converts blacks to whites and whites to blacks and inverts gray levels proportionally, because we found that fine details were more clearly visualized. The resulting images are referred to as "inverted images." Statistics were done using the Student's *t* test.

Western Blotting

Western blot analyses were performed according to established procedures (Sambrook *et al.,* 1989). Neurons cultured in plastic dishes were suspended with cold 1 × PBS and lysed in the sample buffer with SDS, and then the proteins were resolved in 10% SDS-PAGE gels and transferred onto nitrocellulose membranes (90 mA; overnight at 4°C). Transfers were probed with Sp/AAA antibody against spastin. A goat anti-rabbit secondary HRP-conjugated antibody (Jackson ImmunoResearch Laboratories, West Grove, PA) was used. After reaction with chemiluminescent peroxidase substrate (Super Signal; Pierce, Rockford, IL), the blot was covered with x-ray film. We used three different exposure times (5, 15, and 30 s). Films were imaged using an Epson (Long Beach, CA) Perfection 1280 scanner. Protein markers were used to indicate the appropriate molecular weights. GAPDH was used as the internal control in each group to show that the same amount of protein was loaded in each group.

RESULTS

For the studies here, we used cultures of fetal rat hippocampal neurons, which are a well-characterized model for neuronal development (Dotti *et al.,* 1988; Yu *et al.,* 2005). Shortly after they adhere to the substrate, these neurons extend a broad lamellipodium (stage 1) that subsequently coalesces into multiple immature "minor" processes (stage 2). One of these minor processes then becomes the axon, usually by the second day after plating (stage 3), and then, a few days later, the remaining minor processes develop into dendrites (stage 4). Experiments conducted on these neurons utilized a previously described rat EGFP-P60-katanin construct (Karabay *et al.,* 2004; Yu *et al.,* 2005) and a new mouse EGFP-spastin construct developed in our laboratory (see *Materials and Methods*). In the case of the spastin construct, we used the sequence corresponding to that produced by the second start codon, which is the only detectable form expressed during development (Claudiani *et al.,* 2005; Salinas *et al.,* 2005).

Depletion of Spastin from Cultured Neurons Reduces Axonal Branch Frequency

In previous studies, we documented that inhibition of P60-katanin produces profoundly deleterious effects on axonal outgrowth (Ahmad *et al.,* 1999; Karabay *et al.,* 2004). Inhibition of P60-katanin compromises release of microtubules from the centrosome and results in significantly longer microtubules in the cell body and throughout the neuron. These results suggest that the available spastin is insufficient, in the absence of P60-katanin, to meet the microtubule-severing needs of the neuron. The question remains as to whether inhibiting spastin produces a comparable phenotype or produces a phenotype consistent with a more specialized role for spastin in axonal branch formation. To investigate this, we used siRNA to deplete spastin from cultured rat hippocampal neurons. Neurons were treated with either siRNA to spastin or control siRNA, introduced by nucleofection. After allowing 3 d for the spastin protein to be depleted, the neurons were replated and allowed to grow processes anew for 48 h before being fixed. Westerns blots (Figure 1A) confirmed that the spastin siRNA resulted

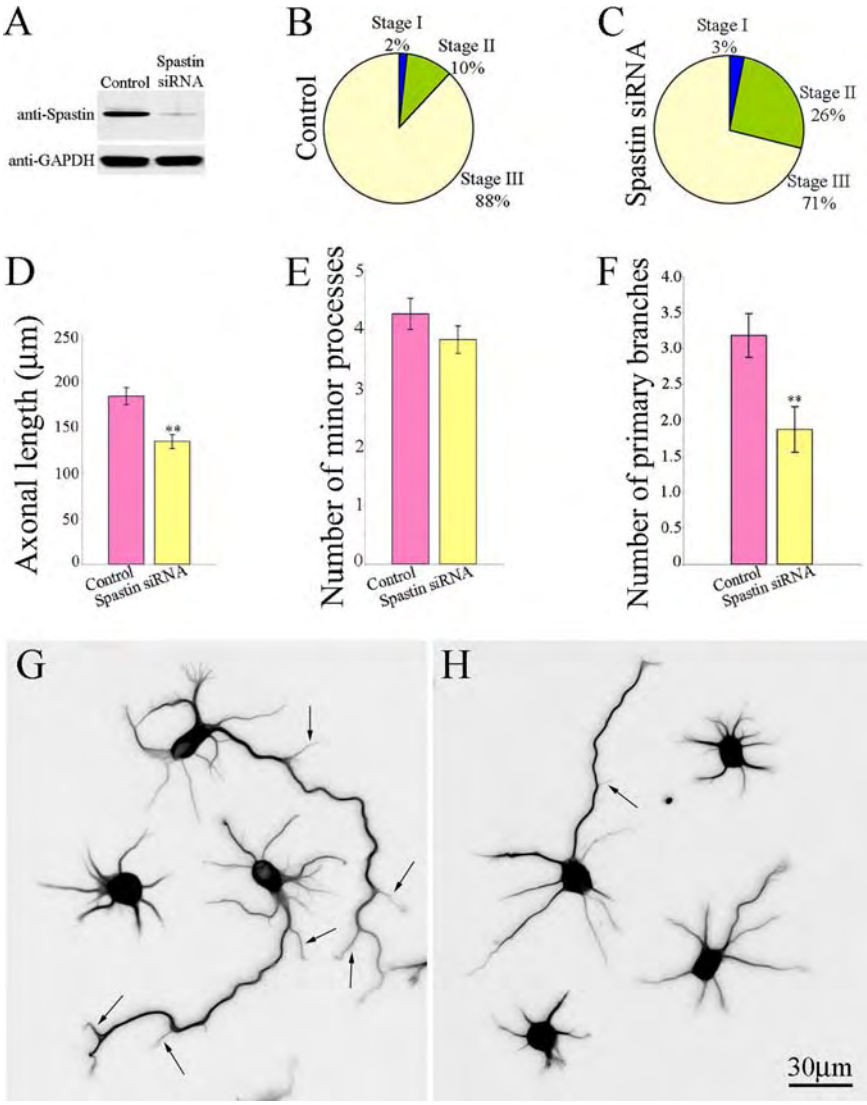

Figure 1. Morphological analysis of control and spastin-depleted hippocampal neurons. (A) Western blot of whole-cell extracts from cultures of rat hippocampal neurons probed with spastin antibody Sp/AAA or GAPDH antibody as an internal control. Cultures were treated with control siRNA or spastin siRNA for 3 d. (B and C) Pie graphs showing the ratio of hippocampal neurons in stage 1, stage 2, or stage 3 in each experimental group ($n > 100$). More neurons remained in stage 1 or stage 2 in spastin-depleted cultures than in control cultures. (D) Quantitative analyses of the lengths of axons in control and spastin-depleted groups ($n > 100$). Axonal length of spastin-depleted neurons is 20% shorter than that of the control group ($p < 0.01$). (E) Quantitative analyses of the number of minor processes in control and spastin-depleted groups ($n > 100$). There is no significant difference between these two groups ($p > 0.05$). (E) Quantitative analyses of the number of primary branches per axon ($n > 100$). For quantification of branches, we chose stage 3 neurons with axons 100–150 μm in length. Depletion of spastin results in 45% reduction of branch numbers ($p < 0.001$). (G and H) Immunostaining of microtubules in control (G) and spastin-depleted (H) hippocampal neurons. Arrows point to axonal branches. Scale bar, 30 μm.

in more than 95% diminution of the spastin protein in the cultures. Spastin-depleted neurons were not dramatically abnormal in their phenotypes, nor did they show indications of being unhealthy. However, as shown in the pie graphs in Figure 1, B and C, 48 h after replating, development was slowed in the neurons depleted of spastin, with more neurons remaining in stages 1 and 2 compared with the control cultures wherein more cells had progressed to stage 3. Comparing cells in stage 3, axons of spastin-depleted neurons were 20% shorter (but had statistically the same number of minor processes) compared with control neurons (Figure 1, D and E). The most dramatic morphological difference was that spastin-depleted neurons displayed 45% fewer axonal branches than control neurons (Figure 1F). Examples of control neurons and spastin-depleted neurons, stained for microtubules, are shown in Figures 1, G and H. More detailed analyses of the microtubule arrays revealed no detectable differences in the overall distribution of microtubules after spastin depletion (data not shown) such as has been reported of neurons with experimentally impaired P60-katanin (Ahmad *et al.*, 1999; Karabay *et al.*, 2004).

Collectively, these results indicate that cultured hippocampal neurons do not require spastin in order to grow axons, to develop branches, or to progress from one developmental stage to the next. However, depletion of spastin does slow or diminish all of these aspects of axonal development. In particular, it is noteworthy that the diminution of axonal branch frequency is over twice as great as the diminution of axonal length, which is consistent with a more specialized role for spastin in branch formation.

Overexpression of Spastin in Cultured Neurons Produces a Markedly Different Phenotype than Overexpression of P60-Katanin

To further test the possibility that the two severing proteins are not identical in their properties, we overexpessed them individually in cultured hippocampal neurons. For controls, neurons were transfected to express EGFP alone. For comparison, neurons were selected from each experimental group that displayed generally similar levels of EGFP fluorescence. For these experiments, neurons were transfected before plating (by nucleofection). Given that high levels of overexpression can severely compromise axonal outgrowth (Karabay *et al.*, 2004), we optimized the parameters of the transfection to achieve levels of expressed P60-katanin or spastin that permitted axons to obtain lengths not dramati-

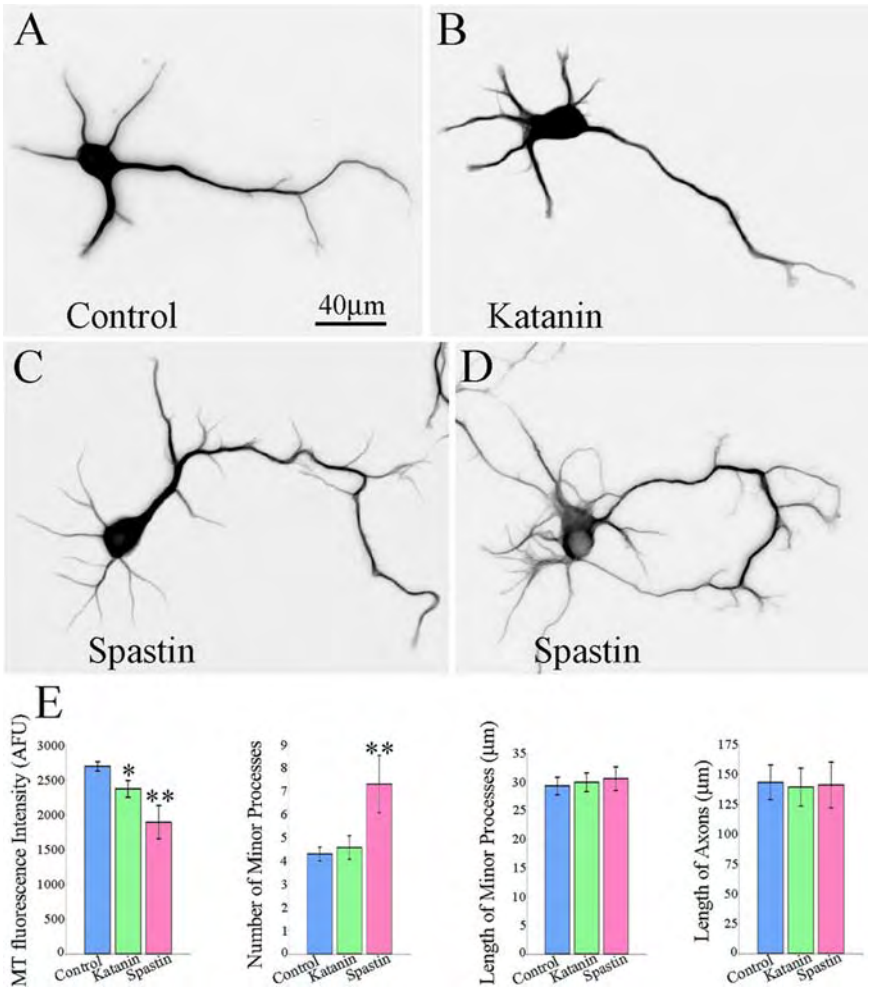

Figure 2. Morphological analyses of stage 3 hippocampal neurons expressing EGFP, EGFP-P60-katanin, or EGFP-spastin. Control (A) and P60-katanin–overexpressing (B) neurons displayed similar morphologies, with 4–6 minor processes and one axon, whereas neurons overexpressing spastin (C and D) displayed more minor processes than control neurons. Quantitative analysis of the microtubule levels, the number of minor process, the length of minor processes and the length of axons are shown in E ($n > 60$). The microtubule levels in the P60-katanin–overexpressing and spastin-overexpressing neurons decreased 12% ($p < 0.05$) and 30% ($p < 0.001$) respectively compared with control neurons. There is a 70% increase of the number of minor processes in hippocampal neurons overexpressing spastin compared with control and P60-katanin–overexpressing neurons ($p < 0.001$). There is no significant difference in the length of minor processes and axons between any of the experimental groups ($p > 0.5$). Scale bar, 40 μm.

cally different from controls. These levels were somewhat lower than in our earlier studies (Karabay *et al.*, 2004; Yu *et al.*, 2005). Figure 2, A–C, shows neurons 24 h after transfection, immunostained for microtubules and then displayed as inverted images to make fine details more obvious. Under these conditions, the neurons overexpressing P60-katanin showed 12% diminution in microtubule mass, whereas the neurons overexpressing spastin showed a somewhat greater loss of microtubule mass (30%). The number of minor processes was not significantly different from controls in neurons overexpressing P60-katanin, but was 70% greater in neurons overexpressing spastin. The lengths of the axon and minor processes were statistically indistinguishable from controls in both cases. Figure 2A shows a control neuron in stage 3. Figure 2B shows a neuron overexpressing P60-katanin. Figure 2C shows a typical spastin-overexpressing neuron. Figure 2D shows another spastin-overexpressing neuron but 48 h after plating to demonstrate that the phenotype continues to become more complex over time. The data, shown in Figure 2E, correspond to the 24-h time point. Figure 3 shows neurons immunostained for microtubules and EGFP. It is apparent from the EGFP staining that the processes are not only more numerous in spastin-overexpressing neurons compared with P60-katanin–overexpressing neurons, and the processes also bear large numbers of short lateral extensions deficient in microtubules.

The most dramatic observation about phenotype was a marked increase in axonal branching in the spastin-overexpressing neurons but not in the P60-katanin–overexpressing neurons. Figure 4 shows higher magnification images of axons overexpressing spastin for 24 h. The first column shows microtubule stains, whereas the second column shows the EGFP-spastin. The third column is a color overlay of the microtubules in red and the EGFP-spastin in green. Shown are axonal arbors from three different neurons displaying varying degrees of branch formation. We defined branches as somewhat thickened lateral extensions containing multiple microtubules. Thin lateral extensions not (yet) invaded by multiple microtubules were called filopodia. The first row shows the early stages of filopodial formation along the length of the axon. The second row shows longer and more numerous lateral extensions (early branches) into which microtubules have started to invade. The third row shows numerous short branches containing microtubules. Panel D shows quantification of the observations. The number of filopodia along minor processes and axons in spastin-overexpressing neurons increased 8 and 28 times, respectively, compared with control neurons ($p < 0.0001$). The axonal branches in spastin-overexpressing neurons increased three times relative to control neurons ($p < 0.001$). There was no significant difference between control and P60-katanin–overexpressing neurons in the number of filopodia along minor processes and axon, or the number of axonal branches ($p > 0.05$). Figure 5 shows inverted images of neurons overexpressing EGFP-spastin and then immunostained for microtubules and EGFP. The dramatic increase

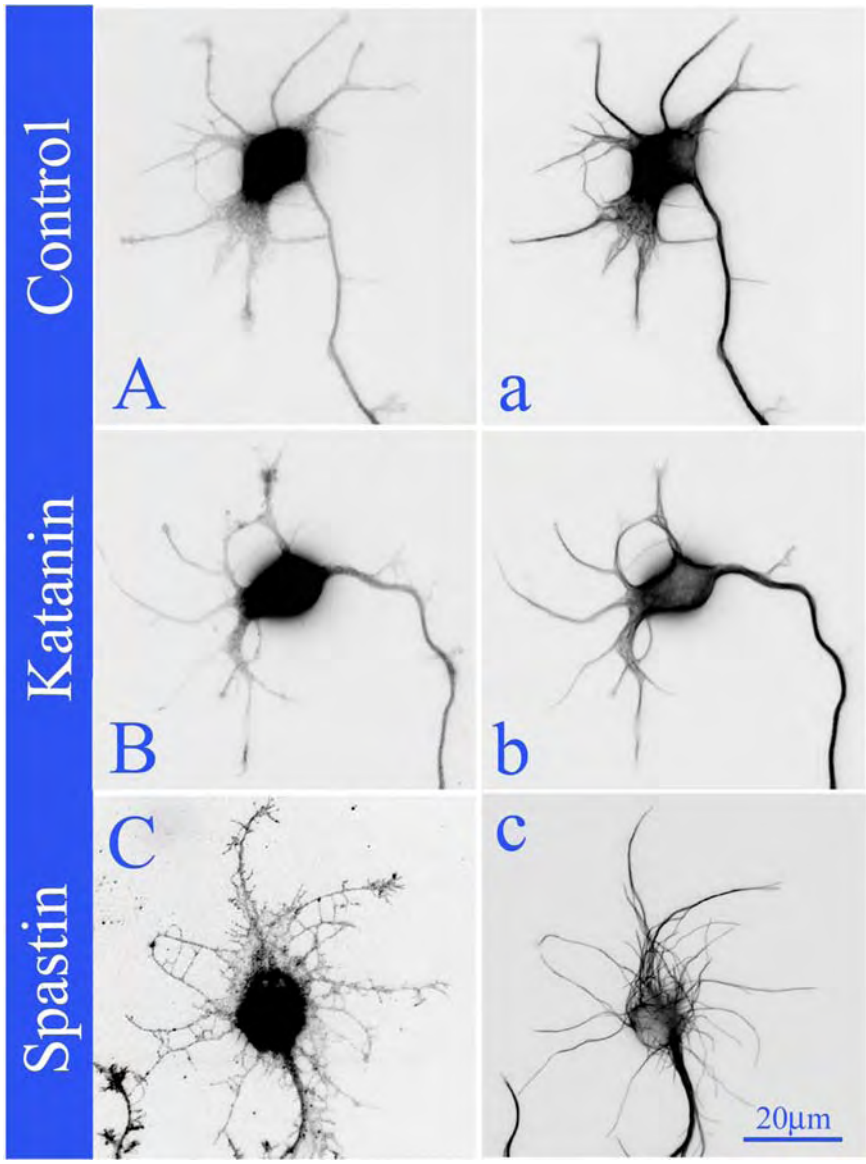

Figure 3. Comparison of hippocampal neurons expressing EGFP (Aa), EGFP-P60-katanin (Bb), or EGFP-spastin (Cc). The left column (A–C) shows EGFP staining, and the right column shows microtubule staining (a–c). To show the cellular morphology in greater detail, the images were displayed as "inverted images" (see *Materials and Methods*). The neurons expressing EGFP and EGFP-P60-katanin showed an average of about five minor processes with a few filopodia (Aa and Bb), whereas the neuron expressing EGFP-spastin showed a dramatic increase of the number of filopodia on the minor processes (Cc). The microtubule levels in the cell body of the EGFP-spastin–expressing neurons (c) are lower than in the cell body of EGFP-P60-katanin-expressing neurons (b). Scale bar, 20 μm.

in branches frequency is apparent at 24 h of overexpression (Figure 5Aa). These newly formed branches are not transient (i.e., they do not retract after reaching ~10 μm in length; see Yu *et al.*, 1994), but rather persist and elongate as shown in images taken at 48 h (Figure 5Bb) and 72 h (Figure 6, Aa and Bb).

Distribution of Spastin in Developing Axons

We previously reported that P60-katanin is relatively evenly distributed along the length of the axon and only slightly enriched in growth cones and branch points of cultured hippocampal neurons (Yu *et al.*, 2005). Our observations thus far described on overexpression of spastin suggest that the distribution of endogenous spastin may be very different from that of P60-katanin, at least during some stages of axonal development. In early axons, the EGFP-spastin appeared to distributed relatively evenly along the axon, but in late stage 3 neurons, with more highly developed axons, it was common for the growth cones to be highly enriched with EGFP-spastin, and the same was true (but to a lesser extent) of many of the sites where early branches emerge (see Figures 4–6). To address the issue of endogenous spastin distribution, we immunostained cultures at various points during development, using the Sp/Sp5 antibody. As shown in Figure 7A, the staining was relatively even along younger axons. In late stage 3 and stage 4 neurons, the immunostains revealed notable enrichments of endogenous spastin in many, but not all, of the growth cones and sites of early branch formation (Figure 7B). Notably, these enrichments, when they occur, are far more dramatic than any of the enrichments ever observed in our previous studies on P60-katanin, with many times the levels of spastin in these growth-related regions compared with other regions along the shaft of the axon. These results are consistent with earlier observations that spastin tends to localize in discrete patches along the length of the axon (Svenson *et al.*, 2005) and also in the distal regions of axons (Errico *et al.*, 2004). We would conclude that, although spastin is less abundant in the neuron than P60-katanin, it has a higher propensity to concentrate at growth-related sites along the axon.

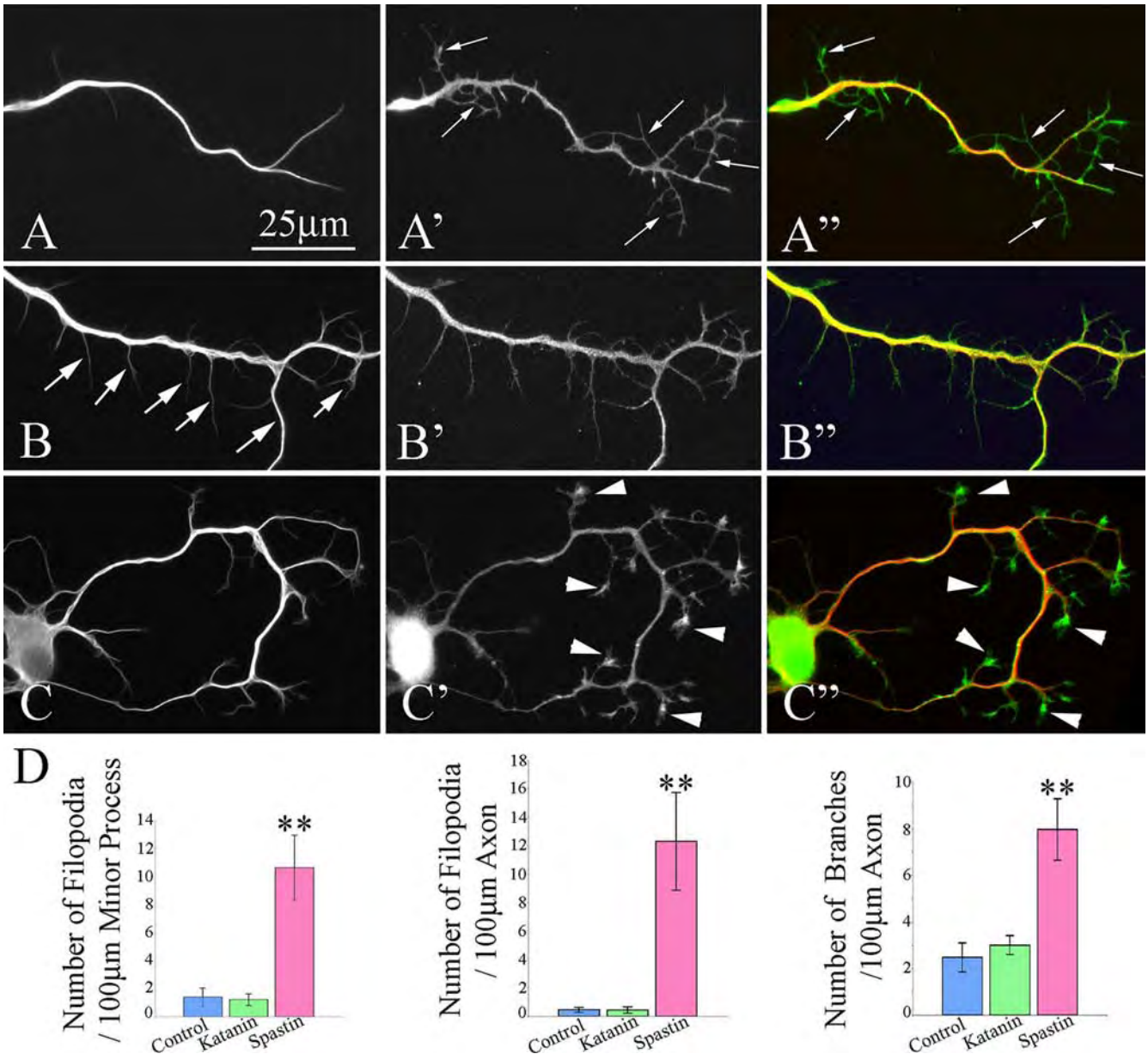

Figure 4. Overexpression of spastin in hippocampal neurons results in a dramatic increase in the number of branches and the number of filopodia on minor processes, axon, and axonal branches. The first column shows microtubule stains, whereas the second column shows the EGFP-spastin. The third column is a color overlay of the microtubules in red and the EGFP-spastin in green. (A, A′, and A″) An axon had many early filopodia along it with no microtubule invasion into the filopodia (small arrows). (B, B′, and B″) An axon with a number of longer filopodia; microtubules have started to invade the filopodia (large arrows). (C, C′, and C″) An axon with several branches. There was an enrichment of EGFP-spastin at the tips of the axons and their branches (arrowheads). Quantitative analyses of the filopodia number on minor processes and axons as well as the number of axonal branches are shown in D ($n > 60$ for each quantitative analysis). Y-axis shows the number of filopodia or branches per 100 μm minor process or axon. There was no significant difference between control and EGFP-P60-katanin–expressing neurons in terms of the number of filopodia along minor process and axon and the number of axonal branches ($p > 0.05$). EGFP-spastin, in contrast, caused a dramatic increase of the filopodia number on minor processes and axons ($p < 0.001$). The number of axonal branches also increased about three times for EGFP-spastin–expressing neurons compared with control neurons ($p < 0.001$). Scale bar, 25 μm.

Overexpression of Spastin Produces a Markedly Different Pattern of Microtubule Severing than Overexpression of P60-Katanin

The results described thus far indicate that overexpressed spastin degrades the microtubule array by 15–20% more than a roughly equal amount of overexpressed P60-katanin. However, neurons expressing higher levels of P60-katanin did not show the morphological characteristics of neurons overexpressing spastin (Karabay *et al.*, 2004; Yu *et al.*, 2005). For this reason, we hypothesized that the patterns of microtubule severing produced by each of the two severing proteins might be distinctive for reasons other than just the degree of microtubule loss. As a first step toward testing this hypothesis, we compared the microtubule arrays in cultured

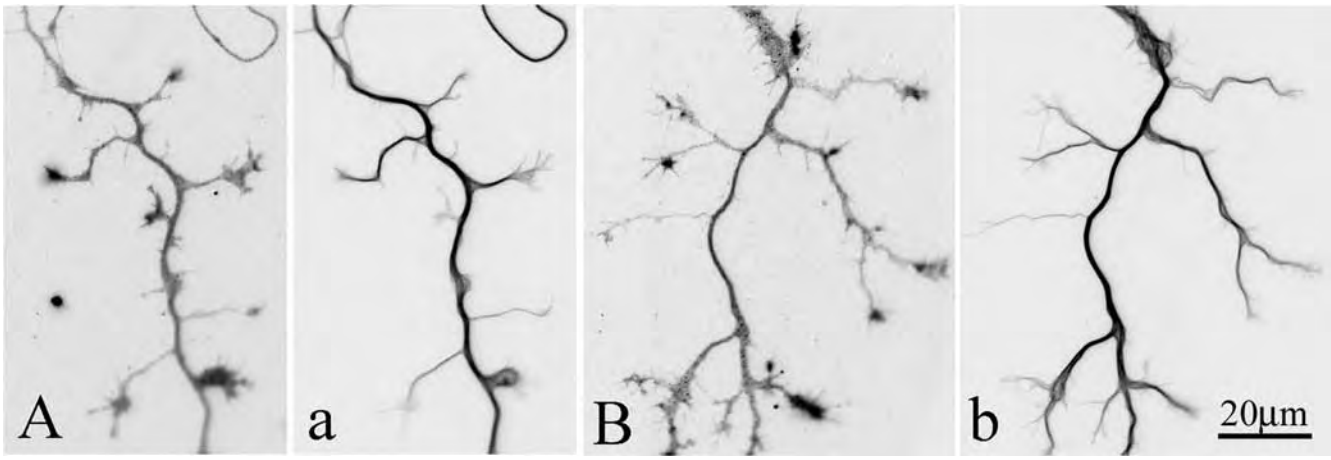

Figure 5. Early stage 3 hippocampal neurons expressing EGFP-spastin, immunostained for EGFP and microtubules. The axons shown here are from the same experiment as shown in Figure 4. Here, two different axons from EGFP-spastin–expressing neurons are displayed as higher magnification "inverted images" to reveal more detail. (A and B) EGFP staining; (a and b) microtubule staining. Aa shows an axon with somewhat shorter branches, whereas the branches of the axon shown in Bb are more developed. The number of filopodia and branches along these axons are much higher than would be observed in controls (see Figure 4). Scale bar, 20 μm.

rat RFL-6 fibroblasts in which we overexpressed each of the two severing proteins. Fibroblasts are very flat and hence permit more spatial resolution than is possible in neurons. Expression was for 12 h, a time frame selected to optimize detection of differences between the two severing proteins. As shown in Figure 8, control cells contained almost exclusively long microtubules (Figure 8A), whereas P60-katanin–overexpressing cells showed a mixture of short and long microtubules (Figure 8B). In sharp contrast, the spastin-overexpressing cells displayed a much more "evenly chopped" microtubule array, with almost exclusively short microtubules, a few microns in length (Figure 8C). Quantification of microtubule free ends showed a fivefold increase in P60-katanin–overexpressing cells ($p < 0.001$), but a 39-fold increase in spastin-overexpressing cells ($p < 0.00001$).

We next examined neurons overexpressing each of the two severing proteins for 12 h (using Lipofectamine 2000 for transfections). We previously reported that the microtubules

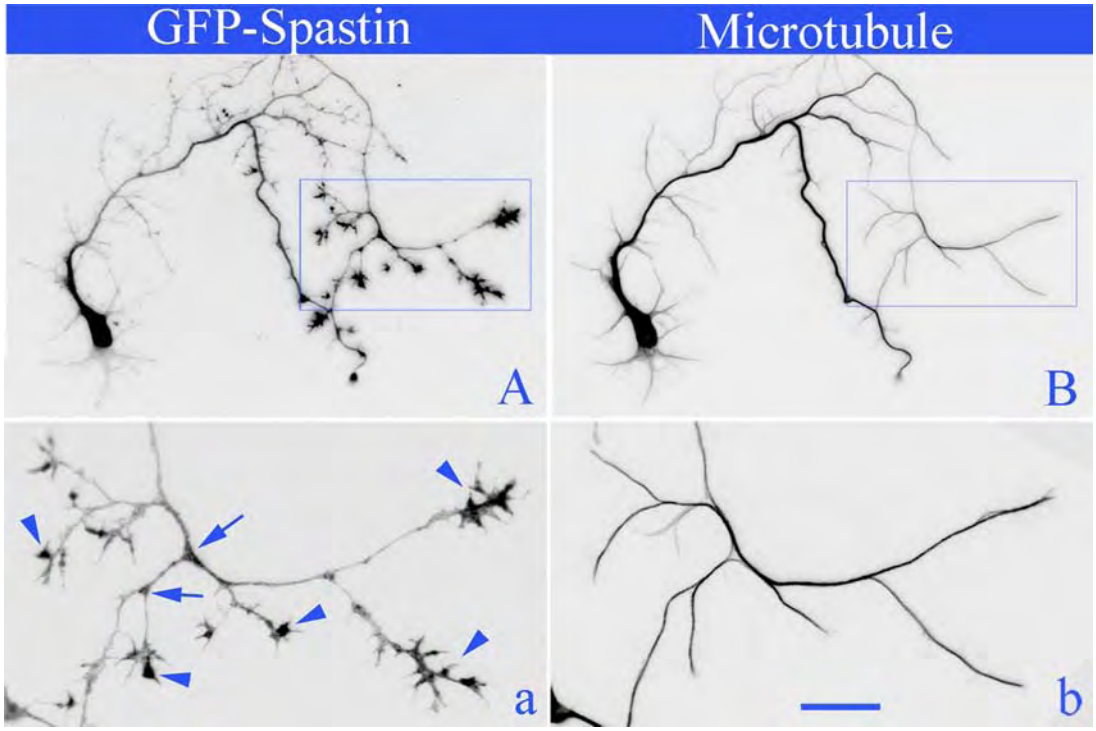

Figure 6. Late stage 3 hippocampal neurons expressing EGFP-spastin, immunostained for EGFP and microtubules. Neurons are displayed as "inverted images" to reveal more detail. Aa shows EGFP staining; Bb show microtubule staining. (a and b) Enlarged images from the regions of A and B indicated by rectangles. Note that GFP-spastin is enriched in growth cones (arrowheads) and also (but to a lesser extent) at branch points (arrows). Scale bar, (A and B) 40 μm; (a and b) 15 μm.

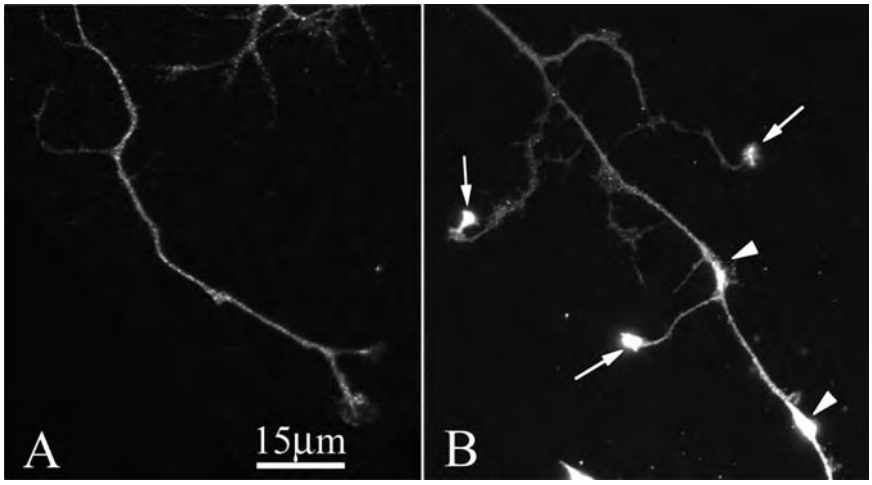

Figure 7. Immunolocalization of spastin in early stage 3 and stage 4 hippocampal neurons. (A) the axon of an early stage 3 (day 2 culture) hippocampal neuron immunostained with Sp/Sp5 antibody; (B) the axon of a stage 4 (day 10 culture) hippocampal neuron immunostained with Sp/Sp5 antibody. The stage 3 axon shows a relatively even distribution of spastin along its length. The stage 4 axon shows accumulations of spastin in growth cones (arrows), some but not all branch points (upper arrowhead) and at sites that we suspect may soon give rise to new branches (lower arrowhead). Scale bar, 15 μm.

in the axon are more resistant to severing over a 12-h bout of overexpression of P60-katanin than microtubules in other compartments of the neuron (Yu *et al.*, 2005; Qiang *et al.*, 2006). Figure 9A shows a control neuron, stained for microtubules. Figures 9, B and C, show neurons overexpressing P60-katanin or spastin, respectively, for 12 h and then stained for microtubules. The neuron overexpressing P60-katanin shows a clear diminution of microtubule mass from the cell body (to about half of control levels), whereas the axon continues to show robust microtubule staining comparable to controls. We then selected spastin-overexpressing neurons that displayed roughly the same degree of diminu-

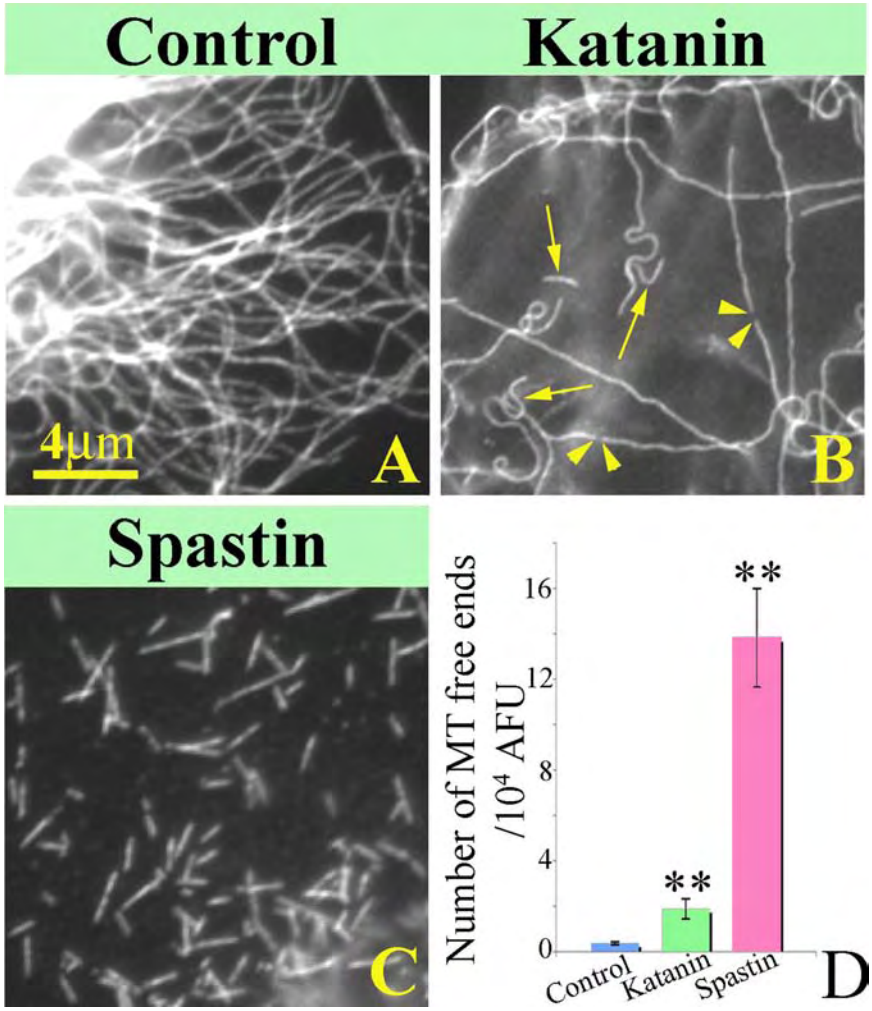

Figure 8. Different microtubule-severing patterns in fibroblasts produced by overexpression of P60-katanin or spastin. (A–C) RFL-6 fibroblasts immunostained for microtubules. (A) Control fibroblast expressing EGFP displaying long continuous microtubules. (B) Fibroblast expressing EGFP-P60-katanin displaying several obvious long microtubules together very few short ones. Arrows point to short microtubules. Arrowheads point to a microtubule being severed. (C) Fibroblast expressing EGFP-spastin displaying only very short microtubules. (D) Quantitative analyses of the number of microtubule free ends per 10^4 AFU of microtubules among the control, P60-katanin–overexpressing, and spastin-overexpressing groups ($n > 100$). Overexpression of P60-katanin creates fivefold more free microtubule ends than in the control group ($p < 0.001$). Overexpression of spastin creates 39-fold more free microtubule ends than in the control group ($p < 0.001$). Scale bar, 4 μm.

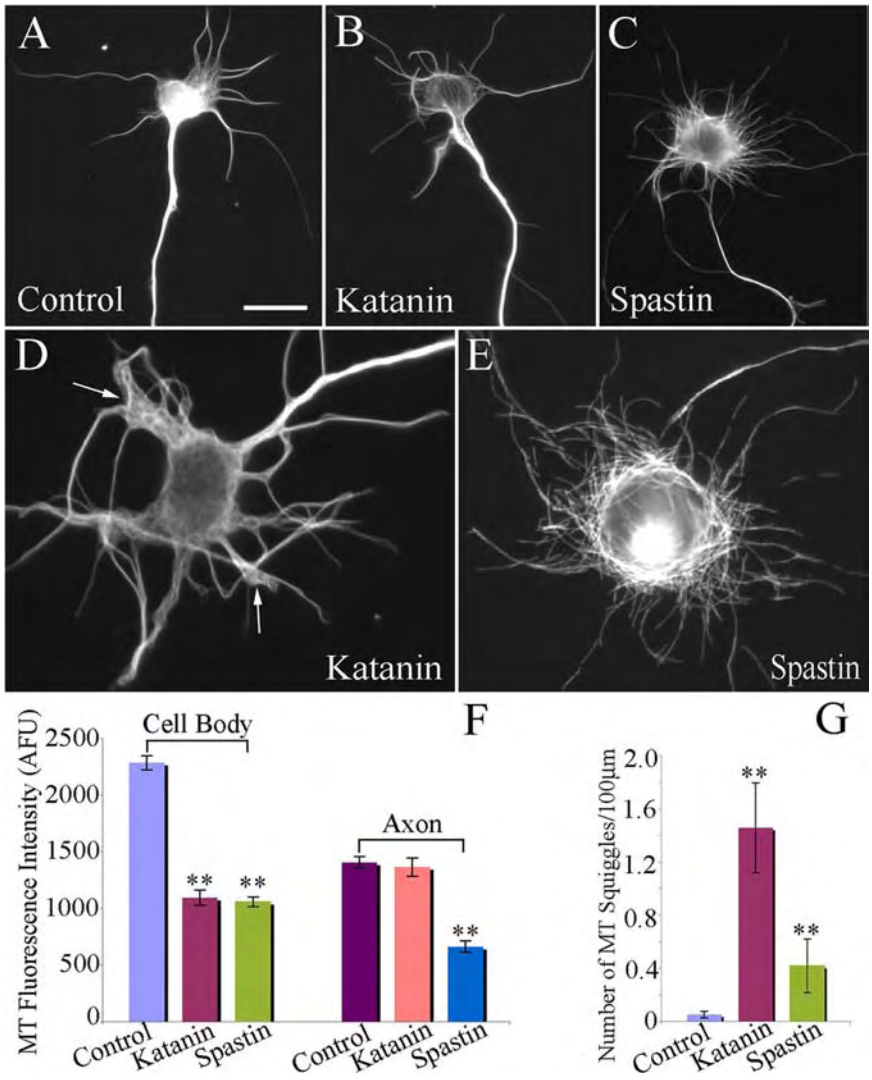

Figure 9. Axonal microtubules are resistant to a 12-h bout of overexpression of P60-katanin, but not spastin. (A–E) The immunostains of microtubules of the hippocampal neurons. (A) Neuron transfected with EGFP control. (B and D) Two neurons transfected to overexpress P60-katanin. (C and E) Two neurons transfected to overexpress spastin. (F) Quantitative analyses of microtubule fluorescence intensity in cell bodies and axons among the three groups (control, overexpression of P60-katanin, and overexpression of spastin). Overexpression of P60-katanin or spastin results in notable microtubule loss from cell bodies compared with control (52% for P60-katanin, $p < 0.001$; 54% for spastin, $p < 0.001$). In axons, overexpression of P60-katanin for 12 h results in no significant diminution of microtubules ($p > 0.05$), whereas overexpression of spastin reduces the microtubule levels by 53% compared with controls ($p < 0.001$). (G) Quantitative analyses of the number of microtubule "squiggles" along the processes per 100 μm ($n > 40$). Overexpression of P60-katanin increased the number of microtubule squiggles by 29-fold ($p < 0.0001$) compared with controls. By contrast, overexpression of spastin increased the number of microtubule squiggles by only eightfold ($p < 0.001$) compared with controls. Arrows point to the microtubule squiggles in the neuron overexpressing P60-katanin. Scale bar, (A–C) 15 μm; (D and E) 8 μm.

tion of microtubule levels from the cell body, so that we could compare the relative effects on the axon. Unlike neurons overexpressing P60-katanin, these neurons also displayed a reduction of microtubule levels in the axon by about half (Figure 9F). Thus, microtubules in the axon are more resistant than microtubules elsewhere in the neuron to P60-katanin but not to spastin. In addition, a marked difference in the microtubule-severing patterns of the two severing proteins is apparent from the micrographs. As previously reported, neurons overexpressing P60-katanin often show very long microtubules that tend to become twisted into shapes we call "squiggles" (Figure 9D). As shown in Figure 9G, such squiggles occurred far less frequently in neurons overexpressing spastin, which is consistent with the lack of a resistant population of long microtubules that fail to be severed by spastin. By contrast, there are abundant short microtubules in the spastin-overexpressing neurons, whereas short microtubules are less plentiful in the P60-katanin overexpressing neurons (Figure 9, D and E).

Tau Protects Microtubules Less Well from Spastin than P60-Katanin

The very different patterns of microtubule severing produced by overexpressing each of the two severing proteins suggest that they have different properties or are regulated differently in cells. We previously reported that the ability of P60-katanin to sever microtubules is attenuated by the presence of tau on the microtubules (Qiang *et al.*, 2006). This was evidenced by the fact that depleting tau from neurons before overexpressing P60-katanin rendered the microtubules in the axon equally sensitive to the microtubules in other regions of the neuron. Moreover, microtubules in RFL-6 fibroblasts were rendered highly resistant to severing when tau was coexpressed with P60-katanin. The fact that axonal microtubules are no more resistant to spastin than microtubules elsewhere in the neuron suggests that tau may not be as good at protecting microtubules against spastin. To investigate this, we performed the same type of overexpression experiments on RFL-6 fibroblasts for spastin as we previously conducted for P60-katanin (Qiang *et al.*, 2006). Figure 10, A and B, shows a control fibroblast and a fibroblast expressing tau (specifically, tau 4R), both stained for microtubules. When P60-katanin is overexpressed in control fibroblasts, there is a severe loss of microtubule mass, with the remaining microtubules appearing shorter than in controls (Figure 10C). Fibroblasts expressing tau display no detectable alterations in the microtubule array when P60-katanin is overexpressed (Figure 10D). When spastin is over-

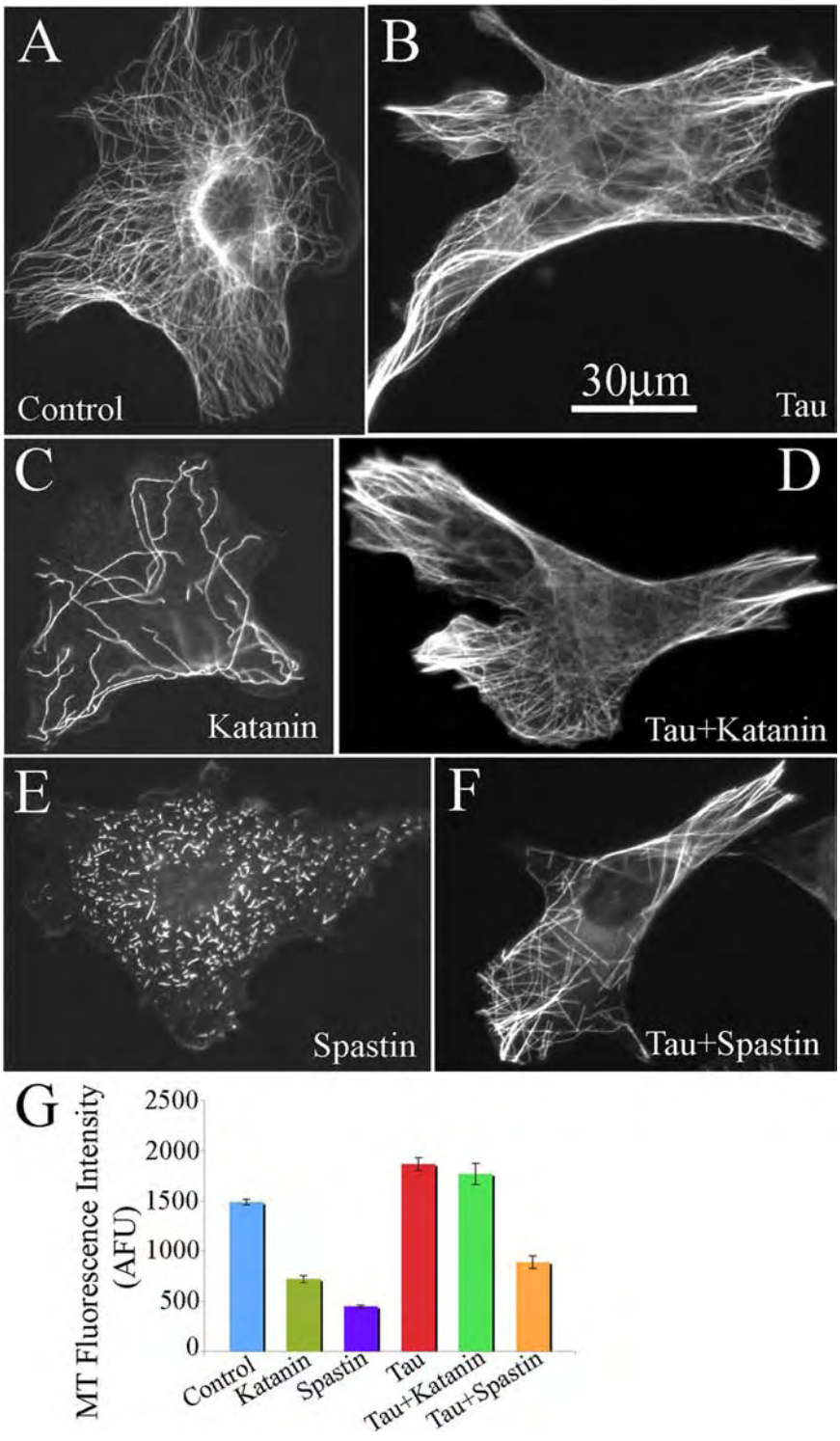

Figure 10. Tau provides stronger protection against microtubule severing by P60-katanin than by spastin. (A–F) RFL-6 fibroblasts immunostained for microtubules. (A) Control cell transfected to express EGFP. (B) Cell transfected to express tau 4R. Tau expression causes the formation of dense bundles of microtubules. (C) Cell transfected to overexpress P60-katanin. Microtubule mass is diminished, with remaining microtubules displaying a variety of lengths. (D) Cell transfected to overexpress P60-katanin and express tau 4R. Microtubules in the tau-expressing cell show no indication of severing by overexpression of P60-katanin, and the microtubule mass is not reduced. (E) Cell transfected to overexpress spastin. Microtubules are severed into a large number of very short ones. (F) Cell transfected to express both spastin and tau. There is a reduction of microtubule mass, but several microtubule bundles together with some individual ones are preserved. (G) Quantitative analyses of microtubule mass in fibroblasts induced to overexpress P60-katanin or overexpress spastin together with tau ($n > 50$). Compared with the control, overexpression of P60-katanin reduces the level of microtubules by 52% ($p < 0.01$), whereas overexpression of spastin reduces the level by 70% ($p < 0.01$). Expression of tau increases the microtubule level by 19%. Compared with the microtubule levels of the cells expressing tau alone, the levels of cells expressing tau and overexpressing P60-katanin are not significantly different ($p > 0.05$); however, expression of both tau and spastin causes 53% loss of microtubule levels compared with the expression of tau alone ($p < 0.01$). Scale bar, 30 μm.

expressed in the fibroblasts, there is a 20% greater loss of microtubule mass compared with when P60-katanin is overexpressed, and the individual remaining microtubules are generally shorter than the microtubules in the fibroblasts overexpressing P60-katanin (Figure 10E). When spastin is overexpressed in the fibroblasts expressing tau, the microtubule mass is diminished by about half (Figure 10F). Quantification of microtubule levels is shown in Figure 10G. Taken together, these results indicate that tau affords some protection of microtubules from each of the severing proteins, but that the protection is greater in the case of P60-katanin than spastin.

Depletion of tau from Hippocampal Neurons Enhances Axonal Branch Formation Whether or Not Spastin Is Also Depleted

In previous studies, we documented that P60-katanin's access to the microtubule lattice is restricted by the presence of

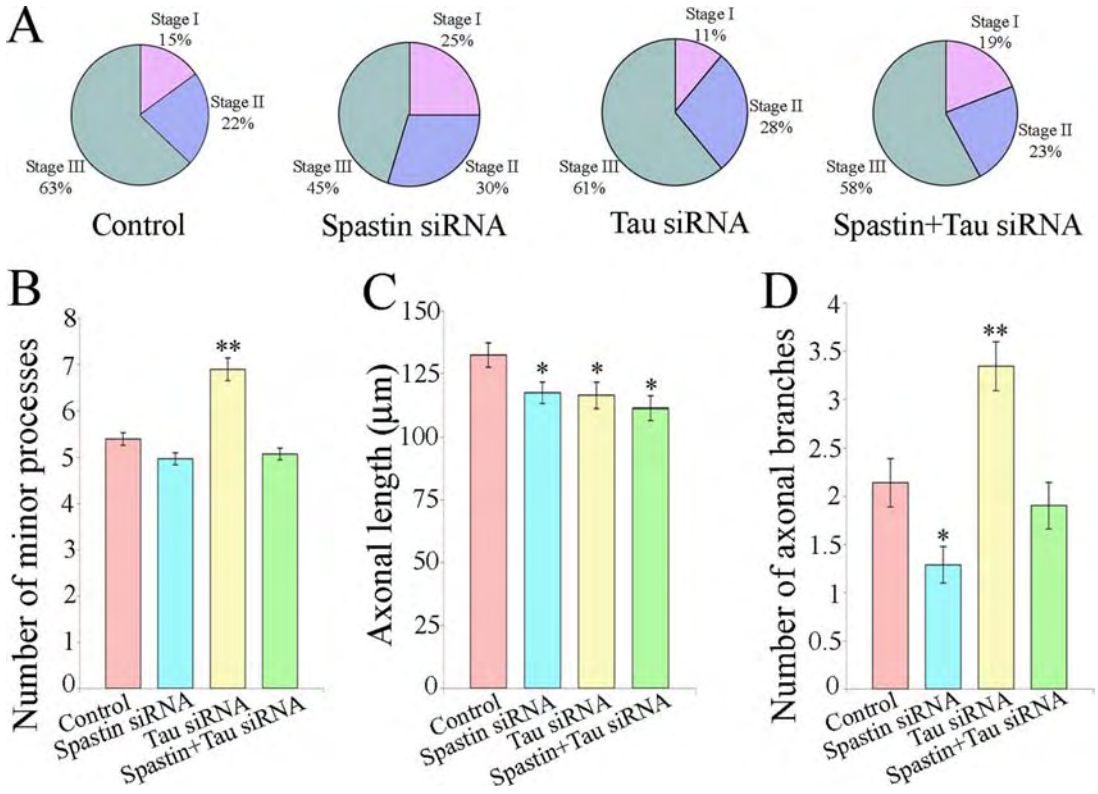

Figure 11. Depletion of tau from hippocampal neurons increases the numbers of axonal branches by a mechanism that does not require spastin. Neurons were treated with either control siRNA, tau siRNA, spastin siRNA, or a combination of tau siRNA and spastin siRNA. (A) Pie graphs showing the ratio of hippocampal neurons in stage 1, stage 2, or stage 3 in each experimental group ($n > 200$). More neurons remained in stage 1 or stage 2 in spastin-depleted cultures than in control cultures. There is no significant difference between the tau-depleted group and the control group or between the spastin+tau-double-depleted group and the control group. (B) Quantitative analyses of the number of minor processes in stage 3 hippocampal neurons. Only in the tau siRNA treated group does the number increase by 28% ($p < 0.001$). Compared with control, the other two groups showed no significant difference ($p > 0.05$; $n > 200$). (C) Quantitative analyses of axonal lengths of stage 3 hippocampal neurons. Compared with control, axonal lengths decrease by 11% ($p < 0.01$), 12% ($p < 0.01$), and 16% ($p < 0.01$) in the spastin-depleted group, the tau-depleted group, and the spastin+tau-double depleted group, respectively ($n > 200$). (D) Quantitative analyses of number of primary axonal branches in stage 3 hippocampal neurons. For quantification of branches, we chose stage 3 neurons with axons 100–150 μm in length. Compared with the control group, there is a 40% ($p < 0.01$) decrease in the number of axonal branches in the spastin-depleted group and a 56% ($p < 0.0001$) increase of the number of axonal branches in the tau-depleted group. There is no significant difference between the control and spastin+tau-double-depleted groups ($p > 0.05$; $n > 200$).

tau molecules on the surface of the microtubule (Qiang *et al.*, 2006). On this basis, we proposed a "tau-protection" model for the formation of axonal branches in which tau is locally detached from microtubules (presumably by its phosphorylation) at sites of impending branch formation; as a result, P60-katanin is able to avidly sever the microtubules into short pieces, specifically in this locale (Baas and Qiang, 2005; Baas *et al.*, 2006). At the time we proposed this model, we had not yet performed any experiments on spastin, but our current studies (see above) suggest that if a tau-protection–based mechanism does exist for axonal branching, that it would probably pertain to P60-katanin more so than to spastin. To investigate this matter, we tested the prediction that axons of neurons depleted of tau with siRNA would display more branches than control axons. We also combined siRNA for tau with siRNA for spastin, to determine whether such an effect still occurs in the absence of spastin. Neurons were treated with control siRNA, or tau siRNA, or spastin siRNA, or the combination of both tau and spastin siRNA. After allowing 3 d for spastin and tau to be depleted (Qiang *et al.*, 2006), the neurons were replated and allowed to develop processes for 24 h before being fixed.

In all cases, the majority of the neurons were in stage 3 after this experimental regime, except in the spastin-depleted group, in which there were greater numbers of neurons in the earlier stages (Figures 1C and 11A). Interestingly, in the double-knockdown (depletion of tau and spastin) group, the suppression of development induced by spastin siRNA was rescued (Figure 11A). This may be because tau depletion results in an increase in microtubule severing, whereas spastin depletion results in a decrease in microtubule severing. The number of minor processes was increased by 28% as a result of tau depletion (Figure 11B); which is reminiscent of the increases in minor processes observed when either P60-katanin or spastin is overexpressed (see Figure 2; see also Yu *et al.*, 2005). Although spastin depletion within itself did not significantly lower the number of minor processes, the depletion of spastin did appear to prevent the depletion of tau from increasing the number of minor processes. In all experimental groups, axonal lengths were shorter than in controls (Figure 11C).

With regard to branching, depletion of tau increased the number of branches by 56% (Figure 11D), consistent with the predictions of our tau-protection hypothesis. In neurons

depleted of spastin, the number of branches was 40% lower than controls. In neurons depleted of both tau and spastin, the number of branches was indistinguishable for controls, indicating that depletion of tau is able to increase branching even, whereas the depletion of spastin is having the opposite effect on branching. These results indicate that the increase in axonal branching associated with tau depletion occurs whether or not spastin is present and hence support the conclusion that a tau-based mechanism for axonal branching functions mainly via P60-katanin.

DISCUSSION

In various studies, including this one, we have never observed an increase in axonal branch formation associated with experimental elevation of P60-katanin (Karabay *et al.*, 2004; Yu *et al.*, 2005; Qiang *et al.*, 2006). However, here we found a very dramatic and consistent elevation in axonal branch formation associated with overexpression of spastin. Thus we would conclude that, in a direct comparison of the two severing proteins, the properties of spastin are more conducive to the formation of branches. In support of this conclusion, depletion of spastin from neurons results in a fairly modest reduction in axonal length, but a far greater reduction in the formation of axonal branches. In addition, spastin has a far greater capacity to concentrate at sites of branch formation (and growth cones) than does P60-katanin. We envision a model wherein neurons contain high levels of P60-katanin that are absolutely essential for the ongoing severing of microtubules needed for axonal growth and contain much lower levels of spastin designed to participate in specialized duties such as axonal branch formation. Even so, it is noteworthy that branches can still form in the absence of spastin, and this is consistent with previous observations on spastin-compromised animals (Sherwood *et al.*, 2004; Trotta *et al.*, 2004; Orso *et al.*, 2005; Tarrade *et al.*, 2006; Wood *et al.*, 2006) and humans (McDermott *et al.*, 2006; Salinas *et al.*, 2007). Our data, presented here, suggest that there are two different modes by which axonal branches can form, one that utilizes spastin and the other than utilizes P60-katanin.

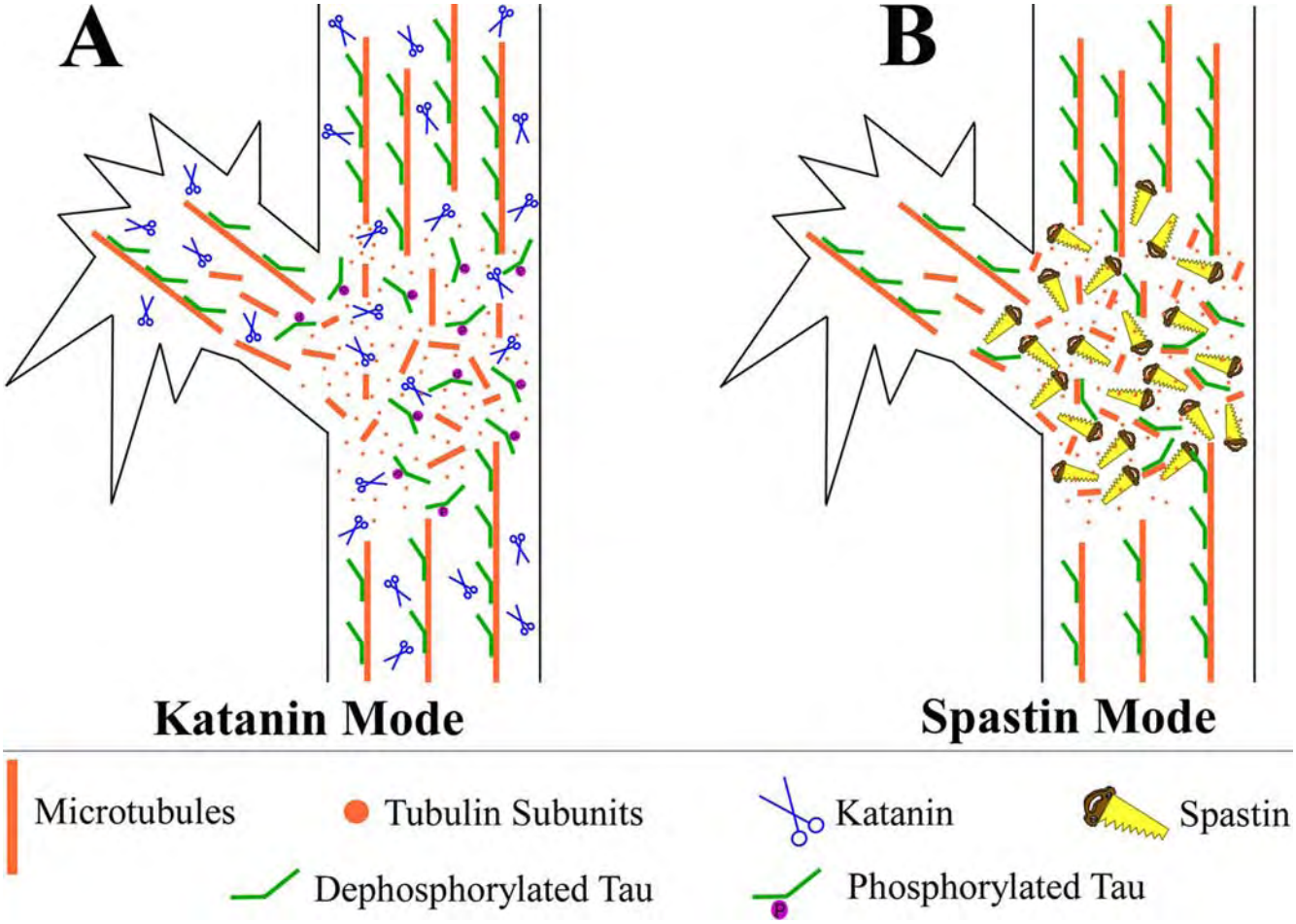

Figure 12. Schematic illustration of two modes by which microtubule severing may be regulated at sites of impending axonal branch formation. Both A and B show the axon undergoing the formation of branch. (A) In the "katanin mode," microtubule severing is enhanced at sites of branch formation by local detachment from the microtubules of proteins such as tau that would otherwise "protect" the microtubule from being accessed by P60-katanin. In the case of tau, which we posit to be the principal protective molecule in the axon, the detachment is induced by local phosphorylation of tau at a site that causes it to lose its attachment to the microtubule. (B) In the "spastin mode," microtubule severing is enhanced at sites of branch formation by the concentration of more spastin molecules specifically at the site where the branch is forming. This mode is independent of whether or not molecules such as tau remain attached to the microtubule. Each of these modes is presumably under the regulation of signaling cascades. The two modes, shown here separately, are not mutually exclusive and may work in tandem during branch formation.

As noted earlier, the sequences of spastin and P60-katanin are very different in regions other than the AAA region responsible for severing microtubules (Errico *et al.,* 2002; Roll-Mecak and Vale, 2005; White *et al.,* 2007). Thus, it may be that the other domains of spastin enable it to influence branch formation by means other than the severing of microtubules. For example, it is known that branch formation requires actin filaments as well as microtubules (Dent and Kalil, 2001), and therefore it is conceivable that spastin influences the actin cytoskeleton in a way that P60-katanin does not. Indeed, the entire morphology of the neuron is markedly altered after spastin overexpression (i.e., greater numbers of filopodia and branches) in a manner not duplicated by P60-katanin overexpression. In the future, it will be of interest to ascertain whether spastin has domains that directly participate in pathways relevant to remodeling of the actin cytoskeleton.

For now, we are persuaded to believe that the dramatic morphological differences produced by the two severing proteins relate directly to their distinct patterns of microtubule severing. We have noticed in the past that overexpression of P60-katanin in neurons can often result in the appearance of very long microtubules that appear to be quite resistant to severing (Yu *et al.,* 2005), and the same observation was made here. By contrast, spastin overexpression appears to produce a far more consistent "even chopping" of the microtubules into small pieces. In other words, we have not detected any evidence for a population of microtubules that are strongly resistant to severing by spastin. Given these different severing patterns, the expectation would be that spastin is capable of producing high concentrations of short microtubules, whereas P60-katanin's properties are more suited for generating mixtures of long and short microtubules. Concentrations of plus ends of microtubules would be expected to recruit a variety of +tips which could also interact with structures within the actin-based cortical regions of the axon (Kornack and Giger, 2005). Thus, the enhanced formation of filopodia and the remodeling of actin required for branches to form could relate directly to the manner by which spastin severs microtubules.

What accounts for the different microtubule-severing patterns of spastin and P60-katanin? Studies on P60-katanin suggest that its severing properties are regulated by phosphorylation, but probably not phosphorylation of P60-katanin itself (Vale, 1991; McNally *et al.,* 2002; Baas and Qiang, 2005). Rather, it appears that in nonneuronal cells, the phosphorylation state of MAP4 is crucial for regulating the degree to which P60-katanin can sever microtubules (McNally *et al.,* 2002). The binding of MAP4 to the microtubule apparently reduces the accessibility of the microtubule to P60-katanin. Phosphorylation of MAP4 causes it to dissociate from the microtubules, thereby permitting more robust severing by P60-katanin. MAP4 is not expressed in CNS neurons, but recent studies from our laboratory indicate that a comparable role is played by tau in the axon (Qiang *et al.,* 2006). The fact that tau and MAP4 are strong protectors against P60-katanin provides an appealing explanation for the severing pattern produced by P60-katanin in fibroblasts and neurons. P60-katanin would preferentially sever microtubules that are less rich in these protective proteins, which would then cause progressively more depolymerization of these microtubules. The molecules of tau or MAP4 that had been associated with these microtubules would then be available to bind to the microtubules that were already richer in these proteins, thereby rendering them even more resistant to severing and enabling them to achieve even greater lengths. In this manner, the properties of P60-katanin would promote a mixture of short and long microtubules.

Our current studies suggest that tau is a far less influential factor in the regulation of spastin's severing properties. The microtubules in the axon, rich in tau, show no greater resistance to spastin overexpression than the tau-deficient microtubules located in other compartments of the neuron. Moreover, axons depleted of tau undergo markedly more branching, and this effect is independent of whether or not spastin is present. These results are consistent with an alternative mechanism for axonal branching based on the properties of P60-katanin. In this mechanism, tau is locally detached from the microtubules at a site of impending branch formation. As a result, P60-katanin can produce the localized chopping of microtubules needed for the branch to form. This idea, which we have discussed in the past (Baas and Qiang, 2005; Baas *et al.,* 2006), does not require a local concentration of P60-katanin, but rather a focal increase in the sensitivity of the microtubules to P60-katanin. This process would presumably be regulated by kinases and phosphatases that phosphorylate or dephosphorylate tau at motifs required for it to bind microtubules. Although our results suggest that tau is probably the main player in such a scenario, there may be other microtubule-associated proteins in the axon that conspire in regulating the sensitivity of the microtubules to P60-katanin.

In conclusion, we propose that there are two modes by which microtubule severing is orchestrated during axonal branch formation, one based on the local concentration of spastin at branch sites and the other based on local detachment from microtubules of molecules such as tau that regulate the severing properties of P60-katanin (see Figure 12). Each of these modes is presumably under the regulation of signaling cascades that regulate such events as the phosphorylation of tau, the attachment or detachment of other protective proteins, and the localization of spastin to sites of impending branch formation. The formation of a particular branch could utilize one mode or the other, or some combination of the two modes, working in tandem.

ACKNOWLEDGMENTS

We thank Kenneth Kosik (University of California, Santa Barbara) for providing a tau construct that we used for some of the studies reported here and Elena Rugarli (National Neurological Institute, Milan, Italy) for providing a human spastin construct that we used for preliminary studies. This work was funded by grants to P.W.B. from the National Institutes of Health, the Spastic Paraplegia Foundation, the Alzheimer's Association, the Department of Defense, and the Craig H. Neilsen Foundation, and by a grant to W.Y. from the Craig H. Neilsen Foundation.

REFERENCES

Ahmad, F. J., Yu, W., McNally, F. J., and Baas, P. W. (1999). An essential role for katanin in severing microtubules in the neuron. J. Cell Biol. *145*, 305–315.

Baas, P. W., and Qiang, L. (2005). Neuronal microtubules: when the MAP is the roadblock. Trends Cell Biol. *15*, 183–187.

Baas, P. W., Karabay, A., and Qiang, L. (2005). Microtubules cut and run. Trends Cell Biol. *15*, 518–524.

Baas, P. W., Vidya, Nadar, C., and Myers, K. A. (2006). Axonal transport of microtubules: the long and short of it. Traffic *7*, 490–498.

Buster, D., McNally, K., and McNally, F. J. (2002). Katanin inhibition prevents the redistribution of gamma-tubulin at mitosis. J. Cell Sci. *115*, 1083–1092.

Claudiani, P., Riano, E., Errico, A., Andolfi, G., and Rugarli, E. I. (2005). Spastin subcellular localization is regulated through usage of different translation start sites and active export from the nucleus. Exp. Cell Res. *309*, 358–369.

Dent, E. W., and Kalil, K. (2001). Axon branching requires interactions between dynamic microtubules and actin filaments. J. Neurosci. *21*, 9757–9769.

Dent, E. W., Callaway, J. L., Szebenyi, G., Baas, P. W., and Kalil, K. (1999). Reorganization and movement of microtubules in axonal growth cones and developing interstitial branches. J. Neurosci. *19*, 8894–8908.

Dotti, C. G., Sullivan, C. A., and Banker, G. A. (1988). The establishment of polarity by hippocampal neurons in culture. J. Neurosci. *8*, 1454–1468.

Errico, A., Ballabio, A., and Rugarli, E. I. (2002). Spastin, the protein mutated in autosomal dominant hereditary spastic paraplegia, is involved in microtubule dynamics. Hum. Mol. Genet. *11*, 153–163.

Errico, A., Claudiani, P., D'Addio. M., and Rugarli, E. I. (2004). Spastin interacts with the centrosomal protein NA14, and is enriched in the spindle pole, the midbody and the distal axon. Hum. Mol. Genet. *13*, 2121–2132.

Evans, K. J., Gomes, E. R., Reisenweber, S. M., Gundersen, G. G., and Lauring, B. P. (2005). Linking axonal degeneration to microtubule remodeling by Spastin-mediated microtubule severing. J. Cell Biol. *168*, 599–606.

Karabay, A., Yu, W., Solowska, J. M., Baird, D. H., and Baas, P. W. (2004). Axonal growth is sensitive to the levels of katanin, a protein that severs microtubules. J. Neurosci. *24*, 5778–5788.

Kornack, D. R., and Giger, R. J. (2005). Probing microtubule +TIPs: regulation of axon branching. Curr. Opin. Neurobiol. *15*, 58–66.

Ma, D. L., Chia, S. C., Tang, Y. C., Chang, M. L., Probst, A., Burgunder, J. M., and Tang, F. R. (2006). Spastin in the human and mouse central nervous system with special reference to its expression in the hippocampus of mouse pilocarpine model of status epilepticus and temporal lobe epilepsy. Neurochem. Int. *49*, 651–664.

McDermott, C. J. *et al.* (2006). Clinical features of hereditary spastic paraplegia due to spastin mutation. Neurology *67*, 45–51.

McNally, K. P., Buster, D., and McNally, F. J. (2002). Katanin-mediated microtubule severing can be regulated by multiple mechanisms. Cell Motil. Cytoskelet. *53*, 337–349.

Orso, G., Martinuzzi, A., Rossetto, M. G., Sartori, E., Feany, M., and Daga, A. (2005). Disease-related phenotypes in a *Drosophila* model of hereditary spastic paraplegia are ameliorated by treatment with vinblastine. J. Clin. Invest. *115*, 3026–3034.

Qiang, L., Yu, W., Andreadis, A., Luo, M., and Baas, P. W. (2006). Tau protects microtubules in the axon from severing by katanin. J. Neurosci. *26*, 3120–3129.

Roll-Mecak, A., and Vale, R. D. (2005). The *Drosophila* homologue of the hereditary spastic paraplegia protein, spastin, severs and disassembles microtubules. Curr. Biol. *15*, 650–655.

Roll-Mecak, A., and Vale, R. D. (2006). Making more microtubules by severing: a common theme of noncentrosomal microtubule arrays? J. Cell Biol. *175*, 849–851.

Salinas, S., Carazo-Salas, R. E., Proukakis, C., Schiavo, G., and Warner, T. T. (2007). Spastin and microtubules: functions in health and disease. J. Neurosci. Res. *85*, 2778–2782.

Salinas, S., Carazo-Salas, R. E., Proukakis, C., Cooper, J. M., Weston, A. E., Schiavo, G., and Warner, T. T. (2005). Human spastin has multiple microtubule-related functions. J. Neurochem. *95*, 1411–1420.

Sambrook, J., Fritsch, E. F., Maniatis, T. (1989). Molecular Cloning: A Laboratory Manual, 2nd ed., Cold Spring Harbor, NY: Cold Spring Harbor Laboratory Press.

Sherwood, N. T., Sun, Q., Xue, M., Zhang, B., and Zinn, K. (2004). *Drosophila* spastin regulates synaptic microtubule networks and is required for normal motor function. PLoS. Biol. *2*, e429.

Svenson, I. K., Kloos, M. T., Jacon, A., Gallione, C., Horton, A. C., Pericak-Vance, M. A., Ehlers, M. D., and Marchuk, D. A. (2005). Subcellular localization of spastin: implications for the pathogenesis of hereditary spastic paraplegia. Neurogenetics *6*, 135–141.

Tarrade, A. *et al.* (2006). A mutation of spastin is responsible for swellings and impairment of transport in a region of axon characterized by changes in microtubule composition. Hum. Mol. Genet. *15*, 3544–3558.

Trotta, N., Orso, G., Rossetto, M. G., Daga, A., and Broadie, K. (2004). The hereditary spastic paraplegia gene, spastin, regulates microtubule stability to modulate synaptic structure and function. Curr. Biol. *14*, 1135–1147.

Vale, R. D. (1991). Severing of stable microtubules by a mitotically activated protein in *Xenopus* egg extracts. Cell *64*, 827–839.

White, S. R., Evans, K. J., Lary, J., Cole, J. L., and Lauring, B. (2007). Recognition of C-terminal amino acids in tubulin by pore loops in Spastin is important for microtubule severing. J. Cell Biol. *176*, 995–1005.

Wood, J. D., Landers, J. A., Bingley, M., McDermott, C. J., Thomas-McArthur, V., Gleadall, L. J., Shaw, P. J., and Cunliffe, V. T. (2006). The microtubule-severing protein Spastin is essential for axon outgrowth in the zebrafish embryo. Hum. Mol. Genet. *15*, 2763–2771.

Yu, W., and Baas, P. W. (1994). Changes in microtubule number and length during axon differentiation. J. Neurosci. *14*, 2818–2829.

Yu, W., Ahmad, F. J., and Baas, P. W. (1994). Microtubule fragmentation and partitioning in the axon during collateral branch formation. J. Neurosci. *14*, 5872–5884.

Yu, W., Solowska, J. M., Qiang, L., Karabay, A., Baird, D., and Baas, P. W. (2005). Regulation of microtubule severing by katanin subunits during neuronal development. J. Neurosci. *25*, 5573–5583.

Zhang. D., Rogers, G. C., Buster, D. W., and Sharp, D. J. (2007). Three microtubule severing enzymes contribute to the "Pacman-flux" machinery that moves chromosomes. J. Cell Biol. *17*, 231–242.